

UCSF

UC San Francisco Electronic Theses and Dissertations

Title

Response and Resistance to Targeted Inhibitors in T-Lineage Leukemias

Permalink

<https://escholarship.org/uc/item/6xs989n3>

Author

Donlan, Kegan Laureen

Publication Date

2013

Peer reviewed|Thesis/dissertation

Response and Resistance to Targeted Inhibitors in T-Lineage
Leukemias

by

Kegan Laureen Donlan

DISSERTATION

Submitted in partial satisfaction of the requirements for the degree of

DOCTOR OF PHILOSOPHY

in

Biomedical Sciences

in the

GRADUATE DIVISION

of the

UNIVERSITY OF CALIFORNIA, SAN FRANCISCO

Copyright 2013

by

Kegan Lauren Donlan

This dissertation is dedicated to my baby sister, whose scrutiny of my life has made me a stronger and better person, and to my husband, who has encouraged and motivated me to be braver than I thought I was.

Acknowledgements

I am grateful to my mentor, Kevin Shannon, for taking me into his lab. Always optimistic and positive, his enthusiasm for research is contagious. His lab is full of people with passion for science and positive attitudes as well. Monique Dail helped me as a lowly roton and has always been a source of advice and friendship. Her expertise in T-ALL was vast and mightily used, and her assistance on everything from Westerns to proliferation assays really made my work so much easier. Ernesto Diaz-Flores was a wonderful resource for FACs experiments, and Jin Xu, Ari Firestone, Anica Wandler, Mike Burgess, Tiffany Chang, and Charissa Cottomham were always there to bounce ideas off of and help guide me in the right experimental direction. I am grateful to Ashley Ward for graciously handing off her cell lines to me and being a wonderful role model. Ben Braun has been such an incredible resource to me, always taking time to help me figure out what to do next, what on earth my data could mean, and I am so grateful for his time and counsel.

I am grateful for the guidance of my Thesis Committee. Frank McCormick has had so many useful insights for my project, and Martin McMahon has been one of the most caring and influential people I have encountered while at UCSF. I am very grateful for the thought and time both of them have invested in me.

During my many long years at UCSF I have been fortunate to have a group of women going through graduate school with me. Lauren Herl Martens, Emily Thornton, Emily Elliott, Kristen Coakley, Renee Greer, and Sara Gierke, our “bookclubs” saved me from loneliness, frustration, and soberness. I am so thankful I

had you all to share the craziness of the last 7 years with and I honestly do not know how I would have gotten through without your support and friendship.

Without Lisa Magargal I would have been so lost on so many separate occasions. I am so thankful for her help on everything from health insurance as a brand new student to dissertation filing. She has made my life infinitely easier.

The fact that I am writing this at all is due to my parents, who encouraged my insatiable curiosity and who actually believed I could do whatever I set out to do, no matter how hard. That they believed this somehow made me believe it too. When I was twelve and wanted to read medical books and figure out how to cure cancer, they went and found me old texts. I actually grew up believing I COULD do anything I set my mind to. Thank you mom, for being my first and best teacher, for gifting me with your fascination with nature and your beautiful curiosity. And thank you dad, for instilling in me your love of learning.

I am so very grateful to my husband for his encouragement and help. For understanding me having to work crazy hours and nearly every weekend, for cheering me on when I felt so tired and just wanted to give up, and for reminding me that there is so much more in my life that is bigger than this. What a gift.

And to my newborn son, Rory. The click of your swing, the little noises you make in your sleep, and the static of your monitor have been the soundtrack to which I have written this dissertation. You will never remember the words I recited out loud to you to see if they sounded right, my sighs of frustration as I tried to format a figure, or the tapping of the keyboard while you napped, but I will never forget looking over from the screen to see you smile in your sleep, the smell of your

head as I held you and tried to type just 1 more sentence, the song your little toy plays that I'd hear as I worked. I hope you someday you have big, silly dreams, and I hope you chase them. I hope you do something harder than you ever imagined and nearly fail, but I hope you stick with it and know the freedom and peace of doing what you always dreamed of and doubted you could do.

Reference to published Materials:

Chapter 2 is a reprint of the material as in the article Shieh A, Ward AF, Donlan KL, Harding-Theobald ER, Xu J, Mullighan CG, Zhang C, Chen SC, Su X, Downing JR, Bollag GE, Shannon KM. Defective K-Ras oncoproteins overcome impaired effector activation to initiate leukemia in vivo. *Blood*. 2013 Jun 13;121(24):4884-93

Research Advisor's Statement Regarding Research Contributions

Kegan (Warner) Donlan made important scientific contributions to and co-authored the two research papers listed below.

Lauchle JO, Kim D, Le DT, Akagi K, Crone M, Krisman K, **Warner K**, Bonifas JM, Li Q, Coakley K, Diaz-Flores E, Gorman M, Przybranowski S, Tran M, Kogan SC, Roose J, Copeland N, Jenkins N, Parada LF, Wolff L, Leopold J, Shannon K. Response and resistance to MEK inhibition in leukemias initiated by hyperactive Ras. *Nature* 2009; **461**:411-414. PMID: 19727076

Shieh A*, Ward A*, **Donlan KL**, Harding-Theobald E, Mullighan CG, Zhang C, Chen S-C, Su X, Downing JR, Bollag GE, Shannon K. Defective K-Ras oncoproteins initiate cancer *in vivo* and evolve to overcome impaired effector interactions. *Blood*; published on-line May 1, 2013. * - these authors contributed equally.

Soon after joining the lab, she contributed data showing that knocking down *Rasgrp1* in primary leukemia cells that developed resistance to a targeted MEK inhibitor *in vivo* restored drug sensitivity. This was a key experiment that was requested by the reviewers and editors of *Nature*, where the work was published. Kegan used a vector developed in the lab of Jeroen Roose (UCSF) to conduct these studies. Jennifer Lauchle, a physician/scientist in my lab, developed these leukemias, treated them, and isolated and analyzed drug-resistant clones. Jennifer was assisted by other members of the lab, including post-docs (D. Le, E. Diaz-Flores,

M. Gorman) and technical staff (D. Kim, K. Krisman, M. Crone, M. Tran). This work was not a central part of Kegan's thesis, but inspired her later studies of MEK inhibitor resistance in T-ALL cell lines (Chapter 2) and provided her with valuable experience for the *Pten* knockdown experiments discussed in Chapter 3.

Kegan made a major scientific contribution to the *Blood* paper, which comprises Chapter 2 of this thesis. Using T cell leukemia cell lines that were generated by another BMS graduate student (Angell Shieh) from an *in vivo* screen of the transforming potential of two second site K-Ras mutant oncoproteins, Kegan fully characterized the response of these cell lines to targeted inhibitors and demonstrated that hyperactive PI3 kinase/Akt signaling protected these cells from apoptosis. Her work is included as a Figure and Supplemental Figure in the final paper and is a key component of the project. Kegan generated and analyzed these data, prepared the figures, and contributed extensively to writing the Material and Methods, Results, and Discussion sections of the paper. In studies described in Chapter 3, she substantially extended her analysis of the mechanisms underlying response and resistance and I believe that this work will ultimately be included in another paper. Angell Shieh and Ashley Ward, a post-doc in my lab, performed the initial screen, generated cell lines and primary leukemias for molecular analysis.

Abstract

Response and Resistance to Targeted Inhibitors in T-Lineage Leukemias
Kegan Lauren Donlan

Ras pathway mutations are prevalent in T lineage leukemias and the Ras/PI3 kinase/PTEN/AKT pathway plays an important role in the maintenance and evolution of this disease. Second-site mutants of Ras are a unique biological system that allows us to study the effects of distinct downstream Ras effectors for cancer initiation and maintenance. By adding chemical inhibitors to this genetically modified system, further information regarding the cells requirements for pathway activation can be assessed.

To accomplish this goal, second site cell lines were exposed to the MEK inhibitor PD0325901, PI3 kinase (PI3K) inhibitor GDC-0941, and the AKT inhibitor MK2206 and proliferation assays were performed. No significant differences were seen between mutational groups when lines were exposed to inhibitors of PI3K or AKT. However, exposing T-ALL cells to PD0325901 revealed significant differences between lines with PTEN expression and those lacking PTEN, despite equal inhibition of the RAF/MEK/ERK pathway. Cells expressing PTEN are uniquely sensitive to MEK inhibition and the cells respond to PD0325901 by undergoing apoptosis.

Dual inhibition of AKT and MEK causes cell lines that are resistant to MEK inhibition to become sensitive, despite significantly higher basal pathway activation. These data implicate AKT as an important mediator of resistance to PD0325901.

Pro-survival proteins BCL-xl and MCL-1 are expressed at low levels in cell lines with PTEN expression, and in the presence of PD0325901, the levels decrease. However, in PTEN negative lines that all show resistance to PD0325901, expression of these proteins is high and remains high or increases in the presence of drug. Our results argue that AKT is activated by loss of PTEN expression, and that AKT mediates drug sensitivity through BCL-xl and MCL-1.

We implicate loss of PTEN expression as integral to PD0325901 resistance in T-ALL cells. DNA sequencing of most lines lacking PTEN expression did not uncover mutations, so we sought to determine whether methylation and epigenetic silencing were the mechanism of *Pten* silencing. Bisulfite sequencing, 5 azacytidine treatment, Trichostatin A treatment, and EpiQ analysis all came back negative, leading us to believe that methylation is not the cause of PTEN silencing in our cells.

Table of Contents

Chapter 1	
Introduction.....	1
Chapter 2	
Defective K-Ras Oncoproteins Overcome Impaired Effector Activation to Initiate Leukemia In Vivo.....	31
Chapter 3	
Mechanism of Resistance to MEK Inhibition.....	91
Chapter 4	
Mechanism of PTEN Silencing in T-ALL Cell Lines.....	117
Chapter 5	
Conclusions and Future Directions.....	143

List of Tables

Chapter 1

Table 1 Ras Mutations in Cancer.....	9
--------------------------------------	---

List of Figures

Chapter 1

Figure 1 Regulation of Ras.....	3
Figure 2 Structure of Ras.....	5
Figure 3 Ras effectors.....	7
Figure 4 Ras pathway mutations in myeloid and lymphoid leukemias.....	12
Figure 5 Ras second site Switch mutants.....	15

Chapter 2

Figure 1 Second site Kras ^{D12} mutant alleles induce hypersensitive myeloid progenitor growth and initiate T-ALL.....	36
Figure 2 Leukemias initiated by Kras ^{D12/G37} and Kras ^{G12/G64} expression demonstrate distinct signaling profiles.....	40
Figure 3 Somatic “third site” Kras mutations in T-ALL.....	42
Figure 4 Acquired “thirdsite” mutations restore oncogenic activity to Kras ^{D12/G37} and Kras ^{G12/G64}	44

Figure 5 PTEN loss confers resistance to inhibition of MEK but not PI3K or AKT.....	47
Figure 6 PI3K activated T-ALL cell lines and human ETP ALLs have similar gene expression profiles.....	50

Chapter 3

Figure 1 PTEN expression does not alter response to PI3K inhibitors.....	94
Figure 2 Second site mutants sensitive to PD0325901 undergo apoptosis...	95
Figure 3 T-ALL lines show no changes in cell cycle in the presence of PD0325901.....	97
Figure 4 Varied expression of pro-survival proteins in the presence of PD0325901.....	99
Figure 5 Inhibition of AKT alters sensitivity to PD0325901 and expression of pro-survival proteins.....	100
Figure 6 Knockdown of PTEN using siRNA vectors.....	102
Figure 7 PTEN knockdown alters sensitivity to PD0325901 and expression of pro-survival proteins.....	103

Chapter 4

Figure 1 Bisulfite sequencing of PTEN deficient cells expression.....	121
---	-----

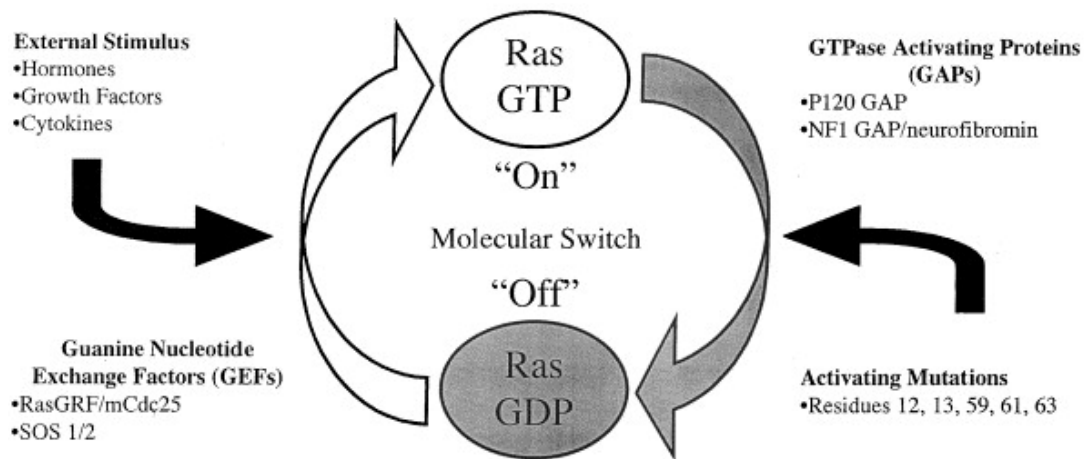
Figure 2 5-azacytidine treatment does not alter PTEN expression.....	123
Figure 3 Cell lines show no changes in proliferation in response to treatment with Trichostatin A.....	125
Figure 4 Trichostatin A does not alter PTEN expression.....	126
Figure 5 Fold change of PTEN in T-ALL cell lines exposed to Trichostatin A	127
Figure 6 EpiQ Analysis of PTEN chromatin structure.....	129

Chapter 1: Introduction

Introduction to Ras

Ras proteins are members of a large family of GTP-binding proteins that function to integrate information from the cell surface and relay it to various parts of the cell by exerting control on numerous signal-transduction pathways.^{1,2} Ras proteins function as molecular switches by cycling between an active GTP-bound form, which interacts productively with downstream pathways, and an inactive GDP-bound form (Figure 1). Ras inactivation is augmented by GTPase activating proteins (GAPs) that bind to Ras proteins and markedly enhance their slow intrinsic GTPase activity.³ Regulation of Ras GTP is crucial to modulate proliferation, survival, differentiation, and various other cellular functions.⁴ Ras-GTP exerts its downstream effects in part by initiating serine/threonine phosphorylation cascades, including the Raf/MEK/ERK, PI3K/AKT, and Ral-GDS pathways, with redundancy and cross-talk between them. Thus, Ras is a nodal signaling molecule that regulates pathways involved in proliferation, apoptosis, stress response, growth, and differentiation.⁵

Ras-GTP is a key transmitter of signals within the cell, but activation of Ras is short-lived as hydrolysis of GTP is rapid, especially in the presence of GTPase activating proteins (GAPs)^{6,7}. Ras GAPs insert an “arginine finger” into the phosphate-binding pocket (P-loop), which markedly increases GTP hydrolysis by stabilizing the transition state between Ras-GTP and Ras-GDP.⁸ The two best-studied Ras GAPs are neurofibromin, which acts as a tumor suppressor and is mutated in many myeloid malignancies and other cancers and p120 GAP.⁹ Guanine nucleotide exchange factors (GEFs) such as SOS are essential positive regulators



Ellis et al, Cellular Signaling (2000)

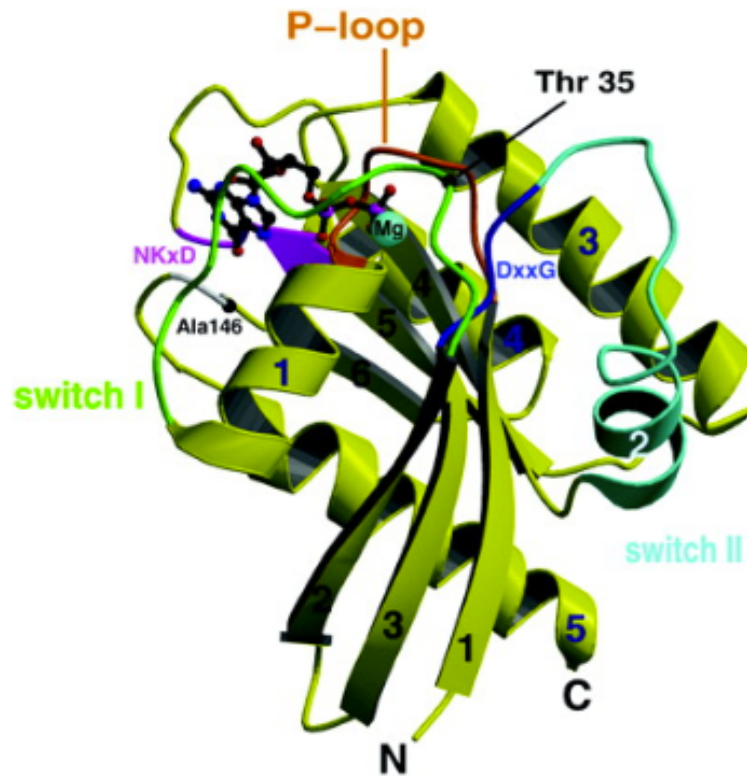
Figure 1 - Regulation of Ras. Ras cycles between an active GTP bound form and an inactive GDP bound form. Activation of Ras is increased by the presence of Guanine Nucleotide Exchange Factors (GEFs) that act to increase the disassociation of guanine nucleotides and allow Ras to bind to prevalent GTP in the cell. Ras has intrinsic GTPase activity that is modulated by GTPase Activating Proteins (GAPs). Common mutations in Ras at residues at residues 12 and 61 decrease the ability of Ras to hydrolyze GTP.

that link activated growth factor receptors and other inputs to Ras. GEFs increase guanine nucleotide dissociation from Ras by binding near the P loop of Ras and inhibiting the interaction of Ras with the guanine phosphate. Negative residues in the switch II region move a lysine away from the guanine nucleotide, resulting in its release from Ras.^{10,11} Ras is then more likely to bind the GTP, which is highly prevalent in cells.¹²

Ras Effector Binding

Ras proteins contain five G domains that bind GTP/GDP. GTP binding induces a conformational change in the switch I and II domains of Ras at regions G2 and G3.¹⁰ When GTP bound, Ras is subtly but essentially altered, existing in a more stable conformation that allows Ras to interact with high affinity with downstream effectors (Figure 2).^{13,14} The switch I (residues 32-40) and switch II (residues 60-76) regions are mobile, but when Ras is bound to GTP, the protein adopts a more stable confirmation due to strong hydrogen bonds between the γ phosphate of GTP and residue 35 (in Switch I) and 60 (in Switch II).¹⁵ This stabilization is essential for efficient binding to effectors and GAPs, with binding of downstream effector PI3K and Ral increased dramatically when Ras is bound to GTP versus GDP.^{16,17}

Oncogenic Ras accumulates in the active, GTP-bound conformation because the most common Ras mutations (in Glycine 12 and Glutamine 61) result in decreased GTP hydrolysis. This increases effector binding and aberrantly activates downstream signaling.¹⁸ In Glycine 12 mutants, the arginine finger required by GAPs to hydrolyze GTP cannot bind in the GTP pocket, so GTP hydrolysis is blocked.



Adapted From Vetter et al, Science (2001)

Figure 2 - Structure of Ras. *Ribbon structure of Ras bound to Magnesium and GTP. The effector loop is shown in orange and the switch I and II regions in lime and aqua, respectively. Conserved sequence elements that facilitate guanine nucleotide binding are indicated.*

Likewise, mutations in Glutamine 61 result in the inability of the protein to form a catalytic residue that is necessary for the hydrolysis of GTP. ^{8,19}

Downstream Effectors of Ras

Ras effectors are defined as proteins that show a markedly increased affinity for Ras-GTP versus Ras-GDP and are important for Ras-regulated cellular function. Endogenous Ras must bind the full-length effector, and Ras-GTP must change the protein, either by causing it to form a complex, changing its localization, or initiating a conformational change. ^{14,20} While there are 10 classes of Ras effectors that meet these criteria, PI3K, Raf, and RalGDS are considered to be the major Ras effectors involved in transformation and oncogenesis (Figure 3). ²¹

PI3Ks are localized to the plasma membrane and become activated by receptor tyrosine kinases or Ras activation. At the membrane, PI3Ks catalyze the reaction of phosphatidylinositol (4,5)-bisphosphate (PIP₂) converted to phosphatidylinositol (3,4,5)-triphosphate (PIP₃). PIP₃ acts as a ligand for AKT, which is recruited and activated at the membrane. AKT is phosphorylated by the mTOR/Rictor complex and PDK1, where it then plays a role in decreasing apoptosis, increasing cell survival, and increasing proliferation. ^{22,23} Phosphatase and tensin homolog (PTEN) is one of the most frequently mutated tumor suppressors in human cancer. A phosphatase that catalyzes second messenger PIP₃ to PIP₂, PTEN plays an essential role in negatively regulating PI3K signaling. ²⁴

The Raf/MEK/ERK pathway is also recruited to the membrane upon Ras activation. Raf is activated at the membrane and in turn activates MEK by

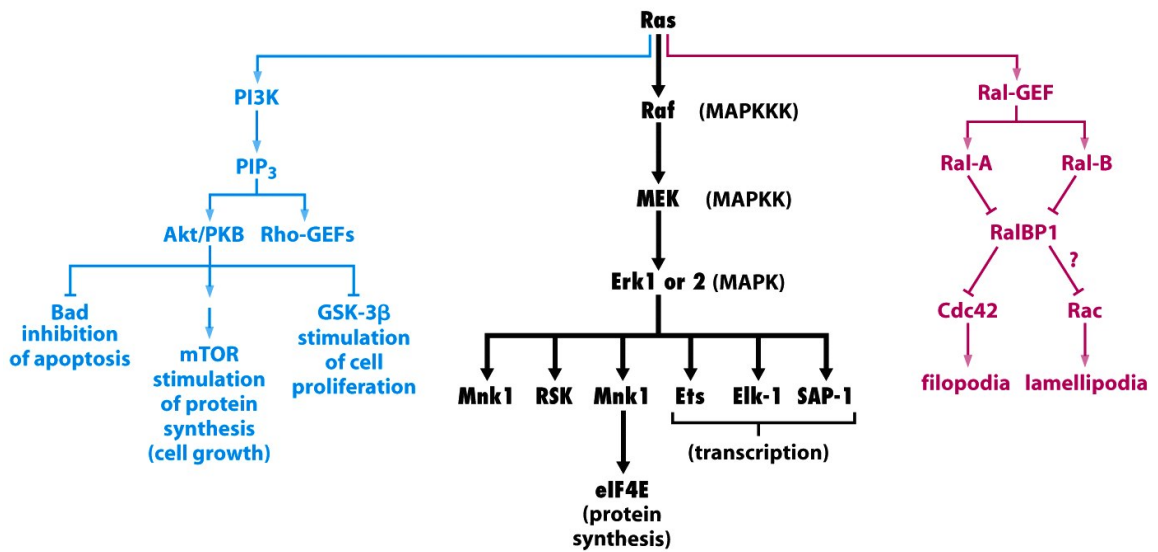


Figure 3 - Ras Effectors. The 3 major Ras effectors PI3K, Raf, and Ral-GEF. Upon activation by binding to Ras, these 3 effectors initiate signal cascades with unique functions within the cell that contribute to Ras transformation. The PI3K and Raf pathway are commonly mutated in human cancers.

phosphorylation, which then activates ERK.²⁵ ERK can localize to the nucleus where it plays a role in translation of genes important in cell survival, proliferation, and mobility.^{26,27} ERK regulates the function of several important transcription factors, including c-Myc.²⁸

RalA and RalB are small GTPases. Like Ras, Ral proteins cycle between an activated GTP bound form and an inactive GDP bound form due to the competing biochemical activities of GAPs and GEFs.²⁹ Activated Ras causes Ral-GDS (a Ral GEF) to localize to the membrane. At the membrane RalGDS interacts with Ral at the membrane to activate it. Additionally, activation of PI3K leads to the activation of Ral through PDK1, which relieves auto-inhibition of RalGDS. RalA functions in gene expression, vesicle trafficking, and control of translation. RalB contributes to immune response, exocyst formation, and cell survival.^{30,31}

Ras Pathway in Cancer

Nearly 30% of human cancers contain mutations in Ras, most often amino acid substitutions at codons 12, 13, and 61.³² These mutations result in resistance to GAPs and decrease the intrinsic GTPase activity of Ras, allowing it to accumulate in the GTP bound form and positively interact with its downstream effectors.^{1,10} Different cancer types show preference for specific Ras isoforms (Table 1), perhaps due to isoform abundance in different tissues, membrane targeting, post-translational modifications, or differences in the ability of Ras isoforms to activate downstream effectors.³³⁻³⁶

Organ/Tissue	H-ras	N-ras	K-ras
Biliary tract	0	2	35
Bladder	12	2	4
Breast	1	2	4
Cervix	9	3	8
Colon	0	2	30
Ganglia	0	8	23
Leukemias	0	11	4
Lymphomas	1	14	6
Liver	0	4	4
Lung	0	1	13
Pancreas	0	3	68
Prostrate	6	2	8
Skin	3	19	5
Stomach	4	2	6
Testis	6	6	6

Table 1 – Ras Mutations in Cancer. Total percentages of cases studied with mutations in the various isoforms of Ras. Data was obtained from the Sanger Catalogue of Somatic Mutations in Cancer and modified from Fernandez-Medarde et al, *Genes and Cancer* (2011).

In addition to mutations that alter Ras, mutations in other Ras pathway proteins are seen in cancer, including loss-of-function mutations in Ras GAP *NF1*. Neurofibromatosis (von Recklinghausen disease) is an autosomal dominant disorder caused by mutations in *NF1*.³⁷ Patients are predisposed to plexiform neurofibromas, myelodysplastic syndromes, leukemias, and optic nerve gliomas.³⁸ Tumors in these patients often reveal somatic inactivation of the normal *NF1* allele, indicating that *NF1* functions as an important tumor suppressor.^{9,39} Recent high-throughput sequencing data have also uncovered frequent somatic *NF1* mutations in glioblastoma and other sporadic cancers.⁴⁰

Mutations in proteins upstream of Ras pathway are also common in cancer. For example, the epidermal growth factor receptor (EGFR) is mutated in 17% of non-small cell lung cancer (NSCLC).⁴¹ A trans-membrane growth factor receptor, EGFR has tyrosine kinase activity signals primarily through the Ras pathway.⁴² Mutations in EGFR can lead to increased copy number and overexpression of the protein, resulting in increased signaling through the Ras pathway. *KRAS* is the most common mutation found in NSCLC, but mutations in *KRAS* and EGFR appear to be mutually exclusive, which is consistent with the idea that EGFR mutations act similarly to activated Ras in the cell and that Ras is essential for EGFR transformation.⁴³

Mutations in proteins downstream of Ras are also often found in cancer. *BRAF* mutations occur in almost 70% of melanoma. The most common mutation is a single amino acid substitution (V600E) which results in a constitutively active BRAF

and signaling through Raf/ MEK/ERK at levels similar to those seen with oncogenic Ras. ⁴⁴ *NRAS* mutations are not found with *BRAF* mutations, which is consistent with the idea that these mutations act similarly in the cell. ⁴⁵

PI3K pathway mutations are also common in many cancer types. In breast cancer, at least 50% of cancers contain mutations in the PI3K pathway, including mutations in *PIK3CA*, *AKT*, and *PTEN*. ⁴⁶ Interestingly, mutations are often found in *RAS* in these tumors as well, indicating that sole activation of the PI3K is not sufficient for transformation. ⁴⁷ It is also worth noting that while Ral has been implicated in aberrant growth of cancer cell lines, mutations in *Ral* are rare in cancer, though the reason for this not yet known. ⁴⁸

Ras Mutations in Hematologic Cancers

Ras-regulated signaling pathways are frequently deregulated in myeloid malignancies through *NRAS* or *KRAS* point mutations or by other mechanisms that deregulate Ras signaling (Figure 4). ^{2,49} *NRAS* and *KRAS2* mutations occur in 40% of chronic myelomonocytic leukemias (CMML) and 25% of juvenile myelomonocytic leukemias (JMML). These aggressive myeloproliferative disorders (MPDs) that share clinical and biologic features and progress to AML in many patients ^{50,51,52}. Proteins upstream of Ras are also commonly mutated in myeloid malignancies, as children with *NF1* have an increased risk of developing JMML, and show a complete loss of *NF1* in tumors. ³⁹ Ras enhancers *CBL* and *PTPN11* are also mutated in JMML, further illustrating that it is indeed a disease of aberrant Ras signaling. ⁵³⁻⁵⁵ *RAS*

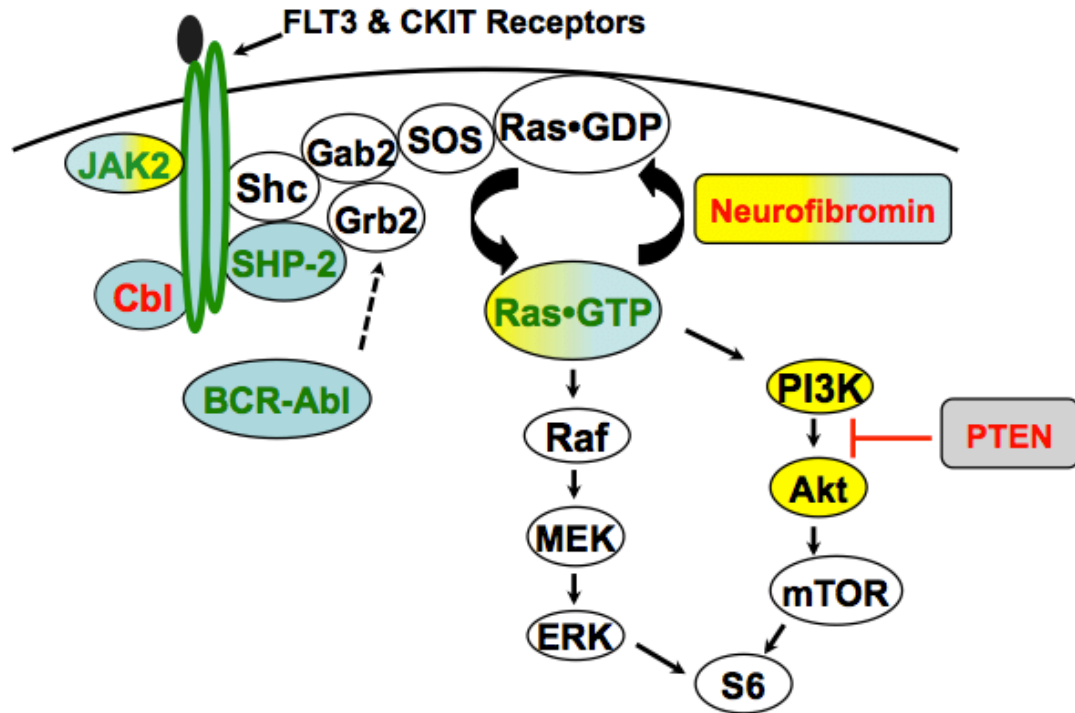


Figure 4 - Ras Pathway Mutations in Myeloid and Lymphoid Leukemias. Red lettering indicates proteins that negatively regulate Ras activation such as Cbl, Neurofibromin, and PTEN. Green indicates positive regulators of Ras activation JAK, cKIT, FLT3, Ras, SHP-2, and BCR-Abl. Proteins colored blue are commonly mutated in myeloid disease. Yellow indicates mutations commonly found in lymphoid disease, and the combination of yellow and blue are mutated in both myeloid and lymphoid leukemias. Myeloid disease is more commonly associated with mutations in Ras or upstream of Ras, while lymphoid disease is most often seen with mutations at or below the level of Ras.

mutations are less common in acute myeloid leukemia (AML), where *NRAS* is mutated in about 10% of patients and *KRAS* in about 5%.^{56,57} However, recent high-throughput studies have found significantly higher percentages of 20-25% of *RAS* mutations in AML.⁵⁸ Importantly, AML is a disease where mutations are often gained and lost, making it possible that *RAS* mutations play an important role early in the development of disease, but less important later on, or vice versa. In multiple myeloma Ras is the most commonly mutated gene family, with mutations in codons 12,13, or 61 found in 23% of patients, most commonly in *NRAS*.⁵⁹

Although Ras pathway mutations are most commonly associated with myeloid disease, sequencing studies have uncovered an increasingly important role of *RAS* mutations in lymphoid leukemias.⁵⁸ A recent deep-sequencing and gene-array study found that over 70% of near haploid ALL patients harbored mutations in genes encoding receptor tyrosine kinases (RTKs) or Ras pathway genes including *NF1*, *NRAS*, *KRAS*, and *MAPK1*. Although less common, *RAS* and RTK mutations were also found in low-hypodiploid and near-diploid ALL at frequencies of 9% and 30%, respectively.⁶⁰ In acute lymphoblastic leukemia (ALL), mutations in *NRAS* and *KRAS* are seen in about 15% of cases, though studies have recently found mutations in *RAS* pathway genes in a far greater number of patients with early T-cell ALL (67%), implicating Ras as an initiator of T-cell disease.^{61,62} Mutations downstream of Ras are common in T lineage ALL, with nearly 50% of cases showing mutations in the PI3K pathway, including 5% with mutations in *PTEN*, a negative regulator of the PI3K, and another 17% with decreased *PTEN* expression.^{63,64} Mutations upstream

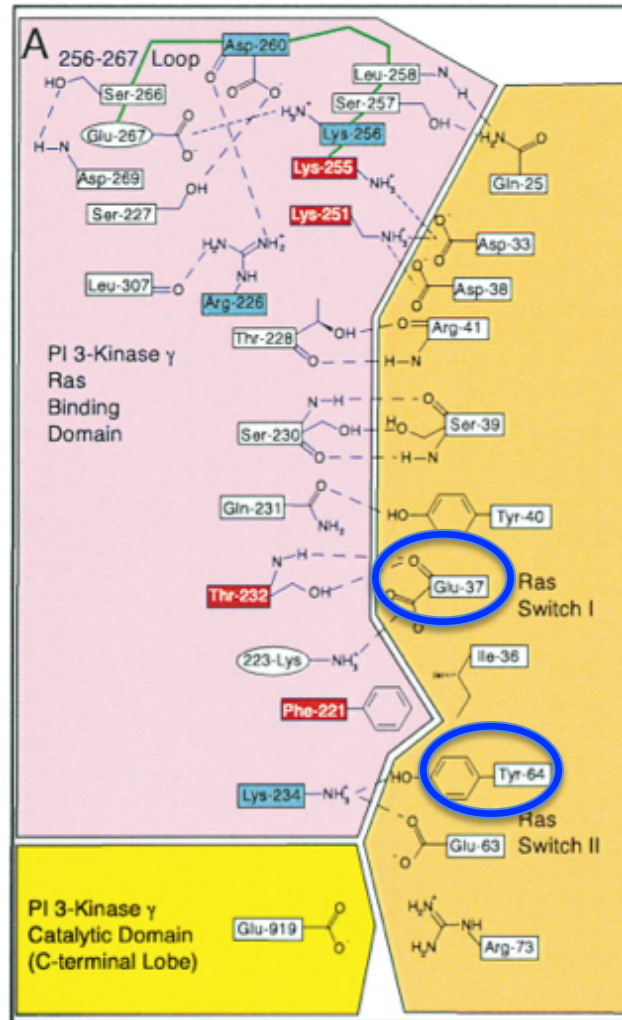
of Ras are found in *NF1* (3%), and *JAK1* (20%) and lead to elevated levels of ERK and AKT, indicating the essential role of Ras signaling in leukemic growth.⁶⁵⁻⁶⁷

Second Site Mutants

Second site mutants of oncogenic Ras are partial loss-of-function proteins with defective binding to one or more classes of effectors. These alleles are generated by introducing an amino acid substitution into one of the Switch domains in the background of a “first site” oncogenic mutation such as G12D. These “second site” mutations alter the ability of Ras proteins to bind specific effectors.^{68,69}

Second-site mutants are useful as a way to help determine which Ras effectors are required for cancer initiation and maintenance, as endogenous Ras signaling is not altered in these mutants. Studies in fibroblasts and epithelial cell lines supported the idea that all three major effectors of Ras are required for transformation.^{8,68} Because Ras itself remains undruggable, determining the minimum pathway activation required for oncogenesis might be used to guide therapeutic strategies combining targeted inhibitors.

Second site mutants were originally created by random mutation of Ras by PCR in a yeast-two hybrid screen.⁶⁹ Crystal studies predicted that amino acid changes at Glu-37 would still allow for Ral and PI3K binding but would decrease affinity for Raf, and that amino acid changed at Tyr-64 would still allow for binding with Raf and Ral but decrease affinity for PI3K (Figure 5).⁷⁰ Drawbacks of this second-site system include that effector binding may not be completely abolished



Adapted From Pacold et al, Cell (2000)

Figure 5 – Ras Second Site Switch Mutants. Diagram of the location of the E37G and Y64G second site mutants. Switch I mutations in Glutamic Acid 37 to Glycine have been predicted to decrease Ras effector binding with Raf, but maintain binding with Ral and PI3K. Mutations in Switch II of Tyrosine 64 to Glycine are predicted to decrease Ras affinity for PI3K but maintain binding affinity with Raf and Ral.

and effectors may still bind weakly to the mutants. In addition, it is difficult to produce a second-site mutant that maintains binding of only one Ras effector.

Mechanisms of Acquired Resistance to Targeted Anti-Cancer Agents

Several over-arching classes of resistance to tyrosine kinase inhibitors (TKIs) have been observed in human cancer. TKI resistance mechanisms in specific cancers can be broadly classified as due to 'on-target' mutations, 'off-target' mutations, or some combination of the two. In chronic myeloid leukemia (CML), acquired resistance to imatinib (Gleevec) most commonly results from mutations to the kinase. Imatinib forms 6 bonds with *BCR-ABL*, and mutations affecting several domains on the kinase cause structural changes such that the drug is unable to exert its inhibition, allowing *BCR-ABL* to continue to signal.⁷¹ There are four distinct classes of *BCR-ABL* mutations seen in acquired resistance, including mutations to the phosphate binding site, imatinib binding site, activation loop, and catalytic loop.⁷² In addition to mutations in *BCR-ABL*, amplification of *BCR-ABL* is also seen in patients with acquired resistance.⁷³

Although most acquired resistance to imatinib results from point mutations that alter *BCR-ABL* kinase activity, other classes of resistance are also seen in CML, though far less commonly. Overexpression of SRC family kinases LYN and HCK have been implicated in acquired resistance, as has expression of efflux proteins.⁷⁴⁻⁷⁶

The epidermal growth factor receptor (EGFR) in lung adenocarcinoma is an example of both on and off-target mechanisms of TKI resistance.⁷⁷ The genetic lesions seen in almost 90% of EGFR mutations are either missense mutations or in-

frame deletions. These mutations confer sensitivity to EGFR kinase inhibitors, specifically erlotinib and gefitinib.⁷⁸⁻⁸⁰ Although patients presenting with EGFR mutations initially respond well to treatment, the majority develop resistance.⁸¹ Approximately 50% of these secondary mutations are also in the EGFR kinase and are responsible for resistance to erlotinib and gefitinib, effectively rendering them unable to inactivate the kinase through the inability of the inhibitor to bind effectively.^{77,82-86} Through genome-wide profiling on the remaining 50% of EGFR resistant tumor samples that do not harbor additional kinase mutations, the *MET* proto-oncogene was implicated in acquired resistance.⁸⁷ Mutations and amplifications in *MET* are often present in tumors resistant to EGFR kinase inhibitors that do not harbor additional kinase mutations. EGFR is still inhibited in these tumors, and resistance is mediated through alternate pathways.

Finally, some tumors acquire “off target” but “on pathway mutations” as the major mechanism of resistance to TKI treatment. *BRAF* (V600E) mutations are common in melanoma and this discovery led to the development of the targeted inhibitors of *BRAF* RG7204/PLX4032.⁸⁸ In patients, response rates were an impressive 81%, but resistance commonly emerged.^{89,90} Studies have implicated mutations in *MAP3K8* as a potential driver of resistance. *MAP3K8* encodes COT/Tpl2, a kinase that can bypass BRAF to activate MEK/ERK signaling.⁹¹ Additionally, some resistant melanomas showed mutations in *MAP2K1* and *NRAS*, which restore aberrant MEK/ERK signaling.⁹² These data indicate that tumors are dependent on over activation of the pathway, and resistance is driven by mutations

that maintain pathway flux even in the presence of potent targeted inhibitors to *BRAF*.

The overall goal of this thesis project was to characterize the response of T cell ALL cell lines generated from bone marrow expressing two second site K-Ras mutant proteins (*Kras*^{D12/G37} and *K-Ras*^{D12/G64}) to targeted inhibitors. I characterized how these second site mutations and PTEN status modulate drug responses. We also performed experiments to investigate potential non-mutational mechanisms of PTEN silencing in these T-ALL lines.

In Chapter 2 we show that second site Ras mutants initiate T-ALL in vivo and that these leukemias undergo secondary genetic alterations to alter signaling, including loss of PTEN expression and reactivation of PI3K signaling. Cell lines that retain PTEN expression are uniquely sensitive to inhibition by the MEK inhibitor PD0325901, and cell lines that have lost expression are resistant.

In Chapter 3 we perform studies with additional targeted inhibitors and elucidate the mechanism underlying sensitivity and resistance to PD0325901. We demonstrate that sensitive cells undergo apoptosis in response to PD0325901 and that sensitivity correlates with decreased expression of pro-survival proteins BCL-xl and MCL-1. Using siRNA to reduce PTEN expression reverses the sensitive phenotype in cell lines with PTEN expression, indicating the importance of PTEN in conferring sensitivity to PD0325901. Inhibition of AKT in combination with PD0325901 causes sensitivity in lines with loss of PTEN expression, implicating AKT as an important component of sensitivity in our system.

Chapter 4 focuses on understanding the mechanism of PTEN loss in our system. We focused on methylation and epigenetic silencing through Bisulfite sequencing, 5 azacytidine treatment, Trichostatin A treatment, and EpiQ analysis. Together, our data indicate that altered methylation is not the cause of PTEN silencing in our lines.

In Chapter 5 we address experiments that will build upon our studies and future directions for this research.

References

1. Donovan S, Shannon KM, Bollag G. GTPase activating proteins: critical regulators of intracellular signaling. *BBA Rev Cancer*. 2002;1602:23-45.
2. Malumbres M, Barbacid M. RAS oncogenes: the first 30 years. *Nat Rev Cancer*. Jun 2003;3(6):459-465.
3. Boguski M, McCormick F. Proteins regulating Ras and its relatives. *Nature*. 1993;366:643-653.
4. Downward J. The *ras* superfamily of small GTP-binding proteins. *Trends Biochem. Sci*. 1990;15:469-472.
5. Barbacid M. *ras* Genes. *Annu Rev Biochem*. 1987;56:779-827.
6. Bollag G, McCormick F. Differential regulation of *ras*GAP and neurofibromatosis gene product activities. *Nature*. 1991;351(6327):576-579.
7. Satoh T, Endo M, Nakafuku M, Akiyama T, Yamamoto T, Kaziro Y. Accumulation of p21^{ras}•GTP in response to stimulation with epidermal

- growth factor and oncogene products with tyrosine kinase activity. *Proc Natl Acad Sci USA*. 1990;87:7926-7929.
8. Scheffzek K, Ahmadian MR, Kabsch W, et al. The Ras-RasGAP complex: structural basis for GTPase activation and its loss in oncogenic Ras mutants. *Science*. Jul 18 1997;277(5324):333-338.
 9. Side L, Emanuel P, Taylor B, et al. Mutations of the *NF1* gene in leukemias from children without evidence of neurofibromatosis, type 1. *Blood*. 1998;92:267-273.
 10. Vetter IR, Wittinghofer A. The guanine nucleotide-binding switch in three dimensions. *Science*. Nov 9 2001;294(5545):1299-1304.
 11. Bollag G, McCormick F. Regulators and effectors of *ras* proteins. *Annu Rev Cell Biol*. 1991;7:601-632.
 12. Bourne HR, Sanders DA, McCormick F. The GTPase superfamily: a conserved switch for diverse cell functions. *Nature*. 1990;348:125-132.
 13. Moodie SA, Paris M, Villafranca E, Kirshmeier P, Willumsen BM, Wolfman A. Different structural requirements within the switch II region of the Ras protein for interactions with specific downstream targets. *Oncogene*. Aug 3 1995;11(3):447-454.
 14. Marshall CJ. Ras effectors. *Current Opinion in Cell Biology*. April 1996 1996;8(2):197-204.
 15. Nassar N, Horn G, Herrmann CxA, Scherer A, McCormick F, Wittinghofer A. The 2.2 Å crystal structure of the Ras-binding domain of the serine/threonine

- kinase c-Raf1 in complex with Rap1A and a GTP analogue. *Nature*. 1995-06-15 1995;375(6532):554-560.
16. Bos JL, Rehmann H, Wittinghofer A. GEFs and GAPs: critical elements in the control of small G proteins. *Cell*. Jun 1 2007;129(5):865-877.
 17. Wittinghofer A, Herrmann C. Ras-effector interactions, the problem of specificity. *FEBS Lett*. Aug 1 1995;369(1):52-56.
 18. Seeburg PH, Colby WW, Capon DJ, Goeddel DV, Levinson AD. Biological properties of human c-Ha-ras1 genes mutated at codon 12. *Nature*. Nov 1-7 1984;312(5989):71-75.
 19. Pai EF, Krenzel U, Petsko GA, Goody RS, Kabsch W, Wittinghofer A. Refined crystal structure of the triphosphate conformation of H-ras p21 at 1.35 Å resolution: implications for the mechanism of GTP hydrolysis. *Embo j*. Aug 1990;9(8):2351-2359.
 20. Hallberg B, Rayter SI, Downward J. Interaction of Ras and Raf in intact mammalian cells upon extracellular stimulation. *J Biol Chem*. Feb 11 1994;269(6):3913-3916.
 21. Shields JM, Pruitt K, McFall A, Shaub A, Der CJ. Understanding Ras: 'it ain't over 'til it's over'. *Trends Cell Biol*. Apr 2000;10(4):147-154.
 22. Vivanco I, Sawyers CL. The phosphatidylinositol 3-Kinase|[ndash]|AKT pathway in human cancer. *Nature Reviews Cancer*. 2002-07-01 2002;2(7):489-501.
 23. Rodriguez-Viciana P, Warne PH, Dhand R, et al. Phosphatidylinositol-3-OH kinase as a direct target of Ras. *Nature*. Aug 18 1994;370(6490):527-532.

24. MESTER J, ENG C. When Overgrowth Bumps Into Cancer: The PTEN - Opathies. *American Journal of Medical Genetics Part C: Seminars in Medical Genetics*.163(2):114-121.
25. Farnsworth CL, Freshney NW, Rosen LB, Ghosh A, Greenberg ME, Feig LA. Calcium activation of Ras mediated by neuronal exchange factor Ras-GRF. *Nature*. 1995;376:524-527.
26. Mercer KE, Pritchard CA. Raf proteins and cancer: B-Raf is identified as a mutational target. *Biochim Biophys Acta*. Jun 5 2003;1653(1):25-40.
27. Repasky GA, Chenette EJ, Der CJ. Renewing the conspiracy theory debate: does Raf function alone to mediate Ras oncogenesis? *Trends Cell Biol*. Nov 2004;14(11):639-647.
28. Wellbrock C, Karasarides M, Marais R. The RAF proteins take centre stage. *Nature Reviews Molecular Cell Biology*. 2004-11-01 2004;5(11):875-885.
29. Feig LA. Ral-GTPases: approaching their 15 minutes of fame. *Trends Cell Biol*. Aug 2003;13(8):419-425.
30. Feig LA, Urano T, Cantor S. Evidence for a Ras/Ral signaling cascade. *Trends Biochem Sci*. 1996;21:438-441.
31. Bodemann BO, White MA. Ral GTPases and cancer: linchpin support of the tumorigenic platform. *Nature Reviews Cancer*. 2008-02-01 2008;8(2):133-140.
32. Bos JL. The *ras* gene family and human carcinogenesis. *Mutation Research*. 1988;195:255-271.

33. Fernandez-Medarde A, Santos E. Ras in cancer and developmental diseases. *Genes Cancer*. Mar 2011;2(3):344-358.
34. Downward J. Targeting RAS signalling pathways in cancer therapy. *Nat Rev Cancer*. Jan 2003;3(1):11-22.
35. Johnson L, Greenbaum D, Cichowski K, et al. K-ras is an essential gene in the mouse with partial functional overlap with N-ras. *Genes Dev*. Oct 1 1997;11(19):2468-2481.
36. Umanoff H, Edelmann W, Pellicer A, Kucherlapati R. The murine N-ras gene is not essential for growth and development. *Proc Natl Acad Sci U S A*. Feb 28 1995;92(5):1709-1713.
37. Weiss B, Bollag G, Shannon K. Hyperactive Ras as a therapeutic target in neurofibromatosis type 1. *Am J Med Genet*. 1999;89(1):14-22.
38. Dasgupta B, Yi Y, Chen DY, Weber JD, Gutmann DH. Proteomic analysis reveals hyperactivation of the mammalian target of rapamycin pathway in neurofibromatosis 1-associated human and mouse brain tumors. *Cancer Res*. Apr 1 2005;65(7):2755-2760.
39. Side L, Taylor B, Cayouette M, et al. Homozygous inactivation of the NF1 gene in bone marrow cells from children with neurofibromatosis type 1 and malignant myeloid disorders. *N Engl J Med*. Jun 12 1997;336(24):1713-1720.
40. Koso H, Takeda H, Yew CCK, et al. Transposon mutagenesis identifies genes that transform neural stem cells into glioma-initiating cells. *PNAS*. 2012-10-30 2012;109(44):E2998.

41. da Cunha Santos G, Shepherd FA, Tsao MS. EGFR mutations and lung cancer. *Annu Rev Pathol.* 2011;6:49-69.
42. Wells A. EGF receptor. *Int J Biochem Cell Biol.* Jun 1999;31(6):637-643.
43. Roberts PJ, Stinchcombe TE. KRAS mutation: should we test for it, and does it matter? *J Clin Oncol.* Mar 10 2013;31(8):1112-1121.
44. Davies H, Bignell GR, Cox C, et al. Mutations of the BRAF gene in human cancer. *Nature.* 2002-06-09 2002;417(6892):949-954.
45. Wan PT, Garnett MJ, Roe SM, et al. Mechanism of activation of the RAF-ERK signaling pathway by oncogenic mutations of B-RAF. *Cell.* Mar 19 2004;116(6):855-867.
46. Miled N, Yan Y, Hon WC, et al. Mechanism of two classes of cancer mutations in the phosphoinositide 3-kinase catalytic subunit. *Science.* Jul 13 2007;317(5835):239-242.
47. Wong KK, Engelman JA, Cantley LC. Targeting the PI3K signaling pathway in cancer. *Curr Opin Genet Dev.* Feb 2010;20(1):87-90.
48. Chien Y, White MA. RAL GTPases are linchpin modulators of human tumour-cell proliferation and survival. *EMBO Rep.* Aug 2003;4(8):800-806.
49. Bos JL. *ras* oncogenes in human cancer: a review. *Cancer Res.* 1989;49:4682-4689.
50. Onida F, Kantarjian HM, Smith TL, et al. Prognostic factors and scoring systems in chronic myelomonocytic leukemia: a retrospective analysis of 213 patients. *Blood.* 2002;99(3):840-849.

51. Vogelstein B, Civin CI, Presinger A, et al. Ras gene mutations in childhood acute myeloid leukemia. *Genes Chromosomes Cancer*. 1990;2:159-162.
52. Van Etten RA, Shannon KM. Focus on myeloproliferative diseases and myelodysplastic syndromes. *Cancer Cell*. Dec 2004;6(6):547-552.
53. Niemeyer CM, Kang MW, Shin DH, et al. Germline CBL mutations cause developmental abnormalities and predispose to juvenile myelomonocytic leukemia. *Nature Genetics*. 2010-08-08 2010;42:794-800.
54. Loh ML, Vattikuti S, Schubbert S, et al. Mutations in PTPN11 implicate the SHP-2 phosphatase in leukemogenesis. *Blood*. Mar 15 2004;103(6):2325-2331.
55. Xu D, Wang S, Yu WM, et al. A germline gain-of-function mutation in Ptpn11 (Shp-2) phosphatase induces myeloproliferative disease by aberrant activation of hematopoietic stem cells. *Blood*. Nov 4 2010;116(18):3611-3621.
56. Bacher U, Haferlach T, Schoch C, Kern W, Schnittger S. Implications of NRAS mutations in AML: a study of 2502 patients. *Blood*. May 15 2006;107(10):3847-3853.
57. Bowen DT, Frew ME, Hills R, et al. RAS mutation in acute myeloid leukemia is associated with distinct cytogenetic subgroups but does not influence outcome in patients younger than 60 years. *Blood*. Sep 15 2005;106(6):2113-2119.

58. Tyner JW, Erickson H, Deininger MW, et al. High-throughput sequencing screen reveals novel, transforming RAS mutations in myeloid leukemia patients. *Blood*. Feb 19 2009;113(8):1749-1755.
59. Chng WJ, Gonzalez-Paz N, Price-Troska T, et al. Clinical and biological significance of RAS mutations in multiple myeloma. *Leukemia*. 2008-06-05 2008;22(12):2280-2284.
60. Holmfeldt L, Wei L, Diaz-Flores E, et al. The genomic landscape of hypodiploid acute lymphoblastic leukemia. *Nature Genetics*. 2013-01-20 2013;45:242-252.
61. Neri A, Knowles DM, Greco A, McCormick F, Dalla-Favera R. Analysis of RAS oncogene mutations in human lymphoid malignancies. *Proc Natl Acad Sci USA*. 1988;85(23):9268-9272.
62. Zhang, Ding L, Holmfeldt L, et al. The genetic basis of early T-cell precursor acute lymphoblastic leukaemia. *Nature*. 2012-01-11 2012;481:157-163.
63. Gutierrez A, Sanda T, Grebliunaite R, et al. High frequency of PTEN, PI3K, and AKT abnormalities in T-cell acute lymphoblastic leukemia. *Blood*. Jul 16 2009;114(3):647-650.
64. Palomero T, Sulis ML, Cortina M, et al. Mutational loss of PTEN induces resistance to NOTCH1 inhibition in T-cell leukemia. *Nature Medicine*. 2007-09-16 2007;13(10):1203-1210.
65. Graux, Cools J, Michaux L, Vandenberghe P, Hagemeijer A. Cytogenetics and molecular genetics of T-cell acute lymphoblastic leukemia: from thymocyte to lymphoblast. *Leukemia*. 2006-07-06 2006;20(9):1496-1510.

66. Balgobind BV, Van Vlierberghe P, van den Ouweland AM, et al. Leukemia-associated NF1 inactivation in patients with pediatric T-ALL and AML lacking evidence for neurofibromatosis. *Blood*. Apr 15 2008;111(8):4322-4328.
67. Appelbaum FR, Gundacker H, Head DR, et al. Age and acute myeloid leukemia. *Blood*. May 1 2006;107(9):3481-3485.
68. Rodriguez-Viciana P, Warne PH, Khwaja A, et al. Role of phosphoinositide 3-OH kinase in cell transformation and control of the actin cytoskeleton by Ras. *Cell*. May 2 1997;89(3):457-467.
69. White MA, Nicolette C, Minden A, et al. Multiple Ras functions can contribute to mammalian cell transformation. *Cell*. 1995;80:533-541.
70. Pacold ME, Suire S, Perisic O, et al. Crystal structure and functional analysis of Ras binding to its effector phosphoinositide 3-kinase gamma. *Cell*. Dec 8 2000;103(6):931-943.
71. Nagar B, Bornmann WG, Pellicena P, et al. Crystal structures of the kinase domain of c-Abl in complex with the small molecule inhibitors PD173955 and imatinib (STI-571). *Cancer Res*. Aug 1 2002;62(15):4236-4243.
72. Lee TS, Potts SJ, Kantarjian H, Cortes J, Giles F, Albitar M. Molecular basis explanation for imatinib resistance of BCR-ABL due to T315I and P-loop mutations from molecular dynamics simulations. *Cancer*. Apr 15 2008;112(8):1744-1753.
73. Gorre ME, Mohammed M, Ellwood K, et al. Clinical resistance to STI-571 cancer therapy caused by BCR-ABL gene mutation or amplification. *Science*. Aug 3 2001;293(5531):876-880.

74. Elrick LJ, Jorgensen HG, Mountford JC, Holyoake TL. Punish the parent not the progeny. *Blood*. Mar 1 2005;105(5):1862-1866.
75. Donato NJ, Wu JY, Stapley J, et al. BCR-ABL independence and LYN kinase overexpression in chronic myelogenous leukemia cells selected for resistance to STI571. *Blood*. Jan 15 2003;101(2):690-698.
76. Lionberger JM, Wilson MB, Smithgall TE. Transformation of myeloid leukemia cells to cytokine independence by Bcr-Abl is suppressed by kinase-defective Hck. *J Biol Chem*. Jun 16 2000;275(24):18581-18585.
77. Pao W, Miller VA. Epidermal growth factor receptor mutations, small-molecule kinase inhibitors, and non-small-cell lung cancer: current knowledge and future directions. *J Clin Oncol*. Apr 10 2005;23(11):2556-2568.
78. Pao W, Miller V, Zakowski M, et al. EGF receptor gene mutations are common in lung cancers from "never smokers" and are associated with sensitivity of tumors to gefitinib and erlotinib. *Proc Natl Acad Sci U S A*. Sep 7 2004;101(36):13306-13311.
79. Paez JG, Janne PA, Lee JC, et al. EGFR mutations in lung cancer: correlation with clinical response to gefitinib therapy. *Science*. Jun 4 2004;304(5676):1497-1500.
80. Lynch TJ, Bell DW, Sordella R, et al. Activating mutations in the epidermal growth factor receptor underlying responsiveness of non-small-cell lung cancer to gefitinib. *N Engl J Med*. May 20 2004;350(21):2129-2139.

- 81.** Jackman DM, Yeap BY, Sequist LV, et al. Exon 19 deletion mutations of epidermal growth factor receptor are associated with prolonged survival in non-small cell lung cancer patients treated with gefitinib or erlotinib. *Clin Cancer Res.* Jul 1 2006;12(13):3908-3914.
- 82.** Kobayashi S, Boggon TJ, Dayaram T, et al. EGFR mutation and resistance of non-small-cell lung cancer to gefitinib. *N Engl J Med.* Feb 24 2005;352(8):786-792.
- 83.** Barrington RE, Subler MA, Rands E, et al. A farnesyltransferase inhibitor induces tumor regression in transgenic mice harboring multiple oncogenic mutations by mediating alterations in both cell cycle control and apoptosis. *Mol Cell Biol.* 1998;18(1):85-92.
- 84.** Kwak EL, Sordella R, Bell DW, et al. Irreversible inhibitors of the EGF receptor may circumvent acquired resistance to gefitinib. *Proc Natl Acad Sci U S A.* May 24 2005;102(21):7665-7670.
- 85.** Balak MN, Gong Y, Riely GJ, et al. Novel D761Y and common secondary T790M mutations in epidermal growth factor receptor-mutant lung adenocarcinomas with acquired resistance to kinase inhibitors. *Clin Cancer Res.* Nov 1 2006;12(21):6494-6501.
- 86.** Kobayashi S, Ji H, Yuza Y, et al. An alternative inhibitor overcomes resistance caused by a mutation of the epidermal growth factor receptor. *Cancer Res.* Aug 15 2005;65(16):7096-7101.
- 87.** Bean J, Brennan C, Shih JY, et al. MET amplification occurs with or without T790M mutations in EGFR mutant lung tumors with acquired resistance to

gefitinib or erlotinib. *Proc Natl Acad Sci U S A*. Dec 26 2007;104(52):20932-20937.

- 88.** Flaherty KT, Puzanov I, Kim KB, et al. Inhibition of mutated, activated BRAF in metastatic melanoma. *N Engl J Med*. Aug 26 2010;363(9):809-819.
- 89.** Villanueva J, Vultur A, Lee JT, et al. Acquired resistance to BRAF inhibitors mediated by a RAF kinase switch in melanoma can be overcome by cotargeting MEK and IGF-1R/PI3K. *Cancer Cell*. Dec 14 2010;18(6):683-695.
- 90.** Emery CM, Vijayendran KG, Zipser MC, et al. MEK1 mutations confer resistance to MEK and B-RAF inhibition. *Proc Natl Acad Sci U S A*. Dec 1 2009;106(48):20411-20416.
- 91.** Johannessen CM, Boehm JS, Kim SY, et al. COT drives resistance to RAF inhibition through MAP kinase pathway reactivation. *Nature*. 2010-11-24 2010;468:968-972.
- 92.** Nazarian R, Shi H, Wang Q, et al. Melanomas acquire resistance to B-RAF(V600E) inhibition by RTK or N-RAS upregulation. *Nature*. 2010-11-24 2010;468:973-977.

**Chapter 2: Defective K-Ras Oncoproteins Overcome Impaired Effector
Activation to Initiate Leukemia In Vivo**

Abstract

Reversing the aberrant biochemical output of oncogenic Ras proteins is one of the great challenges in cancer therapeutics; however, it is uncertain which Ras effectors are required for tumor initiation and maintenance. To address this question, we expressed oncogenic K-Ras^{D12} proteins with “second site” amino acid substitutions that impair PI3 kinase/Akt or Raf/MEK/ERK activation in bone marrow cells and transplanted them into recipient mice. In spite of attenuated signaling properties, defective K-Ras oncoproteins initiated aggressive clonal T lineage acute lymphoblastic leukemia (T-ALL). Murine T-ALLs expressing “second site” mutant proteins restored full oncogenic Ras activity through diverse mechanisms, which included acquiring novel somatic “third site” *Kras*^{D12} mutations and silencing PTEN. T-ALL cell lines lacking PTEN had elevated levels of phosphorylated Akt, a gene expression pattern similar to human early T precursor ALL, and were resistant to the potent and selective MEK inhibitor PD0325901. Our data demonstrating strong selective pressure to overcome defective activation of PI3 kinase/Akt and Raf/MEK/ERK implicate both Ras effector pathways as drivers of aberrant growth in T-ALL, and further suggest that leukemia cells will deploy multiple mechanisms to develop resistance to targeted inhibitors *in vivo*.

Introduction

Somatic *RAS* mutations encode oncogenic proteins that accumulate in an active signaling conformation.¹⁻³ Although the biophysical properties of Ras oncoproteins render them exceedingly challenging targets for rational drug discovery, recent data suggest that this might be feasible.⁴ There is also intensive interest in inhibiting Ras-regulated kinase cascades in cancer, particularly the Raf/MEK/ERK and PI3K/Akt/mTOR pathways.^{1,5} To maximize the efficacy of either therapeutic strategy, it is essential to identify Ras effectors required for cancer initiation and maintenance.

Expressing Ras oncoproteins with “second site” amino acid substitutions that mediate binding to individual effectors is a robust approach for investigating this question, complementing the use of small molecule inhibitors while avoiding potential confounding problems such as off target activities and unpredictable levels of kinase inhibition *in vivo*.⁶⁻⁸ Previous studies in fibroblasts and epithelial cells support the idea that simultaneous activation of PI3K, Raf, and Ral-GDS is essential for Ras-induced tumorigenesis.^{1-3,6-8} Determining requirements for hyperactive signaling through different effector pathways in hematologic cancers has translational implications given the high prevalence of somatic *RAS* mutations.^{4,9}

A glycine to aspartic acid substitution at codon 12 (D12) is the most common *KRAS* mutation found in human cancer. Here we show that oncogenic K-Ras^{D12} proteins containing second site substitutions at glutamate 37 (K-Ras^{D12/G37}) or tyrosine 64 (K-Ras^{D12/G64}) are impaired for activating Raf/MEK/ERK and PI3K signaling, respectively. Expressing either mutant protein in mouse bone marrow

cells unexpectedly deregulated the growth of myeloid progenitors *in vitro*, and initiated aggressive T lineage acute lymphoblastic leukemia (T-ALL) *in vivo*. These leukemias displayed biochemical properties that correlated with responses to targeted inhibitors and with distinct secondary genetic alterations, including acquired “third site” mutations within *Kras^{D12}* transgenes. We conclude that aberrant PI3K/Akt and Raf/MEK/ERK signaling contribute to T-ALL growth, and suggest that leukemia cells will deploy both “on target” and “off target” mechanisms to overcome targeted inhibitors.

Results

Kras^{D12} substitutions at codons 37 and 64 retain GM-CSF hypersensitivity. We constructed MSCV-IRES-GFP retroviruses encoding WT K-Ras, K-Ras^{D12}, or K-Ras^{D12} proteins containing amino acid substitutions within the switch I and switch II domains (Supplemental Table 1).^{2,6,7} After infection, GFP⁺ mouse fetal liver cells were plated in methylcellulose. As expected, cells infected with the *MSCV-Kras^{D12}-IRES-GFP* vector formed CFU-GM colonies without added cytokines, and those that grew in plates containing GM-CSF were abnormally large and monocytic.^{1,11} Second site mutant K-Ras proteins that interact with a single class of effectors^{6,7} did not perturb colony growth (Supplemental Table 1 and Supplemental Figure 1A). However, *Kras^{D12}* alleles encoding glycine substitutions at either glutamate 37 (K-Ras^{D12/G37}) or tyrosine 64 (K-Ras^{D12/G64}) induced modest hypersensitivity, characterized by an increase in the number of CFU-GM colonies formed at low concentrations of GM-CSF (Figure 1A). These data indicate that K-Ras^{D12/G37} and K-

Ras^{D12/G64} exhibit “gain of function” compared to WT K-Ras, but are biologically less activated than oncogenic K-Ras^{D12}.

Glu-37 and Tyr-64 substitutions selectively impair Ras effector activation. The crystal structures of Ras bound to Raf, Ral-GDS, and PI3K suggest how amino acid substitutions at codons 37 and 64 of Ras selectively impair effector interactions.^{2,19} Glu-37 is expected to form two hydrogen bonds with Raf, and substitutions at Glu-37 impair Raf binding while only weakly affecting Ral binding.²⁰ Glu-37 also interacts with a basic residue on the p110 α subunit of PI3K that is not present on p110 δ or p110 γ . Tissue-specific differences in PI3K isoform expression likely underlie the variable effects of H-Ras^{D12/G37} expression on PI3K signaling.^{7,8} Notably, blood cells express high levels of p110 δ and p110 γ , suggesting that Ras proteins containing substitutions at Glu-37 will retain the ability to activate PI3K signaling in hematopoietic tissues.²¹ Substitutions at switch II residue Tyr-64 selectively disrupt the interaction between Ras and PI3K, as Raf and Ral-GDS do not bind to this effector domain.²² Consistent with these data, mutating amino acids within p110 α that contact Tyr-64 abolished Ras binding.²³ Supplementary Table 1 summarizes what has been learned about substitutions at codons 37 and 64 from *in vitro* binding assays, structural studies, and biochemical investigation. Notably, Ras proteins containing E37G and Y64G substitutions retain the ability to bind to and activate Ral-GDS.^{6,22}

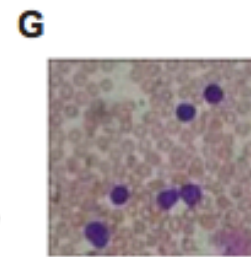
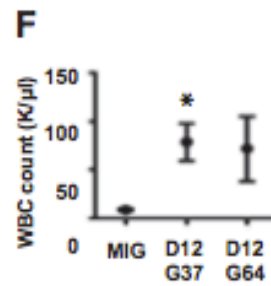
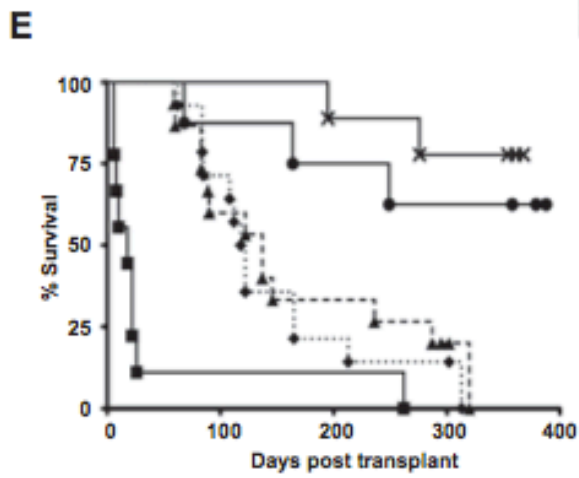
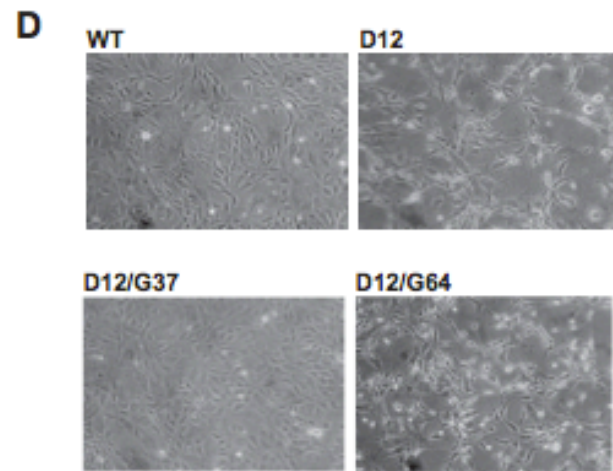
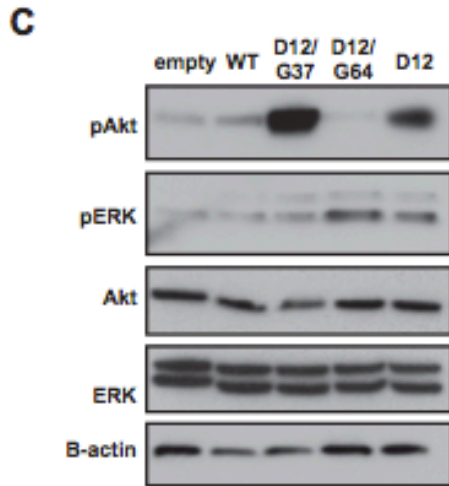
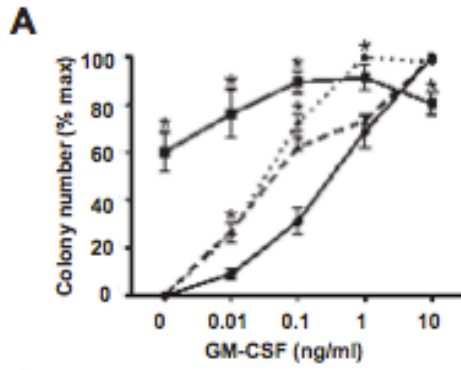


Figure 1 - Second site *Kras*^{D12} mutant alleles induce hypersensitive myeloid progenitor growth and initiate T-ALL. (A) CFU-GM formation by fetal liver cells expressing WT *Kras* (closed circle), *Kras*^{D12} (closed square), *Kras*^{D12/G37} (closed triangle), or *Kras*^{G12/G64} (closed diamond). Mean +/- SEM of 5 independent experiments is shown. Data points marked with an asterisk (*) are significantly different from WT by paired, one-tailed t-test ($p < 0.05$). (B) Signaling in transfected COS-7 cells under basal (B), starved (S), and EGF-stimulated (E) conditions. (C) Signaling in transduced S49 cells under starved conditions. These cells were infected with MSCV-GFP-*Kras* vectors and sorted to equalize Ras expression levels. GFP-K-Ras fusion proteins run at a different molecular weight than endogenous Ras proteins. (D) Morphology of 3T3 cells expressing WT *Kras*, *Kras*^{D12}, *Kras*^{D12/G37}, or *Kras*^{G12/G64}. Note that *Kras*^{D12} and *Kras*^{G12/G64} induce morphologic changes. (E) Survival of lethally irradiated WT mice transplanted with bone marrow cells transduced with MIG vector (; $n=8$) or MIG vectors expressing WT *Kras* (closed circle; $n=10$), *Kras*^{D12} (closed square ; $n=9$), *Kras*^{D12/G37} (closed triangle; $n=15$) or *Kras*^{G12/G64} (closed diamond; $n=14$). (F) White blood cell (WBC) counts at death in recipients of bone marrow transduced with MIG vector ($n=8$), *Kras*^{D12/G37} ($n=15$) or *Kras*^{G12/G64} ($n=14$) viruses. Data plotted as mean +/- SEM with an asterisk (*) indicating data points significantly different from WT by unpaired, one-tailed t-test ($p < 0.05$). (G) Peripheral blood smear showing blast morphology in a mouse with T-ALL.

We expressed K-Ras^{D12/G37} and K-Ras^{D12/G64} in COS-7 cells and the murine T-ALL cell line S49²⁴ and assayed the phosphorylation of downstream effectors. The serum-starved state was most informative for differentiating WT K-Ras from K-Ras^{G12D}, and for testing the effects of the G37 and G64 second site substitutions. Phosphorylated Akt (pAkt) levels were elevated in serum-deprived cells expressing K-Ras^{D12/G37}, while phosphorylated ERK (pERK) levels were normal (Figures 1B and 1C). By contrast, K-Ras^{D12/G64} increased pERK, but not pAkt, levels (Figures 1B and 1C). K-Ras^{D12/G64} expression in 3T3 fibroblasts induced morphological changes consistent with Raf/MEK/ERK pathway activation (Figure 1D).²⁵

Kras^{D12/G37} and Kras^{D12/G64} induce T-ALL in vivo. We infected bone marrow cells from 5-fluorouracil-treated WT donor mice with a control *MSCV-IRES-GFP* vector (MIG) or with viruses encoding WT *Kras*, *Kras^{D12}*, *Kras^{D12/G37}*, or *Kras^{D12/G64}* and transferred them into lethally irradiated WT mice. Recipients of cells transduced with the *Kras^{D12}* virus died early from hematopoietic failure (Figure 1E). Endogenous *Kras^{D12}* reduces the size of the hematopoietic stem cell compartment;²⁶ ectopic expression from the MSCV promoter likely exacerbates this defect, resulting in engraftment failure.

Mice transplanted with cells expressing K-Ras^{D12/G37} or K-Ras^{D12/G64} recovered hematologic function but began to die after 60 days (Figure 1E) from T-ALL characterized by elevated blood leukocyte counts, circulating GFP⁺ blasts, and thymic enlargement with invasion by CD4⁺/CD8⁺ blasts (Figures 1F, 1G and Supplemental Figures 1B, 1C). Secondary recipients died of fulminant leukemia with

a latency of 26.6 days (data not shown). The morphology and immunophenotype were identical in T-ALLs initiated by K-Ras^{D12/G37} or K-Ras^{D12/G64} expression, and Southern blot analysis revealed clonal retroviral integrations (Supplemental Figure 1D). None of the mice transplanted with cells transduced with the MIG vector or with a virus encoding WT K-Ras developed hematologic disease.

Somatic *NOTCH1* mutations are found in ~50% of human T-ALLs,²⁷ and are also observed in mouse models of T-ALL characterized by endogenous *Kras*^{D12} expression.^{12,26,28} Western blot analysis of K-Ras^{D12/G37} and K-Ras^{D12/G64} leukemias with an antibody that detects activated (cleaved) Notch1 revealed abnormal fragments, and DNA sequencing confirmed *Notch 1* PEST domain mutations in 7 out of 11 primary T-ALLs that persisted in secondary recipients (Supplemental Figure 1E and Supplemental Table 2).

Ras and PTEN expression in Kras^{D12/G37} and Kras^{D12/G64}-induced leukemias. We hypothesized that leukemias initiated by K-Ras^{D12/G37} or K-Ras^{D12/G64} might be under selective pressure to augment signaling through Ras effector pathways. To address this question, we biochemically assessed cell lines generated from four independent K-Ras^{D12/G37} (E1-E4) and six independent K-Ras^{D12/G64} (Y1-Y6) leukemias.

T-ALL cell lines expressing K-Ras^{D12/G37} showed elevated Ras protein levels, particularly lines E2 and E4 (Figure 2A), which corresponded to elevated expression of K-Ras^{D12/G37} (Figure 2B), and elevated viral *Kras* DNA copy number (Figure 2C). Three of four K-Ras^{D12/G37} cell lines retained PTEN expression. Of these, two had low levels of pAkt and pERK, while cell line E3 showed a modest increase in pAkt under

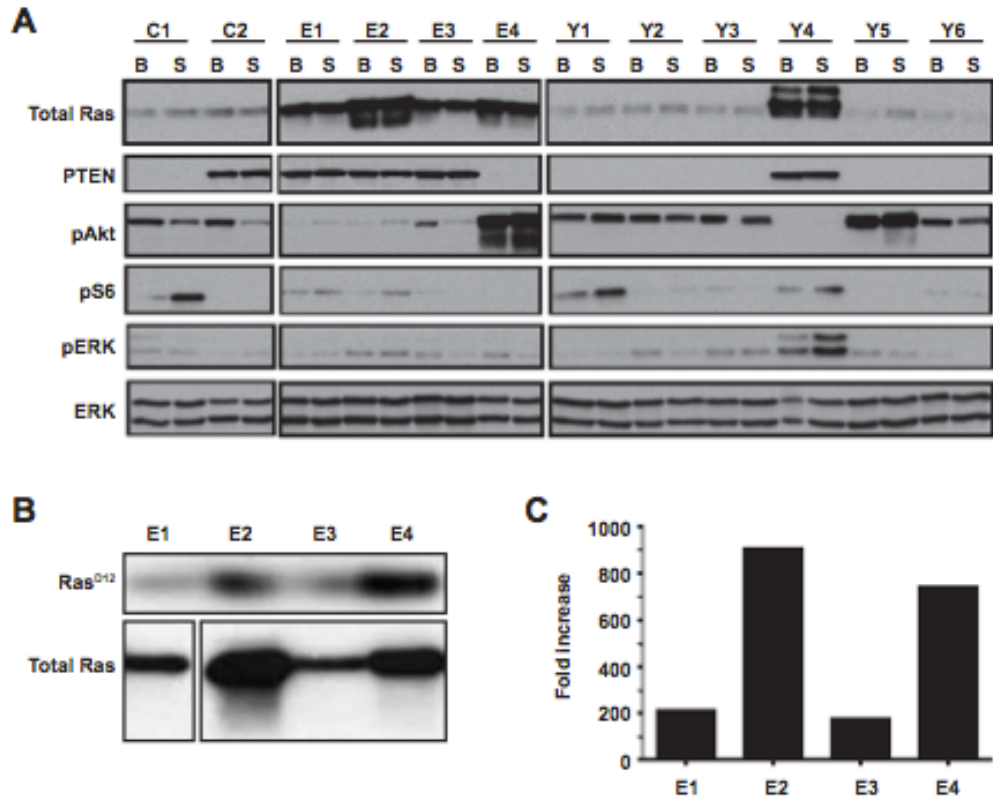


Figure 2 - Leukemias initiated by *Kras*^{D12/G37} and *Kras*^{G12/G64} expression demonstrate distinct signaling profiles. (A) Immunoblot of T-ALL cell lines under basal (B) and starved (S) conditions. Two control T-ALL cell lines with WT *Kras* (C) from a retroviral insertional mutagenesis screen¹¹ were included. Ten cell lines were generated from independent leukemias induced by either *Kras*^{D12/G37} (E1-E4) or *Kras*^{G12/G64} (Y1-Y6). (B) Ras was immunoprecipitated from cell lines E1-E4, then probed with an antibody that recognizes the D12 substitution. (C) Q-PCR analysis of *Kras* expression in T-ALL cell lines compared to WT thymus.

basal growth conditions (Figure 2A). We unexpectedly identified a somatic *Pten* mutation in cell line E4, which also had no detectable PTEN protein or mRNA expression and exhibited markedly elevated levels of pAkt (Figure 2A and Supplemental Figures 2A and 2B). This mutation was also found in the T-ALL that gave rise to the cell line (Supplemental Figure 2A).

By contrast, 5 of 6 K-Ras^{D12/G64} T-ALL cell lines had normal Ras protein levels. PTEN was absent or barely detectable in all 5, and RT-PCR analysis revealed markedly reduced *Pten* mRNA levels, but no *Pten* mutations (Figure 2A, Supplemental Figure 2B, and data not shown). K-Ras^{D12/G64} T-ALL cells without PTEN expression had high basal pAkt levels that persisted during serum and cytokine deprivation (Figure 2A). These data support the idea that T-ALL cells overcome the deleterious effects of the Tyr-64 substitution by down-regulating PTEN expression, thereby activating PI3K signaling.

Acquired “third site” Kras mutations in Kras^{D12/G37} and Kras^{D12/G64} T-ALLs. E1 and E3 had lower levels of Ras expression than E2 and E4 (Figure 2A), and DNA sequencing uncovered the same “third site” *Kras* mutation in both lines that introduced a threonine-to-isoleucine substitution at codon 50 (T50I) (Figures 3A, 3B). Germline T50I *NRAS* mutations cause Noonan syndrome, a developmental disorder characterized by hyperactive Raf/MEK/ERK signaling,²⁹ and ectopic expression of K-Ras^{T50I} increased pERK levels.³⁰ These data suggest that the acquired T50I mutation compensates for defective Raf binding in Kras^{D12/G37}-induced leukemias. Y4 was distinct from the other K-Ras^{D12/G64} lines, exhibiting

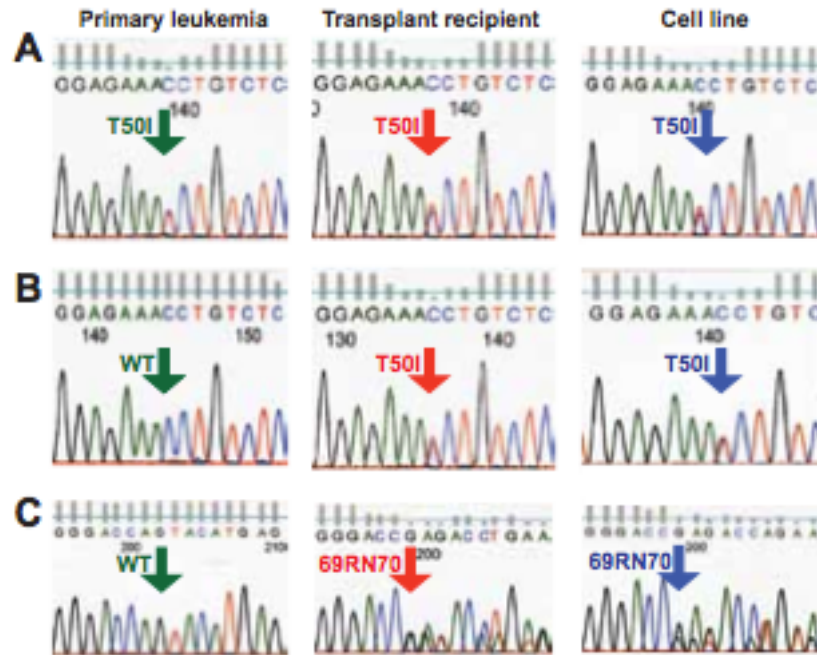


Figure 3 – Somatic “third site” Kras mutations in T-ALL. In cell lines E1 (A) and E3 (B), the single amino acid substitution T50I was present at ~50% frequency based on relative abundance of sequence reads. It was detected at a similar frequency in the spleens of the secondary recipients used to generate these cell lines and in one primary recipient. (C) The sequence GAGACC was inserted between amino acids 69 and 70 of Kras in T-ALL cell line Y4. This mutation is present in ~50% of Kras transcripts in cell line Y4, at lower frequency in the spleen of the secondary recipient used to generate this cell line, and is not seen in the primary leukemia.

elevated Ras levels and persistent PTEN expression (Figure 2A). DNA sequence analysis revealed *Kras* molecules containing the D12 and G64 substitutions along with a *de novo* in frame insertion of an arginine and aspartic acid between codons 69 and 70 (69RN70) of the K-Ras switch II domain (Figure 3C).

To determine when each third site mutation occurred, we analyzed DNA from the recipients of MSCV-infected bone marrow, from secondary recipients, and from cell lines E1, E3, and Y4. Each cell line with a third site mutation also contained viral *Kras* DNA encoding the respective parental second site mutation, suggesting that the third site mutations arose *de novo* (Supplemental Figure 3). Consistent with this idea, PCR-based sequencing of DNA uncovered the T50I mutation in primary T-ALL E1 and in a secondary recipient of T-ALL E3 (Figures 3A, 3B). The 69RN70 third site mutation was not detected in primary T-ALL Y4, but was present in the secondary recipient and further enriched in the cell line (Figure 3C). Together, these data suggest that third site *Kras* mutations are not required to initiate T-ALL, but confer a strong clonal growth advantage.

K-Ras third site mutations restore full oncogenic activity. We assayed CFU-GM colony growth in transduced marrow cells to ask if K-Ras^{D12/G37/I50} and K-Ras^{D12/G64/69RN70} are reactivated compared to the corresponding second site mutant proteins. Remarkably, progenitors expressing either third site mutation fully recapitulated the aberrant K-Ras^{D12} growth phenotype, including cytokine-independent CFU-GM colony formation, pronounced GM-CSF hypersensitivity, and abnormal morphology (Figures 4A, 4B).

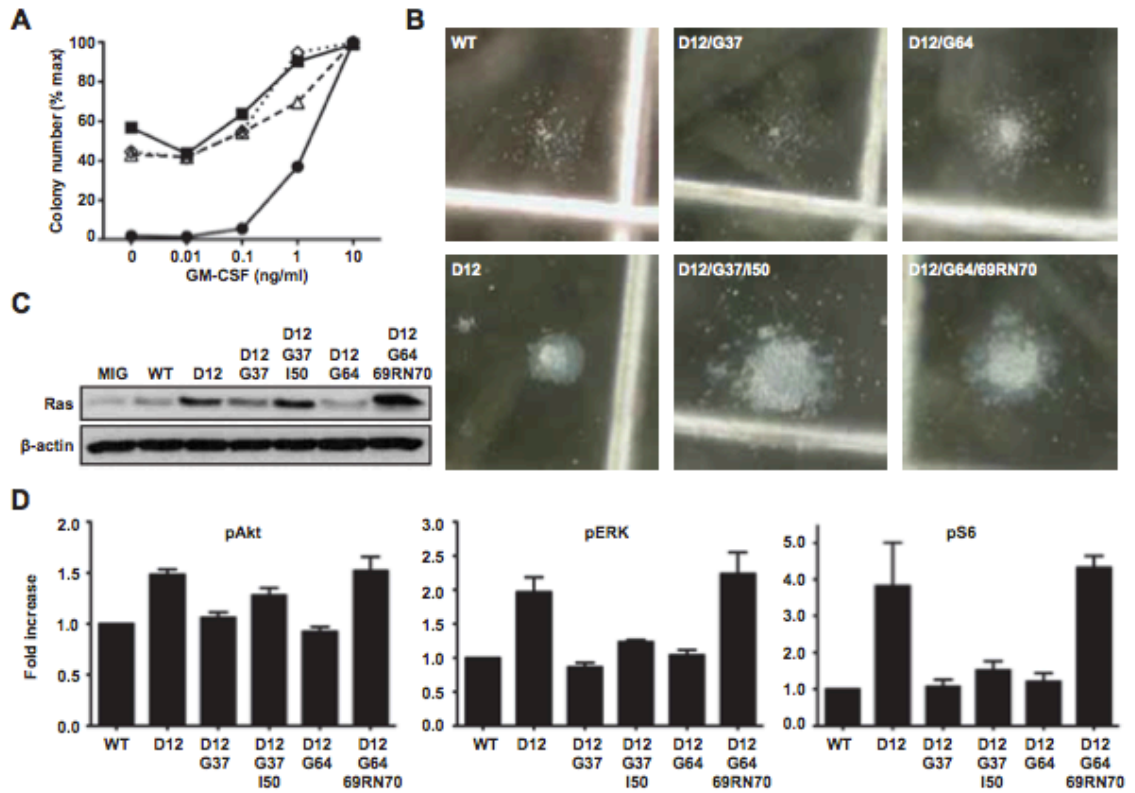


Figure 4 – Acquired "thirdsite" mutations restore oncogenic activity to *Kras*^{D12/G37} and *Kras*^{G12/G64}. (A) CFU-GM formation of fetal liver cells expressing WT *Kras* (closed circle), *Kras*^{D12} (closed square), *Kras*^{D12/G37/150} (open triangle), or *Kras*^{G12/G64/69RN70} (open diamond). Data show the mean of 3 independent experiments. (B) Representative CFU-GM morphology from fetal liver cells expressing *Kras* mutant alleles grown in 0.1 ng/mL GM-CSF. (C) Ras expression in GFP+, Mac1+ fetal liver cells infected with MSCV viruses encoding different *Kras* alleles. (D) Levels of pERK, pAkt, and pS6 in GFP+, Mac1+ fetal liver cells infected with MSCV viruses encoding different *Kras* alleles as determined by flow cytometry using phospho-specific antibodies. Phospho-protein levels in cells expressing WT K-Ras were set at 1 in each experiment. Data shown are derived from 6 independent experiments.

To assess the biochemical consequences of each third site mutation, we expressed K-Ras^{D12/G37/I50} and K-Ras^{D12/G64/69RN70} in mouse fetal hematopoietic cells. Cells expressing oncogenic K-Ras^{D12} or either third site mutant proliferated vigorously and had higher Ras expression than GFP⁺ cells infected with MSCV vectors encoding WT K-Ras or either second site mutant (Figure 4C). K-Ras^{D12/G37/I50} or K-Ras^{D12/G64/69RN70} expression resulted in elevated pERK, pAkt, and pS6 levels compared to cells expressing WT K-Ras or the corresponding second site mutant proteins, which was particularly evident for K-Ras^{D12/G64/69RN70} (Figure 4D and Supplemental Figures 4A and 4B). The modest increase in pERK levels in hematopoietic cells expressing the T50I mutant protein is consistent with data from cell lines E1 and E3 (Figure 2A).

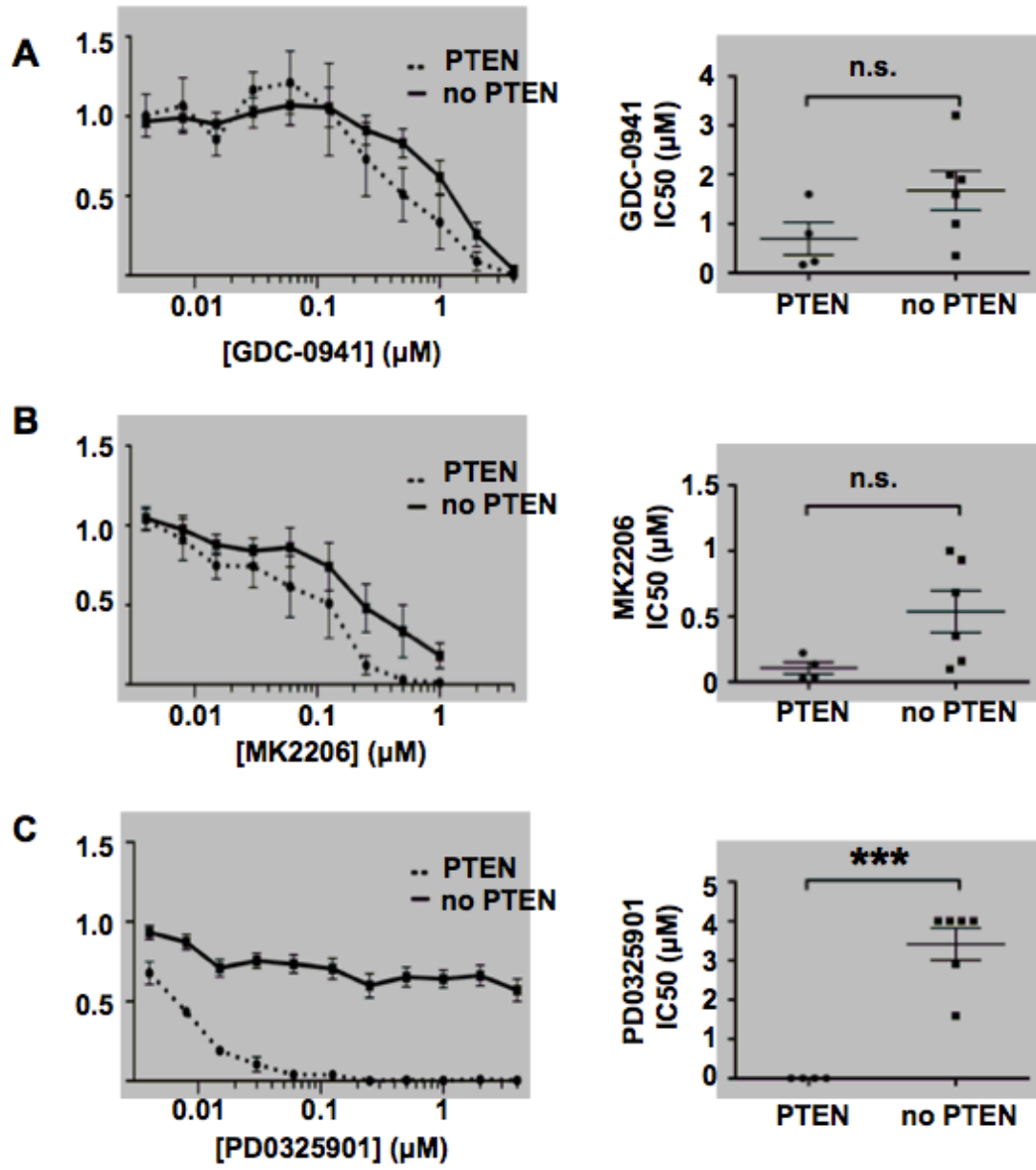
We examined the potential consequences of the T50I substitution and the 69RN70 insertion on predicted Ras-Raf and Ras-PI3K co-crystal structures. While our analysis of T50I suggested potential effects on Ras dimer interactions, with the mutant protein re-orienting the neighboring Ras molecule to enhance binding to Raf-1, we cannot exclude other potential consequences of this substitution (Supplemental Figures 5A and 5B and Supplemental Methods). The 69RN70 insertion is predicted to restore contact with PI3K γ (Supplemental Figure 5C).

Responses of T-ALL cells to chemical inhibitors. We exposed our T-ALL cell lines to inhibitors of PI3K (GDC-0941),³¹ Akt (MK2206),³² or MEK(PD0325901)³³ to ask if

their biochemical characteristics and/or the presence of third site mutations correlated with drug sensitivity. GDC-0941 efficiently reduced pAkt levels in T-ALL cell lines (Supplemental Figure 6A) and blocked their growth (Figure 5A). While the half maximal inhibitory concentration (IC_{50}) was lower for lines that retained PTEN expression, this difference was modest (Figure 5A). Similarly, MK2206 both abrogated Akt phosphorylation and inhibited growth in a dose-dependent manner (Figure 5B and Supplemental Figure 6B). As with GDC-0941, we observed similar IC_{50} values in T-ALL cell lines with and without intact PTEN that were treated with MK2206. Together, these data indicate that T-ALL cells are dependent on PI3K signaling for growth irrespective of basal pathway activation. The somewhat higher IC_{50} values observed in lines lacking PTEN expression likely reflect a requirement for greater drug concentrations to fully suppress pAkt.

We next assessed the effects of blocking Raf/MEK/ERK signaling. Remarkably, loss of PTEN expression and elevated pAkt levels strongly correlated with resistance to PD0325901 despite equivalent target inhibition (Figure 5C and Supplemental Figure 6C). The median IC_{50} values were 0.00625 μ M and $>4\mu$ M in PTEN-positive and PTEN-negative cells, respectively (Figure 5C). Resistance to PD0325901 in PTEN-negative cells appears to occur via abrogation of apoptosis (Figure 5D and supplemental Figure 6D).

T-ALL cell lines with PI3K pathway activation and human early T precursor ALL have similar gene expression profiles. Microarray-based gene expression profiling



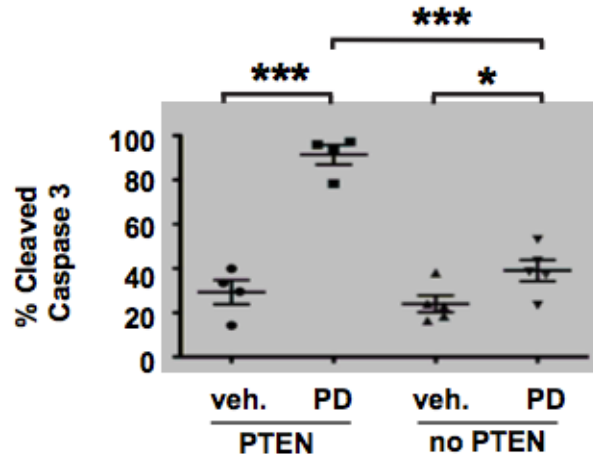
D

Figure 5 - PTEN loss confers resistance to inhibition of MEK but not PI3K or Akt. IC50s and mean growth curves of T-ALL cell lines with and without PTEN expression in varying doses of (A) the PI3K inhibitor GDC-0941, (B) the Akt inhibitor MK-2206 (C) and the MEK inhibitor PD0325901. (D) PD0325901 induces apoptosis in PTEN-positive, but not PTEN-negative cell lines. Curves indicate mean growth of four PTEN positive cell lines (E1, E2, E3 and Y4) and six PTEN negative cell lines (E4, Y1, Y2, Y3, Y5 and Y6) \pm SEM. (***) indicates $p < 0.001$ and (*) indicates $p < 0.05$.

on our T-ALL cell lines revealed one cluster of cell lines without PI3K pathway activation (E1, E2 and Y4) and a second cluster of cell lines with loss of PTEN expression and markedly elevated pAkt levels (Figure 6A). E3, the K-Ras^{D12/G37} line with a modest increase in basal pAkt (Figure 2A), did not clearly segregate with either group (Figure 6A). Gene set enrichment analysis (GSEA) showed that cell lines with PI3K pathway activation demonstrated differential expression of many genes functionally linked to JAK/STAT and Raf/MEK/ERK signaling (Supplemental Tables 3-8). The expression profile of these T-ALL cell lines is highly similar to that of early T precursor (ETP) T-ALL, an aggressive cancer characterized by a high risk of treatment failure and frequent *RAS* mutations (Figures 6B, 6C).^{34,35} This association persisted when the data were reanalyzed to include E4 with either group of T-ALL cell lines (Supplemental Figures 6A, 6B).

Discussion

CFU-GM progenitors expressing second site K-Ras^{D12} mutant proteins that only signal through Raf/MEK/ERK (K-Ras^{D12/E38}) or PI3K/Akt (K-Ras^{D12/C40}) displayed normal growth in methylcellulose cultures over a range of GM-CSF doses (Figure 1A). By contrast, *Kras* oncogenes encoding proteins that retain the ability to engage Ral-GDS, but are defective for either PI3K/Akt (K-Ras^{D12/G64}) or Raf/MEK/ERK (K-Ras^{D12/G37}) pathway activation demonstrated *in vitro and in vivo* transforming activity. The leukemias initiated by these “second site” mutant alleles underwent clonal evolution *in vivo*, characterized by rapid outgrowth of cells with

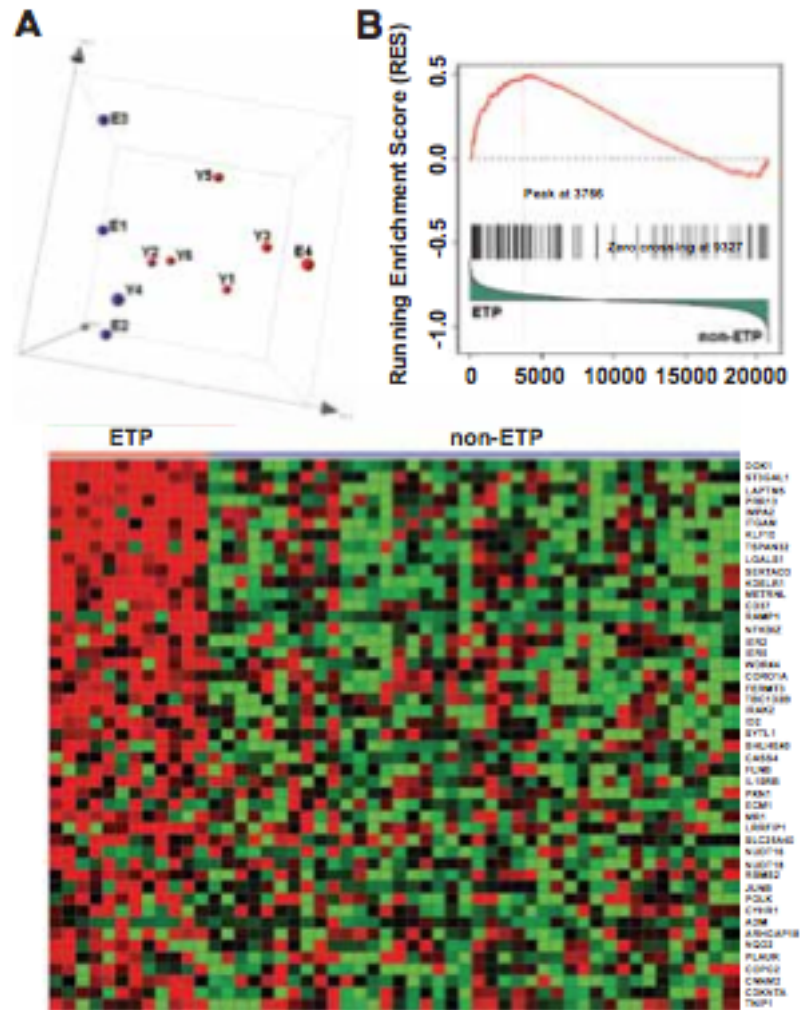


Figure 6 - PI3K activated T-ALL cell lines and human ETP ALLs have similar gene expression profiles. (A) Principal component analysis of the gene expression profiling data of all 10 mouse T-ALL cell lines using 200 representative genes selected by k-means algorithm, showing cases clustered according to PI3K activation status (red=activated, blue=not activated). (B) Gene set enrichment analysis demonstrates significant enrichment of the top 100 mouse PI3K up-regulated genes in ETP ALL ($p=0.057$, $FDR=0.224$). (C) Heatmap of the leading-edge mouse PI3K up-regulated genes in GSEA analysis, showing over-expression of these genes in ETP ALL.

secondary mutations that overcome impaired signaling properties. While the use of a retroviral transduction/transplantation system likely facilitated transformation in our studies, Ras protein levels were not elevated in most K-Ras^{D12/G64} cell lines (Figure 2A). The absence of hematologic cancers in mice transplanted with cells over-expressing WT Kras from the same MSCV vector further demonstrates that K-Ras^{D12/G37} and K-Ras^{D12/G64} have “gain of function” oncogenic activity.

Endogenous *Kras*^{D12} expression causes both T-ALL and myeloid leukemia in mice, which is influenced by a number of factors.^{26,28,36-39} Use of the *Mx1-Cre* transgene to express a latent *Kras*^{D12} oncogene causes an aggressive myeloproliferative neoplasm (MPN),^{36,39} but transferring bone marrow from *Mx1-Cre; Kras*^{D12} mice into irradiated recipients induces T-ALL,^{26,28,38} and *NRAS*, *KRAS*, and other genes commonly mutated in myeloid malignancies are also mutated in ETP T-ALL.³⁵ While the signaling profiles of these aggressive cancers and their susceptibility to targeted therapies have not been reported, our data linking gene expression in ETP-ALL to aberrant PI3K signaling and the observation that T-ALL cell lines with *Kras* mutations are sensitive to PI3K inhibition¹² supports developing clinical trials in which PI3K pathway inhibitors are administered with conventional anti-leukemia therapy. The paradigm of combining targeted and conventional agents has recently been applied successfully to BCR-ABL-positive ALL.⁴⁰

PI3K binds to and is activated by Ras-GTP;^{6,19,41} however, the precise role of PI3K signaling in *Ras*-induced cancer initiation and maintenance is uncertain. An elegant study by Gutpa et al²³ demonstrating dramatic inhibition of *Kras*^{D12}-induced

lung cancer in mice expressing a “knock in” PI3K p110 α protein that is defective for Ras binding supports an essential role of PI3K activation in tumorigenesis.⁴² On the other hand, PI3K/Akt-mediated growth and survival of colon cancer cell lines appears to be dependent on receptor tyrosine kinase (RTK) signaling, but independent of oncogenic *KRAS*.⁴³ Genetic analysis of T-ALL specimens implicated Ras/PI3K pathway mutations as important “drivers” of leukemic growth.⁹ Consistent with this idea, T-ALLs initiated by *Kras* oncogenes with second site mutations frequently silenced PTEN and activated Akt, demonstrating strong selective pressure for leukemia cells to acquire aberrant PI3K/Akt signaling *in vivo*.

The role of aberrant Raf/MEK/ERK signaling in T-ALL is less clear. The identification of somatic “third site” T50I mutations that enhance signaling and fully transform progenitor growth supports the idea that the Raf/MEK/ERK cascade contributes to leukemogenesis. Indeed, T-ALL cell lines that retained PTEN expression were susceptible to the MEK inhibitor PD0325901. However, our studies suggest that PI3K pathway activation confers resistance by providing a survival signal in T-ALL cells that overcomes the pro-apoptotic effects of MEK inhibition. This observation is supported by *in vivo* data showing that administering a MEK inhibitor to *Mx1-Cre; Kras^{D12}* mice abrogated signs of MPN, but that some animals nevertheless progressed to T-ALL during treatment.⁴⁴

The discoveries of *Pten* inactivation in a K-Ras^{D12/G37} T-ALL and a 69RN70 insertion with elevated pERK levels in a K-Ras^{D12/G64} leukemia indicate unexpected plasticity in the spectrum of secondary mutations, and suggest that enhanced signaling through an already-activated pathway can compensate for impaired

binding to another effector. This idea is consistent with recent studies of resistance to MEK inhibitors showing that the underlying mechanisms include amplification of *KRAS* and *BRAF* oncogenes⁴⁵ and over-expression of RasGRP guanine nucleotide exchange factors.⁴⁶

Although the Ras GTPase switch is widely viewed as “undruggable”,⁴⁷ the development of chemical inhibitors of other Ras domains is an emerging area of investigation.⁴ As strategies for targeting oncogenic Ras are tested in advanced cancers, acquired resistance is inevitable. Indeed, our data demonstrate that *Kras*^{D12} can evolve rapidly *in vivo* by acquiring novel secondary mutations, suggesting that “on target” mutations leading to drug resistance will emerge in patients who are treated with inhibitors of oncogenic Ras. Indeed, the recent identification of insertions similar to the 69RN70 alteration in human lung and colorectal cancers^{48,49} underscores the relevance of this potential mechanism in facilitating malignant growth.

Methods

***Kras* expression constructs**

Wild-type (WT) *Kras* mouse cDNA was cloned into the pENTR/D-TOPO vector (Invitrogen). We used a QuikChange site-directed mutagenesis kit (Stratagene) to introduce point mutations, and Gateway technology (Invitrogen) to clone *Kras* cDNAs into the pDEST12.2 vector (Invitrogen) and into a murine stem cell virus (MSCV) vector containing a green fluorescent protein (GFP) cassette driven by an internal ribosome entry site (IRES) downstream of the *Kras* sequence (MIG; MSCV-

IRES-GFP). For some *in vitro* experiments, we used MSCV vectors in which GFP was fused to the NH₂ end of *Kras* (MSCV-GFP-*Kras*).¹⁰

Retroviral transduction and progenitor colony assays

The UCSF Committee on Animal Research approved procedures involving mice. E14.5 C57Bl/6 fetal livers were isolated as described.^{1,5,11} MIG plasmids were co-transfected with packaging plasmids into 293T cells using Lipofectamine2000 (Invitrogen) and viral 3T3 fibroblasts and fetal liver cells transduced with supernatant. GFP-positive (GFP⁺) fetal liver cells were isolated on a FACSAria (BD Biosciences) and seeded in methylcellulose (M3231, StemCell Technologies) containing recombinant mouse granulocyte macrophage colony stimulating factor (GM-CSF). Colony forming unit granulocyte macrophage (CFU-GM) colonies were counted by indirect microscopy after eight days. All cytokines were from Peprotech unless otherwise noted.

Studies in COS-7 and S49 cells

COS-7 cells were transfected with pDEST12.2 plasmids. After 24h, medium was changed to IMDM (UCSF Core; starve) or IMDM + 20% fetal bovine serum (FBS, Hyclone; basal). Cells were harvested 24h later (starve) or after exposure to 50 ng/mL of epidermal growth factor for 5 min (stimulated). Unstarved cells were harvested in parallel (basal). S49 cells were transduced with MIG plasmids and sorted as above. GFP⁺ cells were starved for 2h in DMEM-H21 (UCSF Core) prior to

harvest. Immunoblotting was performed as previously described.^{6-8,12} All immunoblot antibodies were from Cell Signaling except total Akt (Biosource).

Transduction/transplantation procedure

WT Balb/c mice were injected with 150mg/kg of 5-fluorouracil 4 days before euthanasia. Bone marrow cells were collected into IMDM + 20% FBS, cultured in StemSpan SFEM (Stem Cell) with 15% FBS, 100 ng/mL IL-11 (R&D Technologies), 100 ng/mL SCF, 50 ng/mL Flt3, 50 ng/mL IL-6 and 10 ng/mL IL-3, transduced with retroviral supernatant after 24-72h and transplanted 24h later. Male WT Balb/c mice were lethally irradiated with a single 850 cGy dose and retro-orbitally injected with transduced cells 2-3h later. Secondary recipients of established leukemias received a single 500 cGy dose. Blood cells were counted by Hemavet (Drew Scientific) and smears stained with Wright Giemsa (Sigma-Aldrich). The UCSF Mouse Pathology Core analyzed organs. For fluorescence activated cell sorting (FACS) analysis, cells were resuspended after red cell lysis in HBSS+3%FBS and Fc block, then stained with antibodies against myeloid/erythroid (PE-Cy7-Mac1, PacBlue-Gr1, PE-CD71 and APC-Ter119), T-cell (PE-Cy7-CD3, PE-CD8, and APC-CD4) B-cell (PE-Cy7-B220, PacBlue-CD19) and stem cell (PE-Sca1, APC-ckit) markers (BD Biosciences). Data were acquired with LSRII (BD Biosciences) using FACSDiva software and analyzed with FlowJo (Tree Star).

DNA purification and Southern blotting

Hematopoietic tissues were lysed with 100 mM Tris-HCl pH 8.5, 5 mM EDTA pH 8.0,

200 mM NaCl, and 0.2% SDS. Genomic DNA was digested with EcoRI then hybridized with a sequence-verified GFP probe as previously described.¹²

T-ALL cell lines

Single-cell suspensions from bone marrow, thymus, or spleen of sick mice were used to generate T-ALL cell lines as previously described.¹² After serial passage, cells were harvested from basal culture conditions or after 24h starvation in DMEM-H21 and lysed (50mM Tris-HCL pH 8.0, 150mM NaCl, 5mM MgCl, 1% Triton X-100, 0.5% sodium deoxycholate, 0.1% SDS). Ras was immunoprecipitated with H-Ras (sc-259) and probed with pan-*Ras*^{Asp-12} (both Santa Cruz Biotechnology) to detect mutant Ras. Ras-GTP was immunoprecipitated with Raf1-RBD agarose conjugate beads (Millipore). Total Ras (Millipore) was measured prior to immunoprecipitation.

Biochemical analysis of fetal liver cells

E14.5 fetal liver cells transduced as above were resuspended in HBSS+3%FBS and Fc block, then stained with Pac Blue-Mac1. Sorted GFP+, Mac1+ cells were immunoblotted with anti-Ras. For phospho-flow analysis, unsorted cells were resuspended in starve (IMDM+1%BSA) or basal (IMDM+20%FBS) media, then incubated for 2h at 37°C. Fixed and permeabilized cells were incubated with Fc Block, then stained with Pac Blue-Mac1 and either Alexa 647-pAkt (Thr308), anti-pERK plus PE secondary (Jackson Immune Research), or anti-pS6 plus PE. FACS data were collected as above.

Proliferation and Apoptosis Assays

T-ALL cell lines were plated at a density of 30,000/100 μ L in 96 well plates. Drug was added in varying concentrations in triplicate. After 48 hours, 20 μ L CellTiter 96[®] AQueous Non-Radioactive Cell Proliferation Assay (Promega, USA) was added and the plates were incubated for 4 hours. Plates were read according to the manufacturer's instructions. Growth curves were established as percentages of maximal growth in DMSO and IC₅₀ values were calculated. For apoptosis assays, 50,000 cells were plated in 1 μ M PD0325901. After 48 hours, the cells were collected, fixed with PFA, and stained with an antibody against cleaved Caspase-3 (BD). FACS data were acquired as above.

Expression profiling

Gene expression data was generated with GeneChip Mouse Genome 430 2.0 arrays (Affymetrix) with signals normalized to the trimmed average of 500 in MAS 5.0 algorithm. Probe sets with absent calls for all samples were excluded, and probe set signals were variance stabilized by adding 32 and log₂ transformation. Statistical analyses were performed using R 2.11.0 (<http://r-project.org>), Bioconductor 2.6¹³ and Spotfire Decision Site 9.1.1 (Tibco). Supervised analysis to detect differentially expressed genes between PI3K activated and non-activated groups was performed using *limma*¹⁴ with estimation of false discovery rate.¹⁵ Genes with an FDR below 20% were considered significantly differentially expressed and used to assess pathway enrichment in Database for Annotation, Visualization and Integrated Discovery (DAVID) v6.7.^{16,17} Gene expression profiling of 52 T- ALL samples was

performed with Affymetrix GeneChip HT HG-U133+ PM arrays, with signals normalized by RMA algorithm. The correlation between mouse PI3K activation and ETP ALL expression was examined with Gene Set Enrichment Analysis (GSEA)¹⁸ on human ETP against non-ETP using the repository of gene sets available at MSigDB v3.0 and the top 100 up-regulated mouse genes in PI3K activation.

Statistical analysis

Statistics were analyzed with Prism 4 (GraphPad). Kaplan-Meier survival curves were compared by log rank test with a two-tailed P value. % maximum growth = (mean colonies in 3 replicate plates)/(mean colonies in plates with no GM-CSF) x 100. Two-tailed t-tests were used to compare all other data sets.

Accession codes

Gene Expression Omnibus (GEO; <http://www.ncbi.nlm.nih.gov/geo/>): GSE28687 and GSE2870

References

1. Schubbert S, Bollag G, Lyubynska N, et al. Biochemical and functional characterization of germ line KRAS mutations. *Mol Cell Biol.* 2007;27(22):7765–7770.
2. Vetter IR, Wittinghofer A. The guanine nucleotide-binding switch in three dimensions. *Science.* 2001;294(5545):1299–1304.
3. Donovan S, Shannon KM, Bollag G. GTPase activating proteins: critical regulators of intracellular signaling. *Biochim Biophys Acta.* 2002;1602(1):23–

- 45.
4. Maurer T, Garrenton LS, Oh A, et al. Small-molecule ligands bind to a distinct pocket in Ras and inhibit SOS-mediated nucleotide exchange activity. *Proc Natl Acad Sci USA*. 2012;109(14):5299–5304.
 5. Downward J. Targeting RAS signalling pathways in cancer therapy. *Nat Rev Cancer*. 2003;3(1):11–22.
 6. Rodriguez-Viciana P, Warne PH, Khwaja A, et al. Role of phosphoinositide 3-OH kinase in cell transformation and control of the actin cytoskeleton by Ras. *Cell*. 1997;89(3):457–467.
 7. White MA, Nicolette C, Minden A, et al. Multiple Ras functions can contribute to mammalian cell transformation. *Cell*. 1995;80(4):533–541.
 8. Lim K-H, Counter CM. Reduction in the requirement of oncogenic Ras signaling to activation of PI3K/AKT pathway during tumor maintenance. *Cancer Cell*. 2005;8(5):381–392.
 9. Ward AF, Braun BS, Shannon KM. Targeting oncogenic Ras signaling in hematologic malignancies. *Blood*. 2012;120: 3397-40.
 10. Xu J, Hedberg C, Dekker FJ, et al. Inhibiting the palmitoylation/depalmitoylation cycle selectively reduces the growth of hematopoietic cells expressing oncogenic Nras. *Blood*. 2012;119(4):1032–1035.
 11. Schubbert S, Zenker M, Rowe SL, et al. Germline KRAS mutations cause Noonan syndrome. *Nat Genet*. 2006;38(3):331–336.
 12. Dail M, Li Q, McDaniel A, et al. Mutant Ikzf1, KrasG12D, and Notch1 cooperate

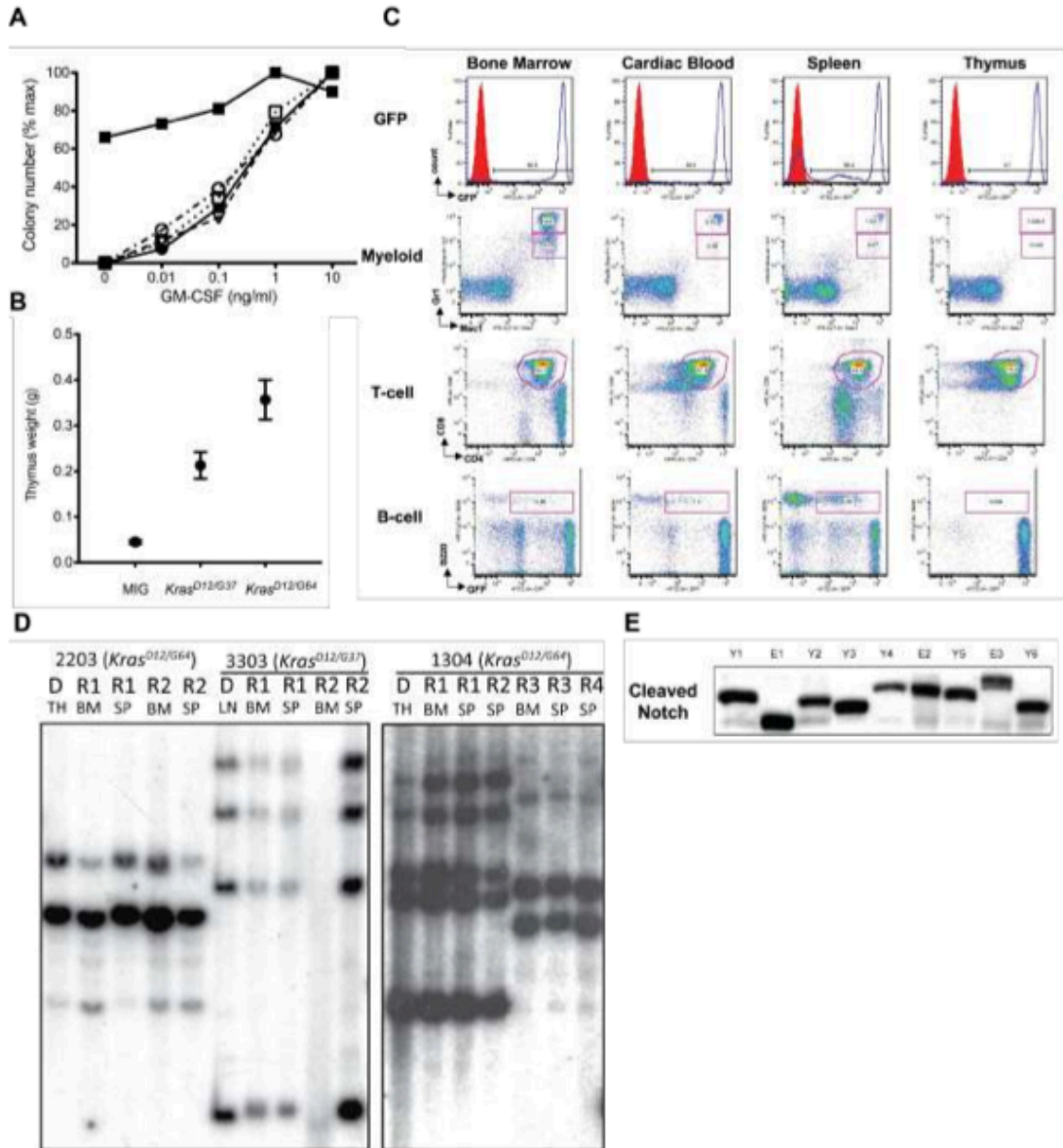
- in T lineage leukemogenesis and modulate responses to targeted agents. *Proc Natl Acad Sci USA*. 2010;107(11):5106–5111.
13. Gentleman RC, Carey VJ, Bates DM, et al. Bioconductor: open software development for computational biology and bioinformatics. *Genome Biol*. 2004;5(10):R80.
 14. Smyth GK. Linear models and empirical bayes methods for assessing differential expression in microarray experiments. *Stat Appl Genet Mol Biol*. 2004;3:Article3.
 15. Benjamini Y, Hochberg Y. Controlling the false discovery rate: a practical and powerful approach to multiple testing. *J R Stat Soc Series B*. 1995;57:289–300.
 16. Huang DW, Sherman BT, Lempicki RA. Systematic and integrative analysis of large gene lists using DAVID bioinformatics resources. *Nat Prot*. 2009;4(1):44–57.
 17. Huang DW, Sherman BT, Lempicki RA. Bioinformatics enrichment tools: paths toward the comprehensive functional analysis of large gene lists. *Nucleic Acids Res*. 2009;37(1):p.1–13.
 18. Subramanian A, Tamayo P, Mootha VK, et al. Gene set enrichment analysis: a knowledge-based approach for interpreting genome-wide expression profiles. *Proc Natl Acad Sci USA*. 2005;102(43):15545–15550.
 19. Pacold ME, Suire S, Perisic O, et al. Crystal structure and functional analysis of Ras binding to its effector phosphoinositide 3-kinase gamma. *Cell*. 2000;103(6):931–943.
 20. Nassar N, Horn G, Herrmann C, et al. The 2.2 Å crystal structure of the Ras-

- binding domain of the serine/threonine kinase c-Raf1 in complex with Rap1A and a GTP analogue. *Nature*. 1995;375(6532):554–560.
21. Vanhaesebroeck B, Leever SJ, Ahmadi K, et al. Synthesis and function of 3-phosphorylated inositol lipids. *Annu. Rev. Biochem.* 2001;70:535–602.
 22. Moodie SA, Paris M, Villafranca E, et al. Different structural requirements within the switch II region of the Ras protein for interactions with specific downstream targets. *Oncogene*. 1995;11(3):447–454.
 23. Gupta S, Ramjaun AR, Haiko P, et al. Binding of ras to phosphoinositide 3-kinase p110alpha is required for ras-driven tumorigenesis in mice. *Cell*. 2007;129(5):957–968.
 24. Harris AW. Differentiated functions expressed by cultured mouse lymphoma cells. I. Specificity and kinetics of cell responses to corticosteroids. *Exp Cell Res*. 1970;60(3):341–353.
 25. Yeh H-H, Wu C-H, Giri R, et al. Oncogenic Ras-induced morphologic change is through MEK/ERK signaling pathway to downregulate Stat3 at a posttranslational level in NIH3T3 cells. *Neoplasia*. 2008;10(1):52–60.
 26. Sabnis AJ, Cheung LS, Dail M, et al. Oncogenic Kras initiates leukemia in hematopoietic stem cells. *PLoS Biol*. 2009;7(3):e59.
 27. Weng AP, Ferrando AA, Lee W, et al. Activating mutations of NOTCH1 in human T cell acute lymphoblastic leukemia. *Science*. 2004;306(5694):269–271.
 28. Kindler T, Cornejo MG, Scholl C, et al. K-RasG12D-induced T-cell lymphoblastic lymphoma/leukemias harbor Notch1 mutations and are

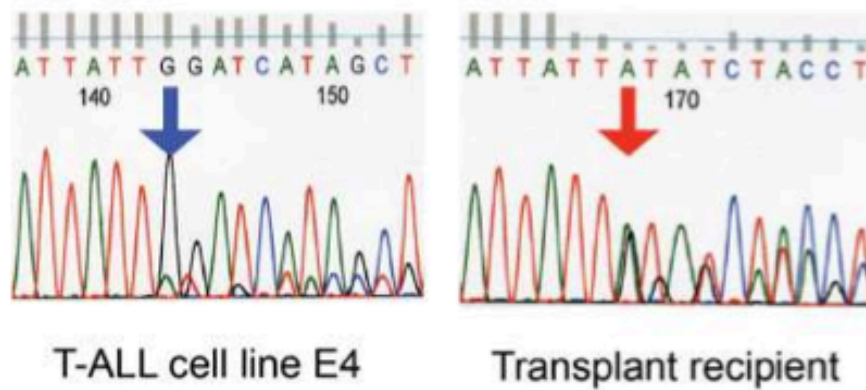
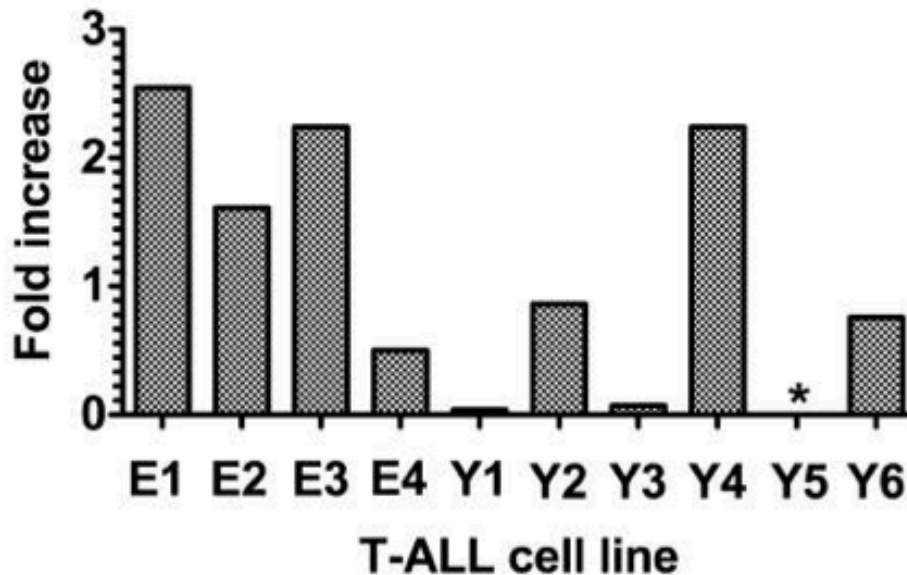
- sensitive to gamma-secretase inhibitors. *Blood*. 2008;112(8):3373–3382.
29. Schubbert S, Shannon K, Bollag G. Hyperactive Ras in developmental disorders and cancer. *Nat Rev Cancer*. 2007;7(4):295–308.
 30. Cirstea IC, Kutsche K, Dvorsky R, et al. A restricted spectrum of NRAS mutations causes Noonan syndrome. *Nat Genet*. 2010;42(1):27–29.
 31. Folkes AJ, Ahmadi K, Alderton WK, et al. The identification of 2-(1H-indazol-4-yl)-6-(4-methanesulfonyl-piperazin-1-ylmethyl)-4-morpholin-4-yl-thieno[3,2-d]pyrimidine (GDC-0941) as a potent, selective, orally bioavailable inhibitor of class I PI3 kinase for the treatment of cancer. *J Med Chem*. 2008;51(18):5522–5532.
 32. Cheng Y, Zhang Y, Zhang L, Ren X, Huber-Keener KJ, Liu X, Zhou L, Liao J, Keihack H, Yan L, Rubin E, Yang JM. MK-2206: MK-2206, a novel allosteric inhibitor of Akt, synergizes with gefitinib against malignant glioma via modulating both autophagy and apoptosis. *Mol Cancer Ther*. 2012 Jan;11(1):154-64.
 33. Barrett SD, Bridges AJ, Dudley DT, et al. The discovery of the benzhydroxamate MEK inhibitors CI-1040 and PD 0325901. *Bioorg Med Chem Lett*. 2008;18(24):6501–6504.
 34. Coustan-Smith E, Mullighan CG, Onciu M, et al. Early T-cell precursor leukaemia: a subtype of very high-risk acute lymphoblastic leukaemia. *Lancet Oncol*. 2009;10(2):147–156.
 35. Zhang J, Ding L, Holmfeldt L, et al. The genetic basis of early T-cell precursor acute lymphoblastic leukaemia. *Nature*. 2012;481(7380):157–163.

36. Braun BS, Tuveson DA, Kong N, et al. Somatic activation of oncogenic Kras in hematopoietic cells initiates a rapidly fatal myeloproliferative disorder. *Proc Natl Acad Sci USA*. 2004;101(2):597–602.
37. Johnson L, Mercer K, Greenbaum D, et al. Somatic activation of the K-ras oncogene causes early onset lung cancer in mice. *Nature*. 2001;410(6832):1111–1116.
38. Zhang J, Wang J, Liu Y, et al. Oncogenic Kras-induced leukemogenesis: hematopoietic stem cells as the initial target and lineage-specific progenitors as the potential targets for final leukemic transformation. *Blood*. 2009;113(6):1304–1314.
39. Chan IT, Kutok JL, Williams IR, et al. Conditional expression of oncogenic K-ras from its endogenous promoter induces a myeloproliferative disease. *J Clin Invest*. 2004;113(4):528–538.
40. Fielding AK. How I treat Philadelphia chromosome-positive acute lymphoblastic leukemia. *Blood*. 2010;116(18):3409–3417.
41. Rodriguez-Viciana P, Warne PH, Dhand R, et al. Phosphatidylinositol-3-OH kinase as a direct target of Ras. *Nature*. 1994;370(6490):527–532.
42. Engelman JA, Chen L, Tan X, et al. Effective use of PI3K and MEK inhibitors to treat mutant Kras G12D and PIK3CA H1047R murine lung cancers. *Nat Med*. 2008;14(12):1351–1356.
43. Ebi H, Corcoran RB, Singh A, et al. Receptor tyrosine kinases exert dominant control over PI3K signaling in human KRAS mutant colorectal cancers. *J Clin Invest*. 2011;121(11):4311–4321.

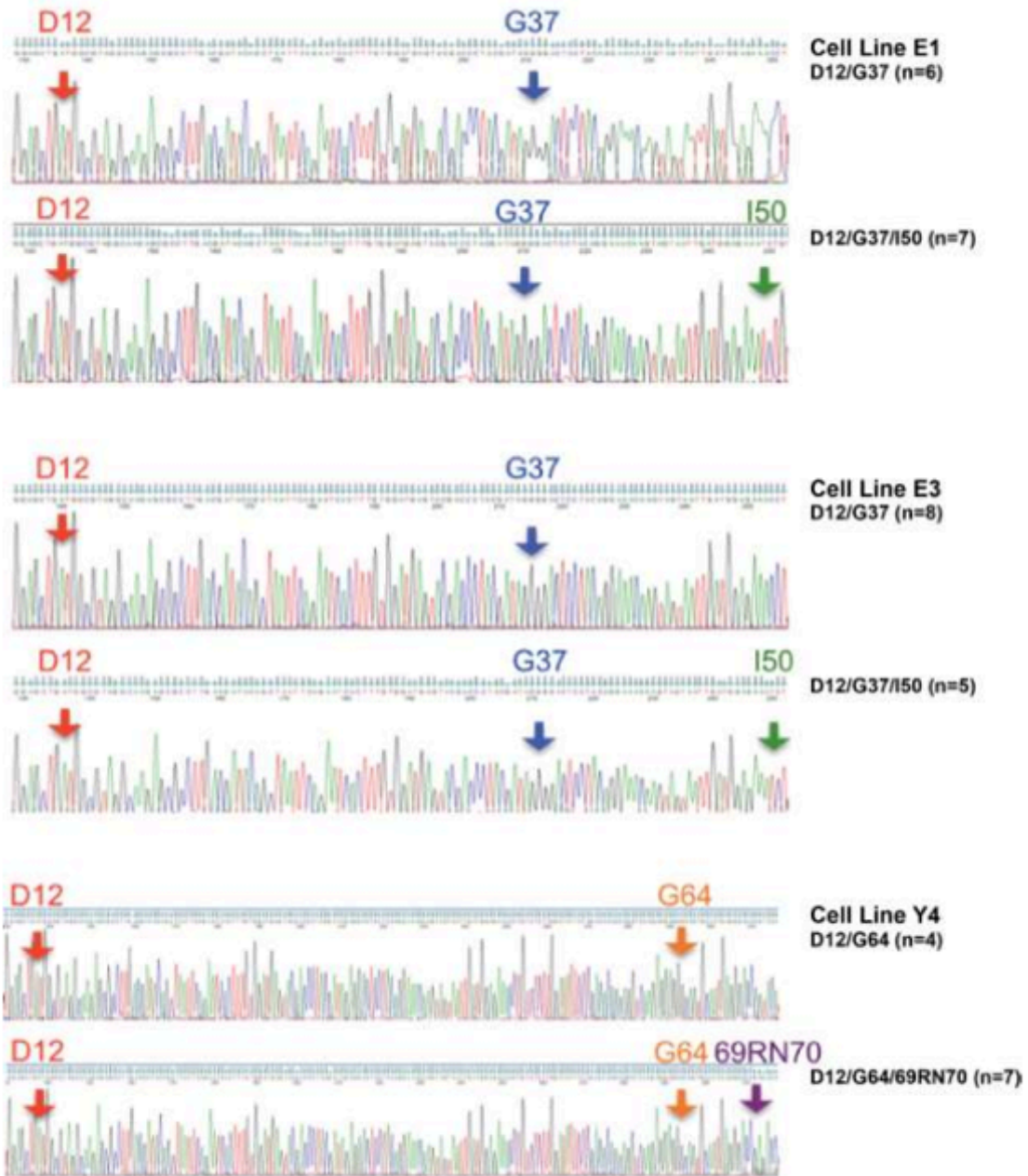
44. Lyubynska N, Gorman MF, Lauchle JO, et al. A MEK inhibitor abrogates myeloproliferative disease in Kras mutant mice. *Sci Transl Med*. 2011;3(76):76ra27.
45. Little AS, Balmano K, Sale MJ, et al. Amplification of the driving oncogene, KRAS or BRAF, underpins acquired resistance to MEK1/2 inhibitors in colorectal cancer cells. *Sci Signal*. 2011;4(166):ra17.
46. Lauchle JO, Kim D, Le DT, et al. Response and resistance to MEK inhibition in leukaemias initiated by hyperactive Ras. *Nature*. 2009;461(7262):411–414.
47. Gysin S, Salt M, Young A, McCormick F. Therapeutic strategies for targeting ras proteins. *Genes & Cancer*. 2011;2(3):359–372.
48. Schmid K, Oehl N, Wrba F, et al. EGFR/KRAS/BRAF mutations in primary lung adenocarcinomas and corresponding locoregional lymph node metastases. *Clin Cancer Res*. 2009;15(14):4554–4560.
49. Wójcik P, Kulig J, Okoń K, et al. KRAS mutation profile in colorectal carcinoma and novel mutation—internal tandem duplication in KRAS. *Pol J Pathol*. 2008;59(2):93–96.



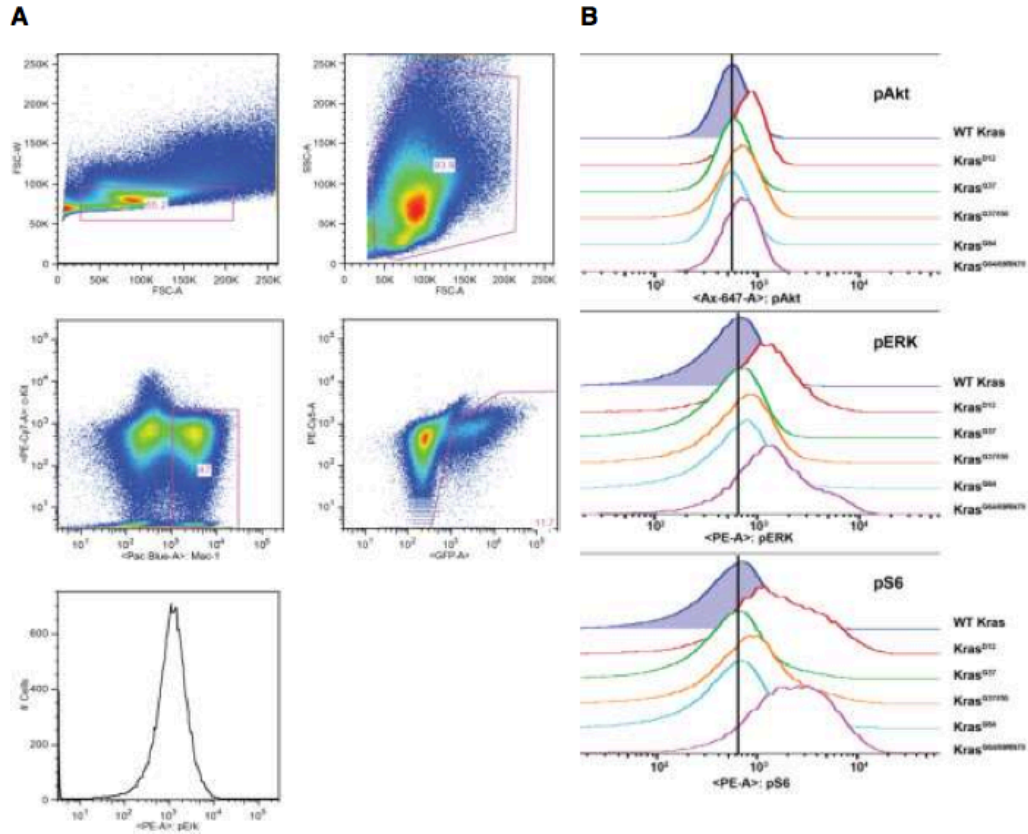
Supplemental Figure 1 - Second site *Kras*^{D12} mutant alleles induce hypersensitive myeloid progenitor growth and initiate T-ALL. (A) CFU-GM colony formation of fetal liver cells expressing WT *Kras* (closed circle), *Kras*^{D12} (closed square), *Kras*^{D12/S35} (open circle), *Kras*^{D12/E38} (open triangle), and *Kras*^{D12/C40} (open square) over a range of GM-CSF concentrations. Representative data from 1 of 2 independent experiments are shown. (B) Thymic weight at time of death of mice that were transplanted with bone marrow cells infected with a control MSCV vector (MIG) or with viruses containing *Kras*^{D12/E37} or *Kras*^{D12/G64}. The data are plotted as mean +/- SEM. (C) Analysis of leukemia cells in hematopoietic tissues of a representative primary recipient with T-ALL. Tissues were homogenized and then labeled with surface marker antibodies to distinguish between the myeloid (Mac1, Gr1+), T-cell (CD4, CD8+), and B-cell (B220+) lineages. Leukemia cells are Mac1-, Gr1-, B220-, CD4+, CD8+, GFP+ and make up the dominant population in bone marrow, cardiac blood, spleen, and thymus. (D) Mouse 2203 (D=donor) was lethally irradiated and transplanted with bone marrow cells expressing *Kras*^{D12/G64}. When the mouse developed leukemia, thymocytes were harvested and injected into the tail vein of irradiated secondary recipients (R), which also developed T-ALL. Southern blot analysis of tissues from these mice (TH=thymus, BM=bone marrow, SP=spleen, LN=lymph node) using an alpha-dCTP radiolabeled 0.7kb-GFP probe reveals clonal retroviral integrations maintained from primary to secondary recipients. A similar finding was seen in mouse 3303 (D), which was transplanted with bone marrow cells expressing *Kras*^{D12/E37}. Cells obtained from the lymph node of this animal caused leukemia in secondary recipients. Interestingly, in mouse 1304 (D), transplanting malignant thymocytes into four secondary recipients yielded two distinct clones. (E) Activated Notch1 was detected in T-ALL cell lines by Western blot using an antibody that detects cleaved Notch1. Y1-6 leukemias express *Kras*^{D12/G64} while E1-3 leukemias express *Kras*^{D12/E37}. Bands ranged in size from 75-110 kDa.

A**B**

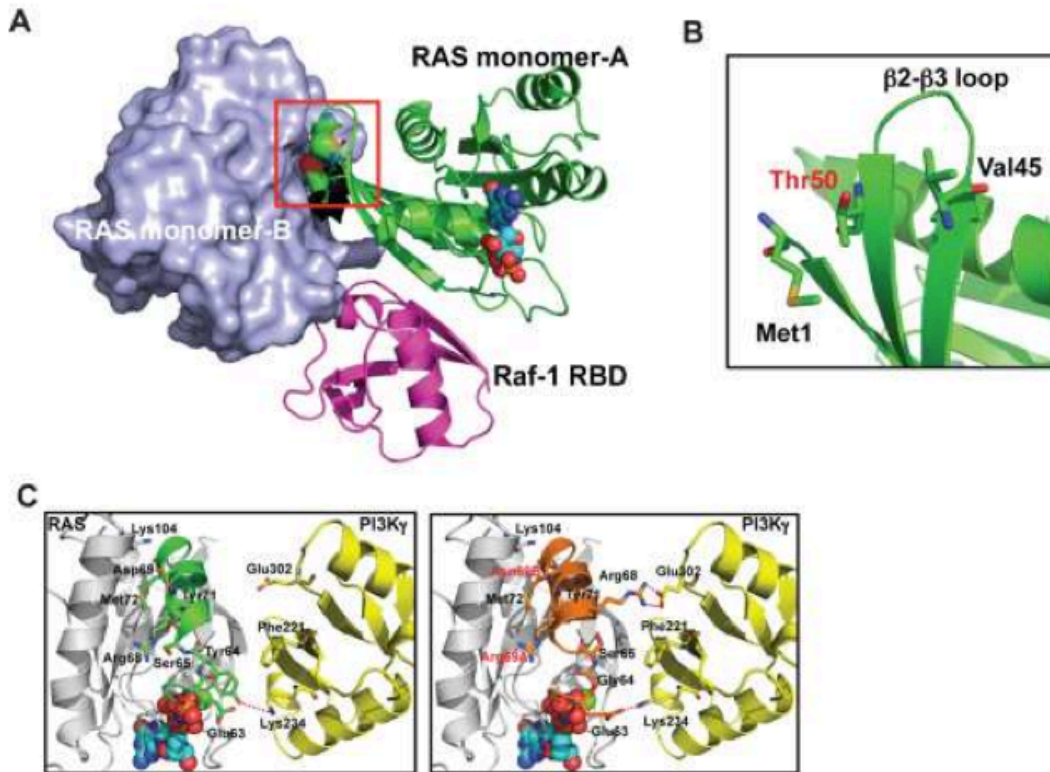
Supplemental Figure 2 - Some leukemias initiated by *Kras*^{D12/E37} and *Kras*^{D12/G64} expression have reduced PTEN expression. (A) The GGATC was inserted into exon 6 of *Pten* in the T- ALL cell line E4 (blue arrow). Based on relative abundance of sequence reads, this mutation is present at high frequency in the cell line and at moderate frequency in the spleen cells of the transplant recipient that were used to generate this cell line (red arrow). (B) Expression of *Pten* was assessed by quantitative RT-PCR in cell lines generated from leukemias expressing *Kras*^{D12/E37} (E) or *Kras*^{D12/G64} (Y), and correlated with *PTEN* protein expression (see Figure 2). Fold-increase is compared to WT thymus and normalized to *GAPDH* expression. Asterisk (*) indicates undetectable levels.



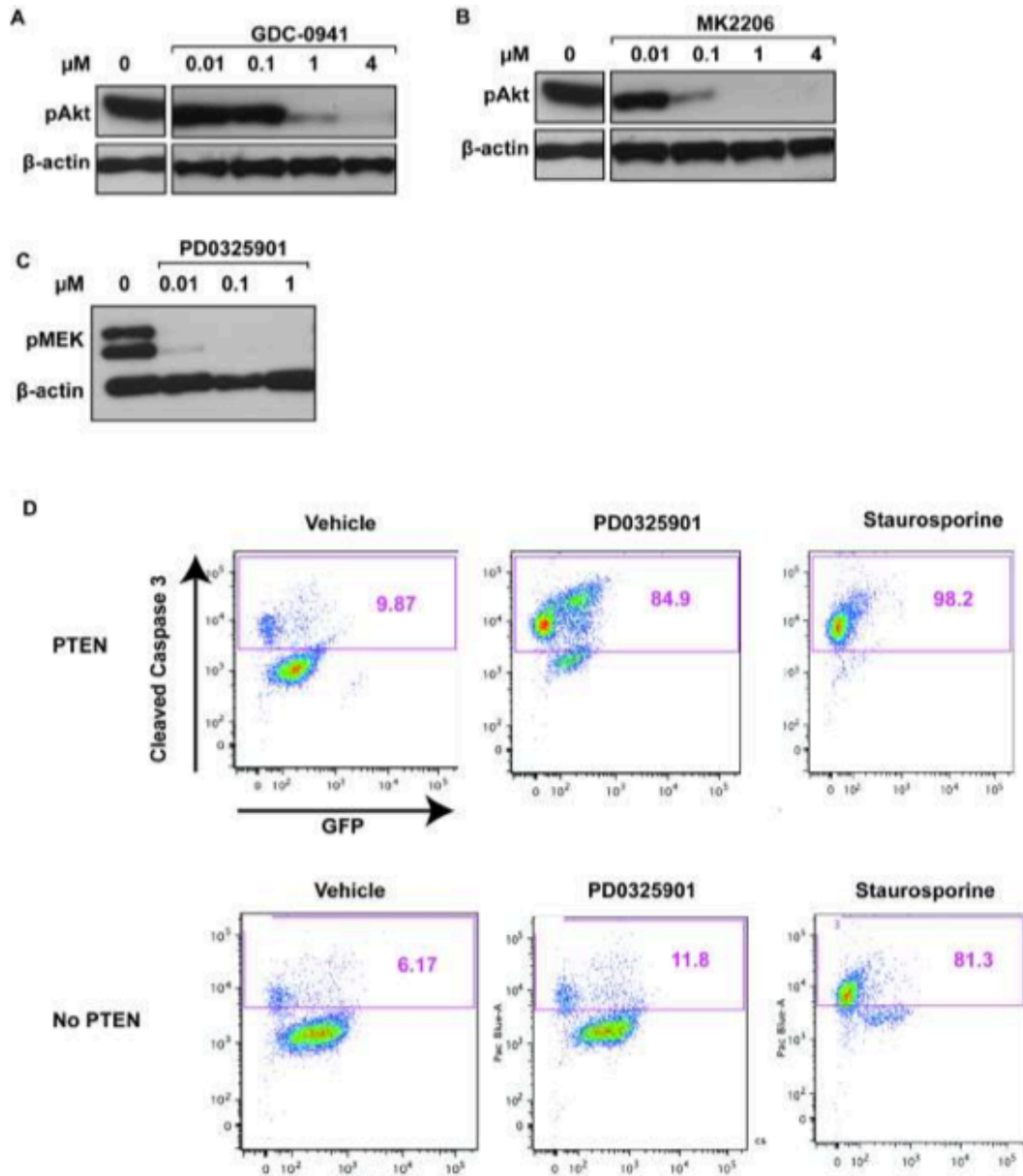
Supplemental Figure 3 - Somatic “third site” Kras mutations in T-ALL. Kras cDNA was amplified from T-ALL cell lines E1, E3, and Y4, cloned, and used to transform competent cells. Fifteen individual colonies were picked for each cell line to assess the relative frequencies of Kras molecules containing two or three mutations. Of these, 11-13 yielded readable sequence from each cell line. The number of individual Kras molecules with two or three mutations is indicated to the right of each representative sequence tracing.



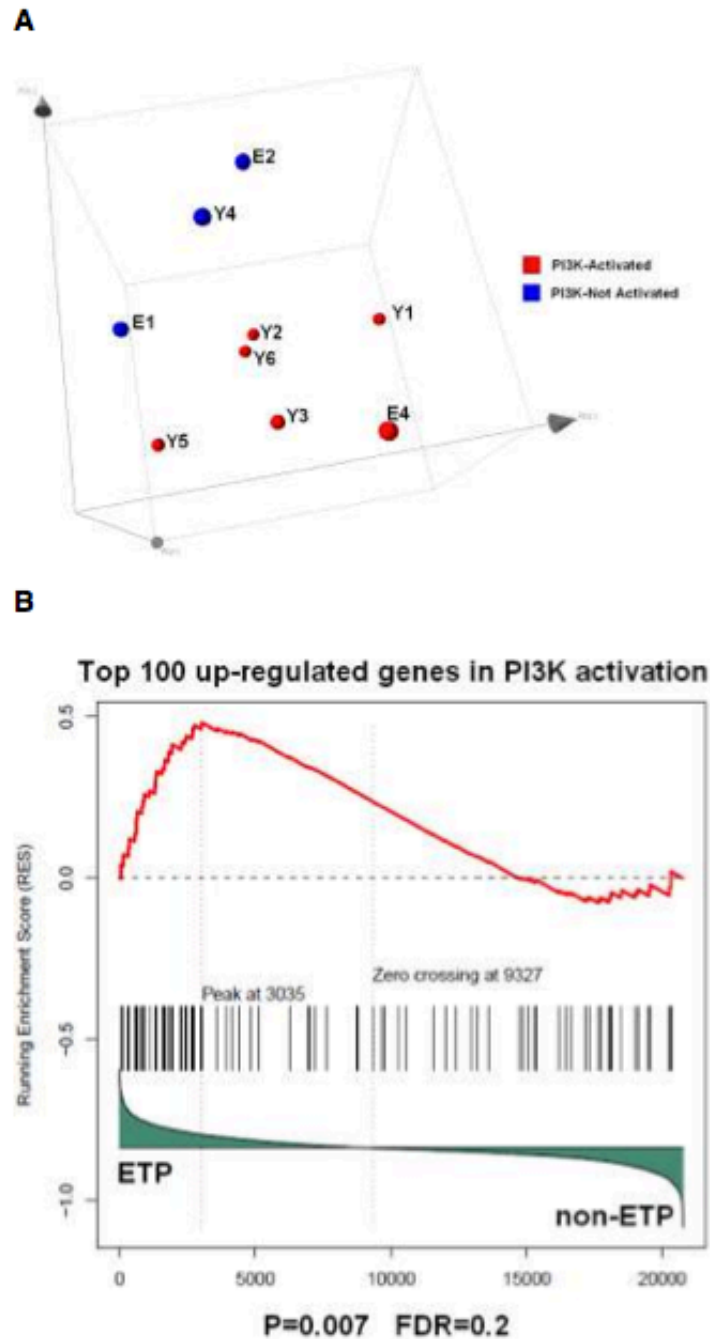
Supplemental Figure 4 - Acquired "third site" mutations restore oncogenic activity to Kras^{D12/E37} and Kras^{D12/G64}. (A) Gating strategy used to analyze transduced primary fetal liver cells doubly positive for GFP and for the myeloid lineage marker (Mac1+). The data presented are from one of six independent experiments that were combined to generate Figure 3D. Gates were set using untransduced WT fetal liver cells at the beginning of each independent experiment, and then used on all transduced samples. (B) Representative original phospho-flow cytometric data from one of six independent experiments used to generate Figure 3D. The black lines depict median fluorescence intensity for cells transduced with the WT Kras vector, which was assigned a value of 1.0 and then compared to cells expressing the 5 Kras mutant alleles in that were transduced and analyzed in same experiment.



Supplemental Figure 5 - Structural and biochemical analysis of the “third site” K-Ras mutants. (A, B (enlarged area)) Superimposing Ras monomer A (K-Ras^{D12/G37/I50}) with the published crystal structure of Rap1A bound to the RBD of Raf-1¹ suggests that Raf-1 RBD forms several contacts with Ras monomer B in addition to a beta-sheet with the switch I region of monomer A. An analysis of the packing between Ras monomers in ~70 published crystal structures showed that Thr-50 frequently appears in or near the contact interface between two Ras monomers, and we speculate that the T50I mutation of one Ras protein may re-orient the neighboring Ras molecule to enhance its binding with Raf-1. This idea implies that the asymmetric dimers found in the crystal are functionally relevant, and is consistent with similar arguments recently proposed for asymmetric Raf dimers.² (C) In silico model of K-Ras^{D12/G37/69RN70} demonstrates a potential mechanism of restored interaction with PI3K. In contrast to other effectors, PI3K makes critical interactions with the switch II domain of Ras. Because of the close homology between the 69RN70 insertion and the two residues just before the insertion site (Arg-68 and Asp-69), we predict that the insertion is likely to occupy the original positions of Arg-68 and Asp-69 in the unmodified protein, thereby extending the $\alpha 2$ helix by a half turn. In its new location, Arg-68 is in position to form a salt bridge with Glu-302 of PI3K. Because the secondary structure is modified, it is difficult to accurately predict the extent of change in the mutant Gly-64 loop caused by the 69RN70 insertion. However, the extended $\alpha 2$ helix is expected to push the Gly-64 loop to restore contact with PI3K. Glu-63 of Ras^{D12/G37/69RN70} may also form additional hydrogen bonds with Lys-234 of PI3K, further strengthening the interaction between the two molecules.



Supplemental Figure 6 - T-ALL cell lines are sensitive to chemical inhibitors and undergo apoptosis. Representative western blot of T-ALL cell line (Y5) shown. (A) GDC-0941 and (B) MK-2206 inhibit pAkt in cell lines after 4 hours of treatment with varying doses of inhibitor. (C) pERK inhibition 48 hours after treatment with PD0325901. (D) Gating strategy used to generate Figure 5D. PTEN-expressing lines induce apoptosis in response to 1 μ M PD0325901 as indicated by an increase in cleaved Caspase-3, while cell lines without PTEN expression do not. Both PTEN positive and negative cell lines undergo apoptosis in the presence of Staurosporine.



Supplemental Figure 7 - PI3K activated T-ALL cell lines and human ETP ALLs have similar gene expression profiles. (A) With the exclusion of E3 cell line, principal component analysis on expression profiling of the remaining nine mouse cell lines using 200 representative genes selected by k-means algorithm. **(B)** With all ten cell lines included in the analysis, gene set enrichment analysis continues to demonstrate significant enrichment of the mouse PI3K up-regulated genes in ETP-ALL.

Ras mutant	Interacts with these effectors	Rationale based on crystal structure
D12/S35	Raf only	Not clear from structure why this mutation affects effector binding differentially.
D12/G37	Ral and PI3K(δ/γ)	Glu37 normally only has a weak ionic bond with Ral but makes two hydrogen bonds with Raf. Glu37 may interact with a basic residue on PI3K α that is not present on the other two isoforms.
D12/E38	Raf only	Residue 38 makes important contact with all three effectors, and mutation introduces a much larger residue. Only Raf has sufficient space for this.
D12/C40	PI3K(α) only	In complexes with Raf and Ral, Tyr40 is required for proper formation of a critical salt bridge. Tyr40 is required for a hydrogen bond with PI3K δ/γ but not α .
D12/G64	Raf and Ral	Neither Raf nor Ral contact any residues in Switch II region so are unaffected by mutations there. Tyr64 forms bonds with three separate contacts on PI3K.

Supplemental Table 1 - Summary of published data on “second site” K-Ras mutants.³⁻⁶

Primary T-ALL	Genotype	Notch1 mutation (nucleotide position)
E3	<i>Kras</i> ^{D12/G37}	None
E4	<i>Kras</i> ^{D12/G37}	Ins CCCTT (7160)
E5	<i>Kras</i> ^{D12/G37}	Del GA (7231)
E6	<i>Kras</i> ^{D12/G37}	None
E7	<i>Kras</i> ^{D12/G37}	Ins CTTC (7160)
Y3	<i>Kras</i> ^{D12/G64}	None
Y4	<i>Kras</i> ^{D12/G64}	Ins TT (7339)
Y6	<i>Kras</i> ^{D12/G64}	Ins CC (7160)
Y7	<i>Kras</i> ^{D12/G64}	Ins TTGGGTC (7273)
Y8	<i>Kras</i> ^{D12/G64}	Ins GG (7275)

Supplemental Table 2 - T-ALLs develop Notch1 mutations. Genomic DNA isolated from diseased organs (peripheral blood, thymus, or spleen) was used to screen for mutations in exon 34 of Notch1, which encodes the PEST domain. All mutations identified are predicted to result in a premature stop codon and were also present in leukemias isolated from transplant recipients. Ins = insertion, Del = deletion.

ProbeSet	Genes	Refseq	FoldChange	Mean G1	Mean G2	FDR	T statistic	P value
1421970_a_at	Gria2	NM_001039195 NM_001083806 NM_013540	-14.070	699.86	49.74	0.003	-13.120	0.000
1418398_a_at	Tspan32	NM_001128080 NM_001128081 NM_001128082 NM_020286	11.954	122.82	1468.19	0.005	11.499	0.000
1448929_at	F13a1	NM_028784	9.073	78.51	712.35	0.013	9.711	0.000
1424638_at	Cdkn1a	NM_001111099 NM_007669	8.023	567.64	4554.38	0.013	9.653	0.000
1419722_at	Klk8	NM_008940	-8.591	1084.37	126.22	0.014	-9.033	0.000
1427484_at	Eml5	NM_001081191	-5.938	241.98	40.75	0.014	-8.984	0.000
1452136_at	Slc5a9	NM_145551	-5.676	256.53	45.20	0.014	-8.978	0.000
1460595_at	1460595_at	---	-5.794	276.71	47.75	0.014	-8.874	0.000
1416029_at	Kif10	NM_013692	2.898	733.73	2126.56	0.017	8.606	0.000
1421861_at	Clstn1	NM_023051 NM_029553	-6.292	346.79	55.11	0.021	-8.164	0.000
1424410_at	Ttc8	NM_198311	-7.294	380.48	52.16	0.021	-8.149	0.000
1453596_at	Id2	NM_010496	3.880	224.44	870.88	0.021	8.095	0.000
1460009_at	Ier5	NM_010500	3.070	77.34	237.47	0.021	7.984	0.000
1434593_at	Eif5a2	NM_177586	-3.284	319.30	97.24	0.021	-7.900	0.000
1443641_at	Fermt3	NM_153795	2.602	160.21	416.89	0.021	7.899	0.000
1436395_at	Card6	NM_001163138 XM_139295 XM_904712	-3.859	510.37	132.24	0.021	-7.856	0.000
1428869_at	Nolc1	NM_001039351 NM_001039352 NM_001039353 NM_053086	-2.268	3132.16	1380.84	0.021	-7.770	0.000
1417790_at	Dok1	NM_010070	2.110	554.53	1169.90	0.021	7.721	0.000
1428508_at	Tbc1d2b	NM_194334	3.229	200.95	648.78	0.021	7.715	0.000
1452831_s_at	Ppat	NM_172146 XM_001002879 XM_001002886 XM_896000 XM_924520 XM_973937 XM_973973	-2.117	2146.41	1013.98	0.023	-7.480	0.000
1451462_a_at	Ifnar2	NM_001110498 NM_010509	2.964	829.29	2457.79	0.023	7.439	0.000
1451722_s_at	Smyd5	NM_144918	-2.511	744.69	296.58	0.023	-7.432	0.000
1423357_at	2610209A20Rik	NM_026010	-2.657	398.15	149.87	0.023	-7.413	0.000
1429893_at	Il17rd	NM_134437	-4.370	271.93	62.23	0.023	-7.411	0.000
1438294_at	Atxn1	NM_009124	2.266	190.92	432.69	0.023	7.402	0.000
1421860_at	Clstn1	NM_023051	-5.391	242.91	45.06	0.024	-7.330	0.000
1426634_at	Slc5a9	NM_145551	-5.153	335.41	65.10	0.024	-7.326	0.000
1434606_at	ErbB3	NM_010153	6.005	136.19	817.82	0.024	7.297	0.000
1436566_at	Rab40b	NM_139147	-5.317	234.00	44.01	0.024	-7.221	0.000
1428091_at	Kih17	NM_001161800 NM_026448	-6.178	295.79	47.88	0.024	-7.203	0.000
1419481_at	Sell	NM_001164059 NM_011346	-6.952	11929.58	1716.01	0.024	-7.194	0.000
1450881_s_at	Gpr137b	NM_031999	-2.660	122.83	46.17	0.026	-7.109	0.000
1424455_at	Gprasp1	NM_001004359 NM_001005385 NM_026081	-3.020	789.78	261.54	0.027	-7.026	0.000
1433656_a_at	Gnl3	NM_153547 NM_178846	-2.089	4707.57	2253.67	0.027	-6.998	0.000
1424829_at	A830007P12Rik	NM_146115	2.092	546.59	1143.32	0.027	6.997	0.000
1425546_a_at	Trf	NM_133977	29.599	91.50	2708.24	0.027	6.967	0.000
1419480_at	Sell	NM_001164059	-8.371	7999.11	955.62	0.027	-6.921	0.000

		NM_011346							
1421898	a at	Mr1	NM_008209	2.039	473.98	966.68	0.027	6.916	0.000
1438005	at	Slc25a40	NM_178766	2.718	629.97	1712.37	0.027	6.905	0.000
1427439	s at	Prmt5	NM_013768	-1.908	3625.20	1900.02	0.028	-6.878	0.000
1417960	at	Cpeb1	NM_007755	4.459	163.16	727.48	0.029	6.798	0.000
1434451	at	Gm10786	---	2.980	259.29	772.72	0.029	6.792	0.000
1452521	a at	Plaur	NM_011113	5.003	97.77	489.10	0.029	6.757	0.000
1428142	at	Etv5	NM_023794	-23.892	1163.69	48.71	0.029	-6.753	0.000
1452117	a at	Fyb	NM_011815	2.855	4572.70	13054.00	0.029	6.751	0.000
1418829	a at	Eno2	NM_013509	3.717	566.11	2104.44	0.031	6.661	0.000
1434444	s at	Anapc1	NM_008569	-1.916	909.47	474.62	0.031	-6.647	0.000
1416593	at	Glrx	NM_053108	2.690	1242.09	3341.23	0.031	6.645	0.000
1426939	at	Tsr2	NM_175146	-1.957	1691.23	864.12	0.031	-6.594	0.000
1450240	a at	Syt11	NM_031393	2.268	988.44	2241.65	0.031	6.592	0.000
1415899	at	Junb	NM_008416	4.397	527.16	2318.03	0.031	6.590	0.000
1449383	at	Adssl1	NM_007421	4.714	311.35	1467.64	0.031	6.578	0.000
1438178	x at	Atad3a	NM_179203	-1.979	5661.40	2861.25	0.031	-6.526	0.000
1448208	at	Smad1	NM_008539	-13.974	1189.65	85.13	0.031	-6.526	0.000
1423890	x at	Atp1b1	NM_009721	-5.509	1547.28	280.87	0.031	-6.507	0.000
1417721	s at	Laptm5	NM_010686	2.691	1319.45	3550.41	0.031	6.491	0.000
1445313	at	LOC636303	XR_033307	2.165	39.26	85.01	0.031	6.488	0.000
1430295	at	Gna13	NM_010303	2.635	739.42	1948.48	0.031	6.483	0.000
1428306	at	Ddit4	NM_029083	2.888	4455.85	12868.70	0.031	6.473	0.000
			NM_001039351 NM_001039352 NM_001039353 NM_053086	-2.266	1864.66	822.82	0.031	-6.466	0.000
			NM_134080 XM_001471989 XM_001472027 XM_001478129 XM_001478141 XM_904364 XM_990154	2.543	49.89	126.85	0.031	6.465	0.000
1442107	at	Flnb	---	-2.649	303.31	114.49	0.032	-6.426	0.000
1454013	at	1810062O18Rik	---	2.775	1212.45	3364.16	0.032	6.398	0.000
1419206	at	Cd37	NM_007645	2.689	725.79	1951.74	0.032	6.395	0.000
1426505	at	Evi2b	NM_146023	1.865	3413.67	6365.67	0.032	6.321	0.000
1418665	at	Impa2	NM_053261	4.157	206.64	858.95	0.032	6.320	0.000
			NM_001159394 NM_001159395	4.468	618.53	2763.64	0.032	6.319	0.000
1457404	at	Nfkbiz	NM_030612	-12.701	1201.92	94.63	0.032	-6.308	0.000
1442166	at	Cpne5	NM_153166	-17.967	1255.62	69.88	0.032	-6.282	0.000
1419086	at	Fgfbp1	NM_008009	2.223	531.53	1181.83	0.032	6.279	0.000
1459843	s at	Smad1	NM_008539	3.110	214.92	668.49	0.032	6.252	0.000
1421899	a at	Mr1	NM_008209	2.384	963.32	2296.10	0.032	6.246	0.000
1431749	a at	Rasgrp1	NM_011246	3.245	157.86	512.31	0.032	6.241	0.000
			NM_001033331 NM_001079876						
1437244	at	Gas2l3	NM_001079876						
1434793	at	Wdr78	NM_146254						
			NM_001005510 XM_001001846 XM_917083	-5.394	676.61	125.44	0.032	-6.233	0.000
1427982	s at	Syne2	NM_133210	2.056	404.69	831.93	0.032	6.229	0.000
1421077	at	Sertad3	NM_145551	-4.390	285.84	65.11	0.032	-6.220	0.000
1440779	s at	Slc5a9	NM_013830	3.054	1257.26	3839.84	0.032	6.217	0.000
1455696	a at	Prpf4b	NM_026077	1.839	545.35	1002.79	0.032	6.216	0.000
1450972	at	3110040N11Rik	NM_009171	-2.470	1630.32	660.04	0.032	-6.213	0.000
1425179	at	Shmt1	NM_179203	-2.079	2803.33	1348.52	0.032	-6.208	0.000
1456541	x at	Atad3a	NM_001033538 NM_001080820	6.813	69.15	471.12	0.032	6.188	0.000
1444426	at	Cass4	NM_015786	3.112	2025.47	6302.36	0.032	6.180	0.000
1416101	a at	Hist1h1c	NM_133643	3.176	149.40	474.52	0.032	6.180	0.000
1437800	at	Edaradd	NM_001039195 NM_001083806						
			NM_013540	-4.066	169.59	41.71	0.032	-6.172	0.000
1434146	at	Gria2	NM_027498	2.082	355.86	740.93	0.032	6.168	0.000
1441947	x at	BC033915							

1430775	at	Wdr44	NM_175180	2.180	93.10	202.98	0.032	6.159	0.000
1447313	at	1447313_at	---	1.877	159.19	298.75	0.032	6.130	0.000
1425479	at	Smyd5	NM_144918	-2.389	408.39	170.95	0.032	-6.116	0.000
1420819	at	Sla	NM_001029841						
1451518	at	Zfp709	NM_145624	-3.292	321.36	97.61	0.032	-6.104	0.000
1423430	at	Mybbp1a	NM_016776	-1.972	2030.63	1029.97	0.032	-6.094	0.000
1451153	a	Cyhr1	NM_019396						
1418478	at	Lmo1	NM_057173	-9.109	495.91	54.44	0.032	-6.083	0.000
1424019	at	Nop2	NM_136747	-1.828	1070.72	585.69	0.032	-6.082	0.000
1450082	s	Etv5	NM_023794	-13.464	654.23	48.59	0.032	-6.070	0.000
1454230	a	Slc25a27	NM_028711	-2.184	80.59	36.90	0.032	-6.066	0.000
1418946	at	Sl3gal1	NM_009177	3.731	262.58	979.56	0.032	6.060	0.000
1455311	at	Dgcr8	NM_033324	-2.079	1193.80	574.26	0.032	-6.045	0.000
1451450	at	2010011I20Rik	NM_025912	2.333	131.48	306.71	0.032	6.041	0.000
1418025	at	Bhlhe40	NM_011498	3.785	756.45	2863.47	0.032	6.036	0.000
1447839	x	Adm	NM_009627	3.907	225.51	881.13	0.032	6.033	0.000
1433847	at	Fam40b	NM_177204	2.432	68.97	167.76	0.032	6.032	0.000
1448659	at	Casp7	NM_007611	-2.701	560.24	207.40	0.032	-6.019	0.000
1460218	at	Cd52	NM_013706	4.281	1719.91	7362.43	0.032	6.018	0.000
1440007	at	D930003E18Rik	---	-2.976	138.36	46.49	0.032	-6.017	0.000
1427324	at	Tmem120b	NM_001039723	2.264	201.68	456.66	0.032	6.014	0.000
1436507	at	Irak2	NM_001113553						
1439036	a	Atp1b1	NM_009721	-8.125	2064.10	254.05	0.033	-5.988	0.000
1452703	at	Ahcy2	NM_021414	4.758	1053.42	5012.19	0.033	5.978	0.000
1435902	at	Nudt18	NM_153136	1.895	364.47	690.70	0.033	5.975	0.000
1435051	at	Wdr44	NM_175180	2.804	389.14	1091.21	0.033	5.965	0.000
1451181	at	Tmem121	NM_153776	-13.719	2123.86	154.81	0.033	-5.956	0.000
1450191	a	Sox13	NM_011439	-4.291	1006.79	234.62	0.033	-5.952	0.000
1448788	at	Cd200	NM_010818	-3.755	162.61	43.30	0.033	-5.948	0.000
1423686	a	Prr13	NM_025385	3.701	548.23	2028.77	0.033	5.939	0.000
1444097	at	Mei2ml	NM_144797	4.262	67.92	289.45	0.033	5.938	0.000
1416077	at	Adm	NM_009627	3.892	174.42	678.85	0.034	5.899	0.000
1440115	at	1440115_at	---	-2.203	92.30	41.89	0.034	-5.897	0.000
1422198	a	Shmt1	NM_009171	-2.645	1069.19	404.22	0.034	-5.881	0.000
1434279	at	1434279_at	---	-1.983	1953.58	985.18	0.034	-5.874	0.000
1422046	at	Ilgam	NM_001082960						
1424436	at	Gart	NM_008401	2.579	75.39	194.44	0.034	5.871	0.000
1415789	a	LOC100045709	NM_010256						
1436595	at	Rbm34	NM_001474845	-5.390	769.14	142.70	0.034	-5.857	0.000
1440205	at	Zmynd19	NM_172762	-1.967	899.60	457.29	0.034	-5.847	0.000
1448613	at	Ecm1	NM_026021	-1.813	423.94	233.87	0.034	-5.847	0.000
1441061	at	1441061_at	NM_007899	3.770	223.56	842.80	0.034	5.841	0.000
1428728	at	Ddx51	---	2.235	165.97	370.94	0.034	5.840	0.000
1447403	a	Zmynd19	NM_027156	-1.829	530.15	289.78	0.035	-5.814	0.000
1438882	at	1438882_at	NM_026021	-1.929	610.94	316.64	0.035	-5.809	0.000
1457142	at	Necab1	---	2.140	98.39	210.56	0.035	5.804	0.000
1434205	at	Ppp2r5c	NM_178617	5.382	54.35	292.51	0.035	5.794	0.000
1455203	at	A930003A15Rik	NM_001081457						
1448147	at	Tnfrsf19	NM_001081458						
1437088	at	Sdad1	NM_001135001						
1417128	at	Plekho1	NM_012023						
1460211	a	Kdelr1	NM_01475293	1.950	2168.87	4228.69	0.036	5.780	0.000
1428333	at	2900062L11Rik	NR_015488						
1448147	at	Tnfrsf19	NR_027896						
1437088	at	Sdad1	XR_035329	2.608	528.13	1377.59	0.036	5.770	0.000
1417128	at	Plekho1	XR_035452						
1460211	a	Kdelr1	NM_001164155						
1428333	at	2900062L11Rik	NM_013869	-7.100	499.79	70.40	0.036	-5.765	0.000
1417128	at	Plekho1	NM_172713	-1.879	760.83	404.83	0.036	-5.753	0.000
1460211	a	Kdelr1	NM_023320	-2.292	273.24	119.21	0.037	-5.738	0.000
1428333	at	2900062L11Rik	NM_133950	1.827	1506.35	2751.53	0.037	5.733	0.000
1428333	at	2900062L11Rik	NR_003641	-3.807	204.38	53.69	0.037	-5.730	0.000

1438385	s_at	Gpt2	NM_173866	-2.184	724.98	332.00	0.037	-5.725	0.000
			NM_172939						
			XM_884335						
1454736	at	Ankrd57	XM_904314	-4.132	243.10	58.83	0.037	-5.714	0.000
1426025	s_at	Laptm5	NM_010686	2.125	2753.57	5851.20	0.037	5.713	0.000
1444372	at	1444372_at	---	2.653	56.57	150.08	0.037	5.696	0.000
1455439	a_at	Lgals1	NM_008495	7.081	4840.70	34277.96	0.037	5.692	0.000
			NM_001161800						
1452660	s_at	Klhl7	NM_026448	-4.973	287.73	57.85	0.037	-5.682	0.000
1416345	at	Timm8a1	NM_013898	-2.203	4004.90	1817.75	0.037	-5.680	0.000
1427689	a_at	Tnip1	NM_021327	2.213	882.16	1951.95	0.037	5.677	0.000
			NM_001037136						
1435433	at	Agap1	NM_178119	-3.257	122.63	37.66	0.037	-5.674	0.000
1423863	at	Abcf2	NM_013853	-1.791	1351.02	754.24	0.037	-5.668	0.000
1419839	x_at	Prpf19	NM_134129	-1.789	4883.28	2728.89	0.037	-5.665	0.000
1458060	at	Ldlrap1	NM_145554	2.985	143.20	427.49	0.037	5.665	0.000
1439589	at	1439589_at	---	2.705	282.34	763.83	0.037	5.660	0.000
			NM_013641						
1436851	at	Pkn1	NM_177262	2.767	478.66	1324.36	0.037	5.656	0.000
1428519	at	2610528E23Rik	NM_025599	-1.816	1270.93	699.87	0.037	-5.648	0.000
1419455	at	Il10rb	NM_008349	4.117	170.93	703.77	0.037	5.647	0.000
			NM_001102471						
1423475	at	Cnnm2	NM_033569	2.283	140.29	320.28	0.037	5.647	0.000
			NR_015468						
1453323	at	2900079G21Rik	XM_001478934	-2.282	441.27	193.38	0.037	-5.635	0.000
1438256	at	Eif5a2	NM_177586	-2.454	173.51	70.71	0.037	-5.620	0.000
1449483	at	Polk	NM_012048	2.030	358.85	728.49	0.037	5.618	0.000
1447585	s_at	Mrps6	NM_080456	-2.211	1630.65	737.47	0.037	-5.616	0.000
1442336	at	1442336_at	---	2.618	53.43	139.90	0.037	5.614	0.000
1421260	a_at	Srm	NM_009272	-2.341	2698.44	1152.51	0.037	-5.613	0.000
1429066	at	4930565B19Rik	---	2.152	227.22	488.91	0.037	5.602	0.000
			NM_029385						
1439884	at	Nudt16	XM_001471758	1.991	835.54	1663.16	0.037	5.600	0.000
1431133	at	Arhgap18	NM_176837	3.350	407.53	1365.28	0.037	5.596	0.000
			NM_028430						
			XM_891672						
1453310	at	Ppil6	XM_908345	2.232	48.74	108.82	0.037	5.575	0.000
			NM_133821						
			XM_001475839						
1426994	at	Phlpp1	NM_129968	-1.975	1244.28	630.15	0.037	-5.571	0.000
1429294	at	Tripp13	NM_027182	-2.054	894.11	435.22	0.037	-5.564	0.000
1426715	s_at	Slc46a1	NM_026740	-2.017	76.78	38.08	0.037	-5.559	0.000
1448761	a_at	Copg2	NM_017478	1.686	1001.07	1687.36	0.037	5.558	0.000
1415917	at	Mthfd1	NM_138745	-2.039	2023.30	992.10	0.037	-5.557	0.000
1435439	at	Dgcr8	NM_033324	-2.048	1051.06	513.11	0.037	-5.556	0.000
1439494	at	Slc5a9	NM_145551	-3.915	245.05	62.59	0.037	-5.553	0.000
1428195	at	Ahcyl2	NM_021414	3.948	413.77	1633.43	0.037	5.550	0.000
1426952	at	Arhgap18	NM_176837	2.436	836.57	2037.84	0.037	5.544	0.000
1428176	at	S1pr2	NM_010333	1.733	454.18	787.04	0.037	5.540	0.000
1449043	at	Naga	NM_008669	2.136	462.47	987.71	0.037	5.536	0.000
1426028	a_at	Cit	NM_007708	2.021	145.79	294.67	0.037	5.532	0.000
1425374	at	Oas3	NM_145226	3.360	77.69	261.05	0.037	5.531	0.000
1459702	at	1459702_at	---	1.766	38.09	67.26	0.037	5.531	0.000
1419522	at	Zmynd19	NM_026021	-1.906	1156.02	606.40	0.037	-5.524	0.000
1422924	at	Tnfsf9	NM_009404	3.430	67.21	230.57	0.037	5.519	0.000
1455729	at	Gnaq	NM_008139	-4.589	269.69	58.77	0.037	-5.516	0.000
1438329	at	Tlr12	NM_205823	-4.443	320.21	72.07	0.037	-5.514	0.000
1419647	a_at	Ier3	NM_133662	5.266	594.30	3129.51	0.037	5.509	0.000
1435288	at	Coro1a	NM_009898	2.840	222.49	631.87	0.037	5.501	0.000
			NM_001111311						
			NM_001111312						
1437477	at	Lrrfp1	NM_008515	2.519	149.56	376.79	0.037	5.496	0.000

1428938_at	Gnaq	NM_008139	-3.387	178.57	52.72	0.037	-5.496	0.000
1459854_s_at	Dynl13	NM_025975	2.764	876.59	2422.90	0.037	5.495	0.000
1428741_at	Elavl4	NM_001038698 NM_001163397 NM_001163399 NM_010488	-2.773	129.34	46.64	0.037	-5.493	0.000
1424211_at	Slc25a33	NM_027460	-4.424	519.19	117.36	0.037	-5.491	0.000
1416442_at	Ier2	NM_010499	4.540	1926.71	8746.97	0.037	5.490	0.000
1424695_at	2010011I20Rik	NM_025912	2.075	112.99	234.43	0.037	5.488	0.000
1415788_at	Ublcp1	NM_024475	-4.730	1614.48	341.35	0.037	-5.486	0.000
1423243_at	Mpp1	NM_008621	2.202	62.36	137.32	0.037	5.478	0.000
1417999_at	Ihm2b	NM_008410	1.941	10295.06	19977.81	0.037	5.472	0.000
1429268_at	2610318N02Rik	NM_183287	-2.392	1067.88	446.43	0.037	-5.471	0.000
1460632_at	1460632_at	---	-3.654	6048.05	1655.20	0.037	-5.471	0.000
1449855_s_at	Uchl3	NM_016723 NM_033607	-2.061	5539.35	2687.51	0.037	-5.463	0.000
1419307_at	Tnfrsf13c	NM_028075	2.052	95.77	196.50	0.037	5.462	0.000
1434285_at	Frm4a	NM_172475	-3.130	1476.67	471.83	0.037	-5.459	0.000
1456885_at	8-Sep	NM_033144	8.851	129.80	1148.84	0.037	5.458	0.000
1435109_at	0710007G10Rik	NM_001163531 NM_001163532 NM_028223	2.263	125.17	283.31	0.037	5.451	0.000
1451180_a_at	Nt5c3l	NM_001102650 NM_026561	-2.005	1503.64	749.84	0.037	-5.448	0.000
1416362_a_at	Fkbp4	NM_010219	-1.724	4110.69	2384.67	0.037	-5.442	0.000
1424161_at	Ddx27	NM_153065	-1.778	1196.04	672.61	0.037	-5.442	0.000
1426980_s_at	E130012A19Rik	NM_175332	-2.853	363.74	127.50	0.037	-5.437	0.000
1425981_a_at	Rbl2	NM_011250	2.166	1010.21	2187.89	0.037	5.433	0.000
1427885_at	Pold4	NM_027196	2.172	840.69	1825.65	0.037	5.432	0.000
1422499_at	Lima1	NM_001113545 NM_023063	-3.272	134.17	41.01	0.037	-5.432	0.000
1455590_at	Nqo2	NM_001163239 NM_001163241 NM_001163242 NM_020282	2.252	175.64	395.47	0.037	5.421	0.000
1422489_at	Mogs	NM_020619	-1.689	2876.42	1703.20	0.037	-5.419	0.000
1429060_at	Malat1	NR_002847	2.313	195.31	451.76	0.037	5.417	0.000
1425178_s_at	Shmt1	NM_009171	-2.217	1282.28	578.36	0.037	-5.415	0.000
1425993_a_at	Hsph1	NM_013559	-1.830	1019.54	556.99	0.037	-5.406	0.000
1450728_at	Fjx1	NM_010218	-4.544	228.48	50.28	0.037	-5.405	0.000
1424440_at	Mrps6	NM_080456	-2.049	1084.27	529.29	0.037	-5.392	0.000
1417481_at	Ramp1	NM_016894 NM_178401	1.875	5215.42	9779.15	0.037	5.391	0.000
1455249_at	1455249_at	---	-8.924	539.74	60.48	0.037	-5.388	0.000
1423540_at	Rbms2	NM_001039080 NM_019711	2.227	307.91	685.81	0.037	5.388	0.000
1452209_at	Pkp4	NM_026361 NM_175464	-3.122	2128.81	681.80	0.037	-5.387	0.000
1430594_at	Rab11flp1	NM_001080813	2.719	195.44	531.45	0.037	5.384	0.000
1421176_at	Rasgrp1	NM_011246 NM_001146346	3.165	202.97	642.34	0.037	5.378	0.000
1417104_at	Emp3	NM_010129	2.083	1672.91	3484.33	0.037	5.373	0.000
1419712_at	Ii3ra	NM_008369	-2.761	127.15	46.05	0.037	-5.368	0.000
1434794_at	Rhof	NM_175092	2.365	320.02	756.94	0.037	5.365	0.000
1450075_at	Polh	NM_030715	2.579	64.40	166.09	0.037	5.364	0.000
1443837_x_at	Bcl2	NM_009741 NM_177410 XM_001476583	3.018	407.14	1228.84	0.037	5.359	0.000
1415762_x_at	Mrpl52	NM_026851	-2.539	2623.57	1033.51	0.037	-5.358	0.000
1432509_at	5033430I15Rik	XM_001473131 XM_001474547	2.198	116.69	256.48	0.037	5.357	0.000
1439181_at	Zfp658	NM_001008549	-3.129	227.03	72.56	0.038	-5.354	0.000
1432543_a_at	Klf13	NM_021366 NM_001025378	2.174	954.23	2074.49	0.038	5.339	0.000
1418226_at	Orc2l	NM_008765	-1.647	1528.87	928.35	0.038	-5.336	0.000
1431212_a_at	Trmt6	NM_175113	-1.870	482.68	258.09	0.038	-5.334	0.000
1419573_a_at	Lgals1	NM_008495	7.673	2922.35	22422.10	0.038	5.329	0.000

1419238_at	Abca7	NM_013850	1.934	389.27	752.95	0.038	5.326	0.000
1438095_x_at	Noc4l	NM_153570	-1.756	1346.28	766.88	0.038	-5.319	0.000
1456079_x_at	Apex1	NM_009687	-1.899	5459.45	2874.91	0.038	-5.319	0.000
1426981_at	Pcsk6	NM_011048 XM_355911 XM_886136 XM_905687 XM_919493	-5.431	361.39	66.54	0.038	-5.319	0.000
1450409_a_at	Slc48a1	NM_026353	2.105	490.72	1033.05	0.038	5.316	0.000
1418293_at	Ifit2	NM_008332	-1.955	699.11	357.57	0.038	-5.313	0.000
1459794_at	1459794_at	---	2.411	55.56	133.95	0.038	5.313	0.000
1415687_a_at	Psap	NM_001146120 NM_001146121 NM_001146122 NM_001146123 NM_001146124 NM_011179	1.818	6282.27	11423.62	0.038	5.312	0.000
1420998_at	Etv5	NM_023794	-9.122	482.29	52.87	0.038	-5.300	0.000
1434327_at	2610020H08Rik	NM_001004187	2.331	167.64	390.80	0.038	5.296	0.000
1447952_at	Auh	NM_016709	3.039	271.93	826.47	0.039	5.283	0.000
1445181_at	Eml5	NM_001081191	-3.687	186.15	50.49	0.039	-5.278	0.000
1449190_a_at	Entpd4	NM_026174 XR_034152	1.945	283.52	551.50	0.039	5.277	0.000
1428786_at	Nckap1l	NM_153505	2.091	1020.06	2133.12	0.039	5.276	0.000
1423021_s_at	Insl3	NM_010589 NM_013564	2.789	439.66	1226.20	0.039	5.271	0.000
1452458_s_at	Ppil5	NM_001081406	-2.212	1703.28	770.19	0.039	-5.268	0.000

Supplemental Table 3 - Top 250 differentially expressed probesets between six PI3K activated (G1) and three non-activated (G2) mouse cell lines. G1: PI3K non-activated mouse cell lines, G2: PI3K activated mouse cell lines.

Term	Count	%	PValue	List Total	Pop Hits	Pop Total	Fold Enrich	Bonferroni	Benjamini	FDR
mmu03040:Spliceosome	45	1.348	0.0000	908	124	5738	2.293	0.0000	0.0000	0.000
mmu04630:Jak-STAT signaling pathway	45	1.348	0.0000	908	152	5738	1.871	0.0045	0.0023	0.030
mmu04120:Ubiquitin mediated proteolysis	40	1.198	0.0001	908	136	5738	1.859	0.0162	0.0054	0.109
mmu04660:T cell receptor signaling pathway	36	1.078	0.0001	908	118	5738	1.928	0.0175	0.0044	0.118
mmu04142:Lysosome	36	1.078	0.0001	908	119	5738	1.912	0.0211	0.0043	0.142
mmu03018:RNA degradation	22	0.659	0.0002	908	60	5738	2.317	0.0361	0.0061	0.245
mmu04144:Endocytosis	52	1.557	0.0003	908	202	5738	1.627	0.0519	0.0076	0.354
mmu03030:DNA replication	15	0.449	0.0005	908	35	5738	2.708	0.0867	0.0113	0.602
mmu04666:Fc gamma R-mediated phagocytosis	29	0.869	0.0009	908	98	5738	1.870	0.1542	0.0184	1.109
mmu00230:Purine metabolism	41	1.228	0.0010	908	157	5738	1.650	0.1770	0.0193	1.288
mmu04662:B cell receptor signaling pathway	24	0.719	0.0023	908	80	5738	1.896	0.3482	0.0382	2.810
mmu05340:Primary immunodeficiency	14	0.419	0.0023	908	36	5738	2.458	0.3525	0.0356	2.853
mmu00240:Pyrimidine metabolism	27	0.809	0.0031	908	96	5738	1.777	0.4391	0.0435	3.777
mmu04210:Apoptosis	25	0.749	0.0034	908	87	5738	1.816	0.4693	0.0443	4.131
mmu00520:Amino sugar and nucleotide sugar metabolism	15	0.449	0.0060	908	44	5738	2.154	0.6765	0.0725	7.239
mmu05210:Colorectal cancer	24	0.719	0.0062	908	86	5738	1.764	0.6852	0.0697	7.407
mmu05212:Pancreatic cancer	21	0.629	0.0066	908	72	5738	1.843	0.7081	0.0699	7.872
mmu04110:Cell cycle	32	0.958	0.0082	908	128	5738	1.580	0.7822	0.0812	9.652
mmu04710:Circadian rhythm	7	0.210	0.0097	908	13	5738	3.403	0.8364	0.0909	11.358
mmu00970:Aminoacyl-tRNA biosynthesis	14	0.419	0.0103	908	42	5738	2.106	0.8550	0.0920	12.064
mmu04914:Progesterone-mediated oocyte maturation	23	0.689	0.0110	908	85	5738	1.710	0.8714	0.0930	12.764
mmu04130:SNARE interactions in vesicular transport	13	0.389	0.0114	908	38	5738	2.162	0.8817	0.0925	13.251
mmu05221:Acute myeloid leukemia	17	0.509	0.0129	908	57	5738	1.885	0.9107	0.0997	14.858
mmu03430:Mismatch repair	9	0.270	0.0153	908	22	5738	2.585	0.9431	0.1126	17.376
mmu04115:p53 signaling pathway	19	0.569	0.0187	908	69	5738	1.740	0.9701	0.1310	20.844
mmu04623:Cytosolic DNA-sensing pathway	16	0.479	0.0205	908	55	5738	1.838	0.9789	0.1379	22.654
mmu04010:MAPK signaling pathway	55	1.647	0.0253	908	265	5738	1.312	0.9915	0.1617	27.176
mmu00670:One carbon pool by folate	7	0.210	0.0297	908	16	5738	2.765	0.9963	0.1813	31.130
mmu04910:Insulin signaling pathway	31	0.928	0.0387	908	138	5738	1.420	0.9993	0.2236	38.651
mmu05222:Small cell lung cancer	21	0.629	0.0396	908	85	5738	1.561	0.9995	0.2216	39.371
mmu05220:Chronic myeloid leukemia	19	0.569	0.0464	908	76	5738	1.580	0.9999	0.2482	44.508
mmu03020:RNA polymerase	9	0.270	0.0516	908	27	5738	2.106	0.9999	0.2652	48.138
mmu05213:Endometrial cancer	14	0.419	0.0571	908	52	5738	1.701	1.0000	0.2819	51.696
mmu05215:Prostate cancer	21	0.629	0.0668	908	90	5738	1.475	1.0000	0.3147	57.496
mmu05200:Pathways in cancer	62	1.857	0.0714	908	323	5738	1.213	1.0000	0.3253	60.028
mmu04150:mTOR signaling pathway	14	0.419	0.0739	908	54	5738	1.638	1.0000	0.3276	61.382
mmu04540:Gap junction	20	0.599	0.0762	908	86	5738	1.470	1.0000	0.3287	62.536
mmu04722:Neurotrophin signaling pathway	28	0.839	0.0774	908	130	5738	1.361	1.0000	0.3258	63.117
mmu04060:Cytokine-cytokine receptor interaction	48	1.438	0.0799	908	244	5738	1.243	1.0000	0.3279	64.360
mmu00790:Folate biosynthesis	5	0.150	0.0813	908	11	5738	2.872	1.0000	0.3259	65.023
mmu00250:Alanine, aspartate and glutamate metabolism	9	0.270	0.0888	908	30	5738	1.896	1.0000	0.3443	68.407
mmu00630:Glyoxylate and dicarboxylate metabolism	6	0.180	0.0945	908	16	5738	2.370	1.0000	0.3558	70.759
mmu04920:Adipocytokine signaling pathway	16	0.479	0.0975	908	67	5738	1.509	1.0000	0.3585	71.946

Supplemental Table 4. DAVID KEGG pathway analysis of T-ALL mouse cell lines. A list of genes in each pathway are available from the authors upon request.

ProbeSet	Genes	Refseq	FoldChange	Mean G1	Mean G2	FDR	T statistic	P value
1451462_a_at	Ifnar2	NM_001110498 NM_010509	2.964	829.29	2457.79	0.023	7.439	0.000
1419455_at	Il10rb	NM_008349	4.117	170.93	703.77	0.037	5.647	0.000
1419712_at	Il3ra	NM_008369	-2.761	127.15	46.05	0.037	-5.368	0.000
1427691_a_at	Ifnar2	NM_001110498 NM_010509	1.741	308.54	537.26	0.039	5.259	0.000
1422021_at	Spry4	NM_011898	-2.936	123.29	41.99	0.041	-5.184	0.000
1449026_at	Ifnar1	NM_010508	1.655	850.69	1407.54	0.047	4.891	0.001
1448575_at	Il7r	NM_008372	8.755	375.51	3287.64	0.048	4.879	0.001
1448576_at	Il7r	NM_008372	8.196	155.17	1271.71	0.050	4.799	0.001
1434745_at	Ccnd2	NM_009829	5.354	454.92	2435.77	0.054	4.557	0.001
1438805_at	Ccnd3	NM_001081635 NM_001081636 NM_007632	-2.066	512.15	247.85	0.056	-4.464	0.001
1425750_a_at	Jak3	NM_010589	2.260	620.13	1401.66	0.056	4.446	0.001
1434403_at	Spred2	NM_033523	-2.067	1590.53	769.61	0.058	-4.353	0.001
1459961_a_at	Stat3	NM_011486 NM_213659 NM_213660	1.811	177.42	321.37	0.059	4.332	0.001
1426587_a_at	Stat3	NM_011486 NM_213659 NM_213660	1.695	2607.73	4418.84	0.060	4.283	0.002
1421570_at	Il9r	NM_001134458 NM_008374	3.081	53.45	164.67	0.061	4.253	0.002
1434980_at	Pik3r5	NM_177320	-2.644	1079.50	408.34	0.063	-4.197	0.002
1423344_at	Epor	NM_010149	-2.234	166.06	74.33	0.067	-4.095	0.002
1460116_s_at	Spred1	NM_033524	-1.882	197.52	104.97	0.067	-4.093	0.002
1416122_at	Ccnd2	NM_009829	4.525	590.52	2672.08	0.070	4.027	0.002
1420888_at	Bcl2l1	NM_009743	2.202	269.75	593.86	0.072	3.964	0.003
1448724_at	Cish	NM_009895	5.753	522.82	3007.64	0.073	3.931	0.003
1441415_at	1441415_at	---	1.910	152.43	291.11	0.075	3.882	0.003
1448731_at	Il10ra	NM_008348	1.873	330.44	618.89	0.079	3.795	0.003
1422707_at	Pik3og	NM_001146200 NM_001146201 NM_020272	-1.571	903.88	575.36	0.081	-3.759	0.004
1443937_at	1443937_at	---	3.830	270.76	1036.97	0.081	3.758	0.004
1452911_at	Spred1	NM_033524	-3.083	317.50	102.98	0.084	-3.712	0.004
1445669_at	Spry4	NM_011898	-3.126	125.16	40.04	0.086	-3.682	0.004
1417546_at	Il2rb	NM_008368	2.493	267.61	667.14	0.086	3.679	0.004
1455956_x_at	Ccnd2	NM_009829	4.015	387.94	1557.66	0.088	3.650	0.004
1420887_a_at	Bcl2l1	NM_009743	1.566	131.80	206.38	0.089	3.611	0.005
1417306_at	Tyk2	NM_018793	1.537	377.60	580.34	0.090	3.584	0.005
1416123_at	Ccnd2	NM_009829	2.355	55.75	131.29	0.090	3.575	0.005
1438767_at	Osm	NM_001013365	4.663	350.76	1635.73	0.091	3.559	0.005
1416296_at	Il2rg	NM_013563	1.565	6072.63	9501.00	0.093	3.537	0.005
1423160_at	Spred1	NM_033524	-3.680	905.34	246.02	0.094	-3.516	0.005
1455703_at	Akt2	NM_001110208 NM_007434 XM_001479739 XM_001479747 XM_001479752	-1.459	208.98	143.23	0.096	-3.478	0.006
1423161_s_at	Spred1	NM_033524	-3.168	616.48	194.57	0.096	-3.476	0.006
1450330_at	Il10	NM_010548	-5.048	322.41	63.87	0.097	-3.466	0.006
1449109_at	Socs2	NM_007706	4.526	210.48	952.62	0.101	3.401	0.006
1428777_at	Spred1	NM_033524	-2.227	256.24	115.06	0.101	-3.401	0.006
1448167_at	Ifnqr1	NM_010511	2.781	1027.32	2856.88	0.102	3.389	0.007
1455899_x_at	Socs3	NM_007707	2.753	835.74	2300.67	0.106	3.336	0.007
1436584_at	Spry2	NM_011897	-2.933	163.30	55.68	0.106	-3.327	0.007
1440047_at	Socs1	NM_009896	4.722	175.61	829.22	0.106	3.323	0.007
1448759_at	Il2rb	NM_008368	3.912	181.51	710.17	0.113	3.243	0.009
1460700_at	Stat3	NM_011486	1.382	1563.31	2160.32	0.116	3.198	0.009

		NM_213659 NM_213660						
1416576_at	Socs3	NM_007707	2.193	488.47	1071.07	0.122	3.128	0.010
1435458_at	Pim1	NM_008842	2.209	1268.21	2801.88	0.126	3.086	0.011
1442222_at	lfnar1	NM_010508	1.770	219.16	387.89	0.127	3.073	0.011
1415907_at	Ccnd3	NM_001081635 NM_001081636 NM_007632	-1.887	10482.55	5556.40	0.128	-3.061	0.012
1421884_at	Sos1	NM_009231	1.566	249.28	390.36	0.130	3.049	0.012
1446085_at	1446085_at	---	2.081	63.61	132.40	0.130	3.043	0.012
1456482_at	Pik3r3	NM_181585	2.083	241.83	503.72	0.132	3.026	0.012
1418674_at	Osmr	NM_011019	1.514	43.44	65.77	0.133	3.011	0.013
1416124_at	Ccnd2	NM_009829	2.161	85.58	184.91	0.136	2.983	0.013
1448229_s_at	Ccnd2	NM_009829	2.030	184.37	374.25	0.145	2.905	0.015
1434834_at	Socs7	NM_138657	1.524	606.15	923.77	0.145	2.904	0.015
1425711_a_at	Akt1	NM_009652	-1.349	1853.33	1373.79	0.149	-2.879	0.016
1418507_s_at	Socs2	NM_007706	4.153	140.72	584.35	0.150	2.864	0.016
1450550_at	Il5	NM_010558	3.631	74.16	269.30	0.152	2.845	0.017
1423006_at	Pim1	NM_008842	2.199	597.30	1313.61	0.154	2.828	0.017
1422397_a_at	Il15ra	NM_008358 NM_133836	1.373	254.23	349.09	0.158	2.791	0.019
1435852_at	Spred3	NM_182927	-2.066	128.43	62.16	0.163	-2.756	0.020
1416295_a_at	Il2rg	NM_013563	1.502	4995.54	7500.97	0.163	2.753	0.020
1422581_at	Pias1	NM_019663	1.286	1379.08	1773.60	0.164	2.749	0.020
1450446_a_at	Socs1	NM_009896	2.366	725.70	1717.36	0.166	2.729	0.021
1448681_at	Il15ra	NM_008358 NM_133836	1.519	330.30	501.65	0.168	2.706	0.022
1422102_a_at	Stat5b	NM_001113563 NM_011489	1.422	850.48	1209.62	0.172	2.683	0.022
1423557_at	lfngr2	NM_008338	1.649	225.06	371.01	0.172	2.682	0.022
1416657_at	Akt1	NM_009652	-1.361	2585.72	1899.71	0.176	-2.652	0.024
1419454_x_at	Pias2	NM_001164167 NM_001164168 NM_001164169 NM_001164170 NM_008602	-1.574	256.88	163.23	0.177	-2.644	0.024
1443602_at	1443602_at	---	1.893	119.29	225.78	0.178	2.636	0.024
1437270_a_at	Clcf1	NM_019952	1.847	84.44	155.97	0.179	2.631	0.025
1421207_at	Lif	NM_001039537 NM_008501	3.273	300.28	982.77	0.182	2.608	0.026
1421886_at	Sos1	NM_009231	1.496	85.68	128.18	0.185	2.596	0.026
1437271_at	Clcf1	NM_019952	1.711	101.68	173.99	0.185	2.592	0.026

Supplemental Table 5. Differentially expressed probesets in the KEGG Jak-STAT signaling pathway. G1: PI3K non-activated mouse cell lines, G2: PI3K activated mouse cell lines.

ProbeSet	Genes	Refseq	FoldChange	Mean G1	Mean G2	FDR	T statistic	P value
1421176_at	Rasgrp1	NM_011246	3.165	202.97	642.34	0.037	5.378	0.000
1438478_a_at	Ppp3ca	NM_008913	2.182	362.58	791.14	0.042	5.163	0.000
1426401_at	Ppp3ca	NM_008913	1.958	1134.96	2222.50	0.050	4.748	0.001
1434295_at	Rasgrp1	NM_011246	5.163	581.01	2999.66	0.054	4.561	0.001
1440442_at	Map2k7	NM_001042557 NM_001164172 NM_011944	1.839	76.20	140.15	0.056	4.434	0.001
1440164_x_at	Cd8a	NM_001081110 NM_009857	2.222	61.19	135.95	0.057	4.401	0.001
1431843_a_at	Nfkbie	NM_008690	-2.000	861.77	430.79	0.058	-4.351	0.001
1450143_at	Rasgrp1	NM_011246	3.932	209.91	825.37	0.060	4.303	0.001
1421926_at	Mapk11	NM_011161	-2.192	91.37	41.69	0.062	-4.205	0.002
1434980_at	Pik3r5	NM_177320	-2.644	1079.50	408.34	0.063	-4.197	0.002
1423100_at	Fos	NM_010234	6.534	740.36	4837.34	0.063	4.185	0.002
1427779_a_at	Cd4	NM_013488	3.572	81.31	290.43	0.064	4.155	0.002
1430257_at	Card11	NM_175362	1.737	67.00	116.37	0.066	4.108	0.002
1448306_at	Nfkbia	NM_010907	2.113	1510.72	3191.68	0.073	3.944	0.003
1449731_s_at	Nfkbia	NM_010907	1.896	1126.53	2136.46	0.073	3.943	0.003
1439205_at	Nfatc2	NM_001037177 NM_001037178 NM_001136073 NM_010899	2.161	269.94	583.23	0.076	3.857	0.003
1422707_at	Pik3cg	NM_001146200 NM_001146201 NM_020272	-1.571	903.88	575.36	0.081	-3.759	0.004
1427705_a_at	Nfkb1	NM_008689	1.747	2162.71	3778.42	0.087	3.667	0.004
1438157_s_at	Nfkbia	NM_010907	2.194	3962.76	8693.03	0.089	3.622	0.004
1420685_at	Grap2	NM_010815 XM_972673	1.590	216.08	343.51	0.090	3.580	0.005
1455200_at	Pak6	NM_001033254 NM_001145854	1.889	76.01	143.61	0.093	3.539	0.005
1460204_at	Tec	NM_001113460 NM_001113461 NM_001113464 NM_013689	2.617	410.52	1074.36	0.096	3.479	0.006
1455703_at	Akt2	NM_001110208 NM_007434 XM_001479739 XM_001479747 XM_001479752	-1.459	208.98	143.23	0.096	-3.478	0.006
1450330_at	Ii10	NM_010548	-5.048	322.41	63.87	0.097	-3.466	0.006
1452056_s_at	Ppp3ca	NM_008913	1.592	764.31	1216.46	0.106	3.322	0.007
1440165_at	Ptprc	NM_001111316 NM_011210	1.850	182.19	337.11	0.109	3.289	0.008
1419696_at	Cd4	NM_013488	4.017	75.68	303.98	0.110	3.272	0.008
1420979_at	Pak1	NM_011035	-2.207	124.75	56.53	0.114	-3.231	0.009
1420088_at	Nfkbia	NM_010907	1.672	6303.65	10542.24	0.116	3.194	0.009
1451979_at	Kras	NM_021284	-2.019	6450.70	3195.67	0.123	-3.126	0.010
1458299_s_at	Nfkbie	NM_008690	-2.375	2285.57	962.26	0.127	-3.072	0.011
1421884_at	Sos1	NM_009231	1.566	249.28	390.36	0.130	3.049	0.012
1434000_at	Kras	NM_021284	-1.765	2307.73	1307.41	0.130	-3.041	0.012
1456482_at	Pik3r3	NM_181585	2.083	241.83	503.72	0.132	3.026	0.012
1438999_a_at	Nfat5	NM_018823 NM_133957	1.585	292.06	462.92	0.133	3.011	0.013
1416797_at	LOC100044 475	NM_010879 XM_001472256	-1.521	1445.24	950.05	0.141	-2.937	0.014
1444078_at	Cd8a	NM_001081110 NM_009857	5.720	176.04	1006.94	0.143	2.928	0.015
1418970_a_at	Bcl10	NM_009740	1.341	1791.98	2403.39	0.146	2.899	0.015
1425711_a_at	Akt1	NM_009652	-1.349	1853.33	1373.79	0.149	-2.879	0.016
1450550_at	Ii5	NM_010558	3.631	74.16	269.30	0.152	2.845	0.017

1457917_at	Lck	NM_001162432 NM_001162433 NM_010693	1.805	209.16	377.59	0.159	2.779	0.019
1416796_at	LOC100044 475	NM_010879 XM_001472256	-1.421	4523.85	3183.24	0.163	-2.754	0.020
1418971_x_at	Bcl10	NM_009740	1.342	1392.26	1868.50	0.168	2.708	0.021
1450070_s_at	Pak1	NM_011035	-2.371	116.87	49.28	0.172	-2.678	0.023
1416657_at	Akt1	NM_009652	-1.361	2585.72	1899.71	0.176	-2.652	0.024
1454369_a_at	Nfatc4	NM_023699	-1.374	125.79	91.57	0.179	-2.633	0.024
1459635_at	1459635_at	---	1.622	50.74	82.29	0.184	2.602	0.026
1421886_at	Sos1	NM_009231	1.496	85.68	128.18	0.185	2.596	0.026
1426396_at	Cd247	NM_001113391 NM_001113392 NM_001113393 NM_001113394 NM_031162	1.350	2879.77	3886.88	0.187	2.578	0.027
1419334_at	Ctla4	NM_009843	-2.826	982.57	347.67	0.193	-2.542	0.029
1435646_at	Ikbg	NM_001136067 NM_001161421 NM_001161422 NM_001161423 NM_001161424 NM_010547 NM_178590	1.288	616.69	794.26	0.196	2.524	0.030
1426170_a_at	Cd8b1	NM_009858	3.318	321.00	1065.09	0.196	2.522	0.030

Supplemental Table 6. Differentially expressed probesets in the KEGG T-cell receptor signaling pathway. G1: PI3K non-activated mouse cell lines, G2: PI3K activated mouse cell lines.

ProbeSet	Genes	Refseq	FoldChange	Mean G1	Mean G2	FDR	T statistic	P value
1442107_at	Flnb	NM_134080 XM_001471989 XM_001472027 XM_001478129 XM_001478141 XM_904364 XM_990154	2.543	49.89	126.85	0.031	6.465	0.000
1434279_at	1434279_at	---	-1.983	1953.58	985.18	0.034	-5.874	0.000
1421176_at	Rasgrp1	NM_011246	3.165	202.97	642.34	0.037	5.378	0.000
1438478_a_at	Ppp3ca	NM_008913	2.182	362.58	791.14	0.042	5.163	0.000
1426750_at	Flnb	NM_134080 XM_001471989 XM_001472027 XM_001478129 XM_001478141 XM_904364 XM_990154	2.820	325.27	917.39	0.044	5.023	0.000
1416896_at	Rps6ka1	NM_009097	2.487	968.19	2408.22	0.046	4.931	0.001
1449519_at	Gadd45a	NM_007836	1.750	541.00	946.94	0.050	4.768	0.001
1426401_at	Ppp3ca	NM_008913	1.958	1134.96	2222.50	0.050	4.748	0.001
1434295_at	Rasgrp1	NM_011246	5.163	581.01	2999.66	0.054	4.561	0.001
1450971_at	Gadd45b	NM_008655	3.719	92.16	342.79	0.054	4.537	0.001
1445534_at	Flnb	NM_134080 XM_001471989 XM_001472027 XM_001478129 XM_001478141 XM_904364 XM_990154	2.408	194.58	468.62	0.056	4.466	0.001
1440442_at	Map2k7	NM_001042557 NM_001164172 NM_011944	1.839	76.20	140.15	0.056	4.434	0.001
1437494_at	Mapkapk3	NM_178907	3.383	84.19	284.80	0.057	4.397	0.001
1449773_s_at	Gadd45b	NM_008655	3.707	69.82	258.80	0.057	4.384	0.001
1440343_at	Rps6ka5	NM_153587	1.674	780.38	1306.40	0.057	4.380	0.001
1450143_at	Rasgrp1	NM_011246	3.932	209.91	825.37	0.060	4.303	0.001
1460251_at	Fas	NM_001146708 NM_007987	5.789	213.35	1235.00	0.062	4.229	0.002
1418448_at	Rras	NM_009101	2.211	347.34	767.92	0.062	4.207	0.002
1421926_at	Mapk11	NM_011161	-2.192	91.37	41.69	0.062	-4.205	0.002
1434815_a_at	Mapkapk3	NM_178907	5.187	40.19	208.48	0.062	4.203	0.002
1423100_at	Fos	NM_010234	6.534	740.36	4837.34	0.063	4.185	0.002
1443897_at	Ddit3	NM_007837	1.874	191.81	359.38	0.066	4.115	0.002
1421026_at	Gna12	NM_010302	-1.896	223.20	117.70	0.067	-4.089	0.002
1425444_a_at	Tgfb2	NM_009371 NM_029575	2.400	200.48	481.20	0.067	4.084	0.002
1428834_at	Dusp4	NM_176933	-8.403	723.66	86.12	0.068	-4.059	0.002
1455560_at	1455560_at	---	1.660	113.56	188.47	0.069	4.044	0.002
1417455_at	Tgfb3	NM_009368	-5.058	566.83	112.07	0.073	-3.948	0.003
1439205_at	Nfatc2	NM_001037177 NM_001037178 NM_001136073 NM_010899	2.161	269.94	583.23	0.076	3.857	0.003
1439004_at	Rps6ka5	NM_153587	1.566	217.13	339.99	0.080	3.775	0.003
1427705_a_at	Nfkb1	NM_008689	1.747	2162.71	3778.42	0.087	3.667	0.004
1440265_at	Jund	NM_010592	1.573	50.47	79.40	0.087	3.662	0.004
1450097_s_at	Gna12	NM_010302	-2.813	199.08	70.78	0.093	-3.530	0.005
1450975_at	Cacng4	NM_019431	-4.413	283.63	64.27	0.094	-3.517	0.005
1440208_at	Rac2	NM_009008	1.689	280.11	473.23	0.094	3.510	0.005
1455703_at	Akt2	NM_001110208 NM_007434 XM_001479739 XM_001479747	-1.459	208.98	143.23	0.096	-3.478	0.006

1438309_at	Acvr1c	NM_001033369 NM_001111030	-1.678	65.15	38.83	0.104	-3.363	0.007
1418093_a_at	Egf	NM_010113	1.630	91.15	148.59	0.106	3.331	0.007
1452056_s_at	Ppp3ca	NM_008913	1.592	764.31	1216.46	0.106	3.322	0.007
1453851_a_at	Gadd45g	NM_011817	4.193	274.52	1151.17	0.107	3.308	0.008
1418401_a_at	Dusp16	NM_001048054 NM_130447	-4.632	409.16	88.33	0.109	-3.293	0.008
1455008_at	1455008_at	---	-1.722	359.57	208.86	0.109	-3.293	0.008
1418513_at	Stk3	NM_019635	1.712	663.61	1135.99	0.109	3.284	0.008
1420979_at	Pak1	NM_011035	-2.207	124.75	56.53	0.114	-3.231	0.009
1449117_at	Jund	NM_010592	2.464	2136.17	5263.87	0.119	3.163	0.010
1450698_at	Dusp2	NM_010090	2.180	1159.42	2527.93	0.121	3.148	0.010
1415834_at	Dusp6	NM_026268	-4.048	1934.77	477.93	0.122	-3.138	0.010
1451979_at	Kras	NM_021284	-2.019	6450.70	3195.67	0.123	-3.126	0.010
1417516_at	Ddit3	NM_007837	1.792	905.75	1623.40	0.125	3.098	0.011
1417080_a_at	Ecsit	NM_012029	-1.412	743.74	526.70	0.128	-3.065	0.012
1421884_at	Sos1	NM_009231	1.566	249.28	390.36	0.130	3.049	0.012
1434000_at	Kras	NM_021284	-1.765	2307.73	1307.41	0.130	-3.041	0.012
1460444_at	Arb1	NM_177231 NM_178220	2.664	229.34	610.90	0.139	2.959	0.014
1426397_at	Tgfb2	NM_009371 NM_029575	2.011	1438.53	2892.21	0.141	2.941	0.014
1422147_a_at	Pla2g6	NM_016915	1.431	486.62	696.45	0.143	2.925	0.015
1418512_at	Stk3	NM_019635	1.571	1039.11	1632.29	0.143	2.922	0.015
1425711_a_at	Akt1	NM_009652	-1.349	1853.33	1373.79	0.149	-2.879	0.016
1455597_at	Map3k2	NM_011946	1.406	384.64	540.81	0.152	2.849	0.017
1434159_at	Stk4	NM_021420	1.416	2687.43	3806.41	0.154	2.825	0.018
1431278_s_at	Pla2g6	NM_016915	1.416	116.31	164.67	0.156	2.809	0.018
1445427_at	1445427_at	---	1.503	95.62	143.74	0.161	2.771	0.019
1455230_at	1455230_at	---	-2.497	290.35	116.30	0.163	-2.756	0.020
1421107_at	Stk4	NM_021420	1.514	734.24	1111.85	0.165	2.739	0.020
1420653_at	Tgfb1	NM_011577	1.364	1317.47	1796.72	0.165	2.738	0.020
1425380_at	Rasgrp4	NM_145149	-3.338	191.06	57.23	0.165	-2.737	0.020
1426759_at	Map4k3	NM_001081357	-3.036	381.60	125.71	0.168	-2.709	0.021
1420611_at	Prkacb	NM_001164198 NM_001164199 NM_001164200 NM_011100	1.447	2889.89	4180.63	0.169	2.701	0.022
1451530_at	Egfr	NM_007912 NM_207655	-1.599	80.31	50.21	0.172	-2.680	0.023
1450070_s_at	Pak1	NM_011035	-2.371	116.87	49.28	0.172	-2.678	0.023
1420932_at	Mapk8	NM_016700	-1.389	1025.14	737.80	0.174	-2.670	0.023
1416437_a_at	Mapk8ip3	NM_001163447 NM_001163448 NM_001163449 NM_001163450 NM_001163451 NM_001163453 NM_013931	1.479	269.94	399.18	0.175	2.663	0.023
1416657_at	Akt1	NM_009652	-1.361	2585.72	1899.71	0.176	-2.652	0.024
1454369_a_at	Nfatc4	NM_023699	-1.374	125.79	91.57	0.179	-2.633	0.024
1421886_at	Sos1	NM_009231	1.496	85.68	128.18	0.185	2.596	0.026
1454737_at	Dusp9	NM_029352	-1.595	85.68	53.73	0.186	-2.586	0.027
1420622_a_at	Hspa8	NM_031165	-1.477	9550.45	6466.60	0.192	-2.548	0.028
1417856_at	Relb	NM_009046	1.454	143.06	207.95	0.195	2.535	0.029
1435646_at	Ikkg	NM_001136067 NM_001161421 NM_001161422 NM_001161423 NM_001161424 NM_010547 NM_178590	1.288	616.69	794.26	0.196	2.524	0.030
1455349_at	Rap1b	NM_024457	1.326	2253.51	2987.98	0.197	2.520	0.030
1455181_at	Rasa2	NM_053268	-1.630	1714.63	1051.61	0.199	-2.506	0.031

Supplemental Table 7. Differentially expressed probesets in the KEGG MAPK signaling pathway. G1: PI3K non-activated mouse cell lines, G2: PI3K activated mouse cell lines.

ProbeSet	Genes	Refseq	FoldChange	Mean G1	Mean G2	FDR	T statistic	P value
1428306_at	Ddit4	NM_029083	2.888	4455.85	12868.70	0.031	6.473	0.000
1416896_at	Rps6ka1	NM_009097	2.487	968.19	2408.22	0.046	4.931	0.001
1451959_a_at	Vegfa	NM_001025250 NM_001025257 NM_001110266 NM_001110267 NM_001110268 NM_009505	1.726	557.41	962.09	0.061	4.255	0.002
1434980_at	Pik3r5	NM_177320	-2.644	1079.50	408.34	0.063	-4.197	0.002
1420909_at	Vegfa	NM_001025250 NM_001025257 NM_001110266 NM_001110267 NM_001110268 NM_009505	1.779	689.47	1226.27	0.070	4.011	0.002
1422707_at	Pik3cg	NM_001146200 NM_001146201 NM_020272	-1.571	903.88	575.36	0.081	-3.759	0.004
1444010_at	Eif4e	NM_007917 XM_001004193	1.902	44.44	84.51	0.082	3.749	0.004
1455703_at	Akt2	NM_001110208 NM_007434 XM_001479739 XM_001479747 XM_001479752	-1.459	208.98	143.23	0.096	-3.478	0.006
1429463_at	Prkaa2	NM_178143	-1.957	106.37	54.35	0.104	-3.356	0.007
1439597_at	1439597_at	---	1.620	110.60	179.17	0.107	3.309	0.008
1456482_at	Pik3r3	NM_181585	2.083	241.83	503.72	0.132	3.026	0.012
1449966_s_at	Cab39l	NM_026908	1.361	935.30	1273.14	0.148	2.888	0.016
1425711_a_at	Akt1	NM_009652	-1.349	1853.33	1373.79	0.149	-2.879	0.016
1418432_at	Cab39	NM_133781	1.361	1391.95	1895.04	0.165	2.736	0.020
1416657_at	Akt1	NM_009652	-1.361	2585.72	1899.71	0.176	-2.652	0.024
1422268_a_at	Rps6kb2	NM_021485	1.286	432.93	556.93	0.190	2.561	0.028

Supplemental Table 8. Differentially expressed probesets in the KEGG mTOR signaling pathway. G1: PI3K non-activated mouse cell lines, G2: PI3K activated mouse cell lines.

Supplemental Methods Quantitative PCR

RNA was prepared with Qiagen RNEasy Midi kit, and 150 ng used to generate cDNA with Superscript III Reverse Transcriptase (Invitrogen). Quantitative PCR was performed using TaqMan Assays (Applied Biosystems) for *Pten* (Mm00477208_m1), *Kras* (Mm00517494_m1) and *GAPDH* (Mm99999915_g1) with the TaqMan Gene Expression Master Mix and 1ul of cDNA. Reactions were run in triplicate on an ABI 7900HT. Cycling conditions were 2 minutes at 50oC and 10 minutes at 95oC, then 40 cycles of 15 seconds at 95oC and 1 minute at 60oC. Target quantities were determined by relative standard curve, normalized to *Gapdh* and compared with WT thymus.

DNA sequencing

Exon 34 of *Notch1*, *Kras* transgenes, and *Pten* were amplified then directly sequenced using standard methodologies.⁷ PCR conditions and primer sequences are available upon request. To sequence individual *Kras* molecules in T-ALL cell lines, PCR products were ligated into pCR®II vector (Invitrogen). Plasmid DNA from individual colonies was sequenced using the M13F primer (5'-GTAAAACGACGGCCAG-3').

Supplemental References

1. Nassar N, Horn G, Herrmann C, et al. The 2.2 Å crystal structure of the Ras-binding domain of the serine/threonine kinase c-Raf1 in complex with

- Rap1A and a GTP analogue. *Nature*. 1995;375(6532):554–560.
2. Rajakulendran T, Sahmi M, Lefrançois M, Sicheri F, Therrien M. A dimerization-dependent mechanism drives RAF catalytic activation. *Nature*. 2009;461(7263):542–545.
 3. Kinashi T, Katagiri K, Watanabe S, et al. Distinct mechanisms of alpha 5beta 1 integrin activation by Ha-Ras and R-Ras. *J Biol Chem*. 2000;275(29):22590–22596.
 4. White MA, Nicolette C, Minden A, et al. Multiple Ras functions can contribute to mammalian cell transformation. *Cell*. 1995;80(4):533–541.
 5. Rodriguez-Viciano P, Warne PH, Khwaja A, et al. Role of phosphoinositide 3-OH kinase in cell transformation and control of the actin cytoskeleton by Ras. *Cell*. 1997;89(3):457–467.
 6. Pacold ME, Suire S, Perisic O, et al. Crystal structure and functional analysis of Ras binding to its effector phosphoinositide 3-kinase gamma. *Cell*. 2000;103(6):931–943.
 7. Dail M, Li Q, McDaniel A, et al. Mutant Ikzf1, KrasG12D, and Notch1 cooperate in T lineage leukemogenesis and modulate responses to targeted agents. *Proc Natl Acad Sci USA*. 2010;107(11):5106–5111.

Chapter 3: Mechanism of Resistance to MEK Inhibition

Introduction

Chapter 1 of this dissertation describes what is known about the molecular pathogenesis of T-ALL, including the role of Ras/PI3K pathway mutations in this aggressive cancer. Chapter 2 is a research article showing that transplanting primary mouse bone marrow transduced with retroviral vectors encoding mutant K-Ras proteins containing “second site” amino acid substitutions that abrogate or impair PI3K/AKT or Raf/MEK/ERK pathway activation initiated aggressive T-ALL in recipient mice. Cell lines generated from 10 independent leukemias carried diverse secondary genetic alterations that correlated with discrete effects on the biochemical activation of Ras effectors. Remarkably, exposing this panel of T-ALL cells to targeted inhibitors of PI3K, AKT, or MEK showed that lines with high levels of pAKT and markedly reduced or absent PTEN expression are resistant to a potent and selective MEK inhibitor. I went on to demonstrate that these cell lines failed to undergo apoptosis in response to PD0325901, while this MEK inhibitor triggered apoptosis in cell lines with low basal pAKT levels and robust PTEN expression. In this Chapter, I describe unpublished studies of additional inhibitors in this system as well as functional and biochemical experiments to elucidate mechanisms of response and resistance to PD0325901 in T-ALL cells.

Results

Sensitivity of T-ALL Cells to Chemical Inhibitors of PI3K/AKT Signaling. To extend the studies of GDC-0941 and MK2206 presented in Chapter 2 (see Figure 5 and Supplemental Figure 6 in Chapter 2), we interrogated the effects of additional

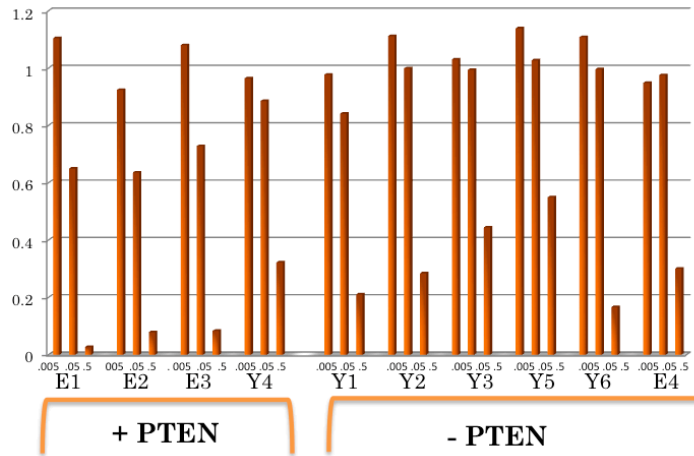
PI3K/AKT/mTOR pathway inhibitors on the growth of T-ALL cell lines. These molecules included: (1) PP242, an ATP competitive mTORC1/2 inhibitor and less potent inhibitor of PKC α , p110Y, and JAK2; and (2) Rapamycin, which inhibits mTOR and mTORC1. ^{1,2} As with GDC-0941 and MK2206, T-ALL cells with and without detectable PTEN expression displayed equivalent sensitivity to these inhibitors (Figure 1).

PD032901 causes sensitive cells to undergo apoptosis. *In vitro* proliferation assays characterized lines as sensitive or resistant to MEK inhibition, but the method of determining proliferation did not distinguish between cell death and cell stasis. In studies presented in the article included as Chapter 2, we assessed the mechanism of action of PD325901 in T-ALL.

We plated T-ALL cell lines with PD0325901 for 48 hours, then fixed and permeabilized them, and stained for activated Caspase-3 and Draq5. Caspase-3 is a member of the cysteine-aspartic acid protease family and is activated by both intrinsic and extrinsic pathways. ³ The caspase-3 zymogen is activated by Caspases 8 and 9 once apoptosis has begun in the cell. ⁴ Draq5 is a far-red DNA stain used in FACS analysis to determine cell cycle distribution. ⁵

Cell lines with PTEN expression that were exposed to PD0325901 underwent apoptosis, while those without detectable PTEN were resistant (Figure 2 and Supplemental Figure 6 in Chapter 2). T-ALL cell lines with and without PTEN were

PP242



RAPAMYCIN

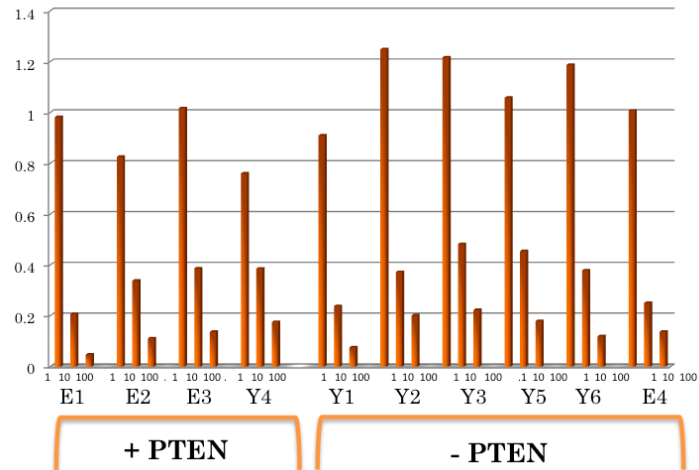


Figure 1 - PTEN expression does not alter response to PI3K inhibitors. Proliferation assays of PP242 and Rapamycin. Data are represented as percent maximum of DMSO wells. Three doses per cell line were run and no significant differences were seen between lines that have lost PTEN expression and those that retain PTEN expression.

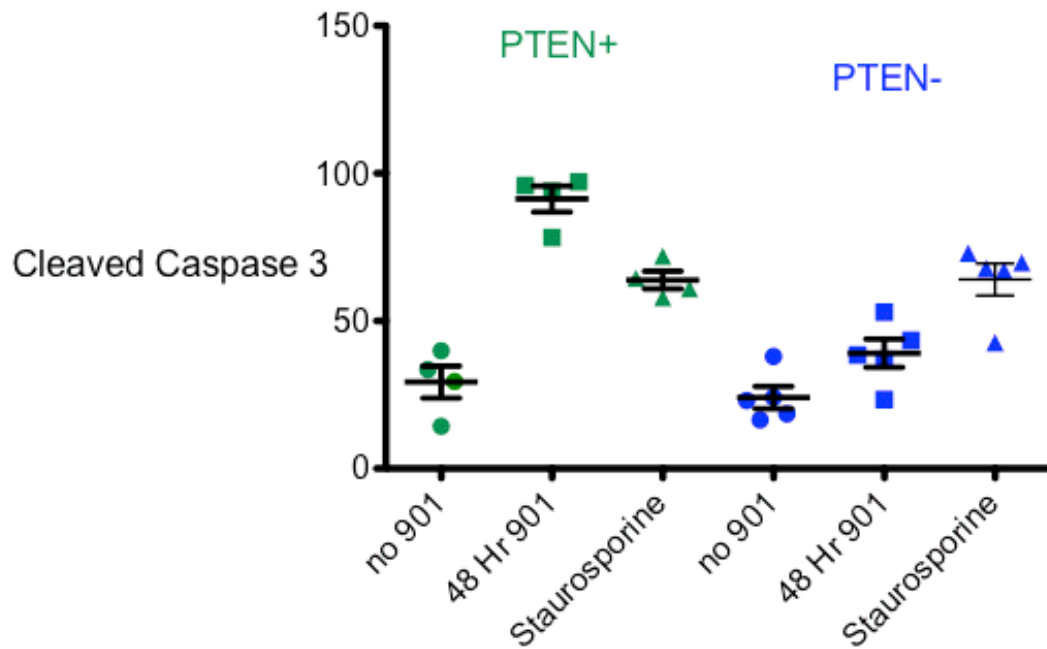


Figure 2 - Second site mutants sensitive to PD0325901 undergo apoptosis. *PTEN* expressing lines undergo apoptosis in the presence of PD0325901 as indicated by expression of cleaved caspase-3. Cells that do not express *PTEN* show no marked increase in apoptosis in the presence of PD0325901. Both lines with and without *PTEN* undergo apoptosis when treated with staurosporine.

able to undergo apoptosis when exposed to staurosporine, a potent protein kinase C inhibitor.⁶ These data indicate that PD0325901-resistant T-ALL cells do not have a global impairment in apoptosis, but they selectively fail to die when Raf/MEK/ERK signaling is inhibited. No difference was observed in cell cycle between lines with and without PTEN (Figure 3).

MEK inhibition alters expression levels of pro-apoptotic proteins. We performed Western blotting of candidate proteins as an initial step toward characterizing the mechanisms underlying whether or not T-ALL cells undergo apoptosis in response to PD0325901. Apoptosis, or programmed cell death, is a cellular response to stress that results when various regulatory signals initiate a conserved “death program” in the cell.^{7,8} The Bcl-2 family of proteins plays an essential role in triggering the apoptotic pathway (ref). This family contains over 25 proteins, both pro-apoptotic members (BAX, BAK, BAD) and anti-apoptotic (MCL-1, Bcl-2, BCL-xl) that primarily reside on the outer mitochondrial surface.⁹ Upon activation, pro-survival Bcl-2 family proteins inhibit the release of cytochrome c from the mitochondria. Conversely, pro-apoptotic proteins activate cytochrome c release, and after it is released into the cytosol it activates caspases 3 and 9, initiating apoptosis.^{9,10}

We exposed sensitive and resistant T-ALL cells to PD0325901 and collected the cells 0, 2, 4, 8, 12, 24, and 48 hours later. We hypothesized that cells that undergo apoptosis in response to MEK inhibition and might differentially express proteins associated with apoptosis. Consistent with this, we found that sensitive cell

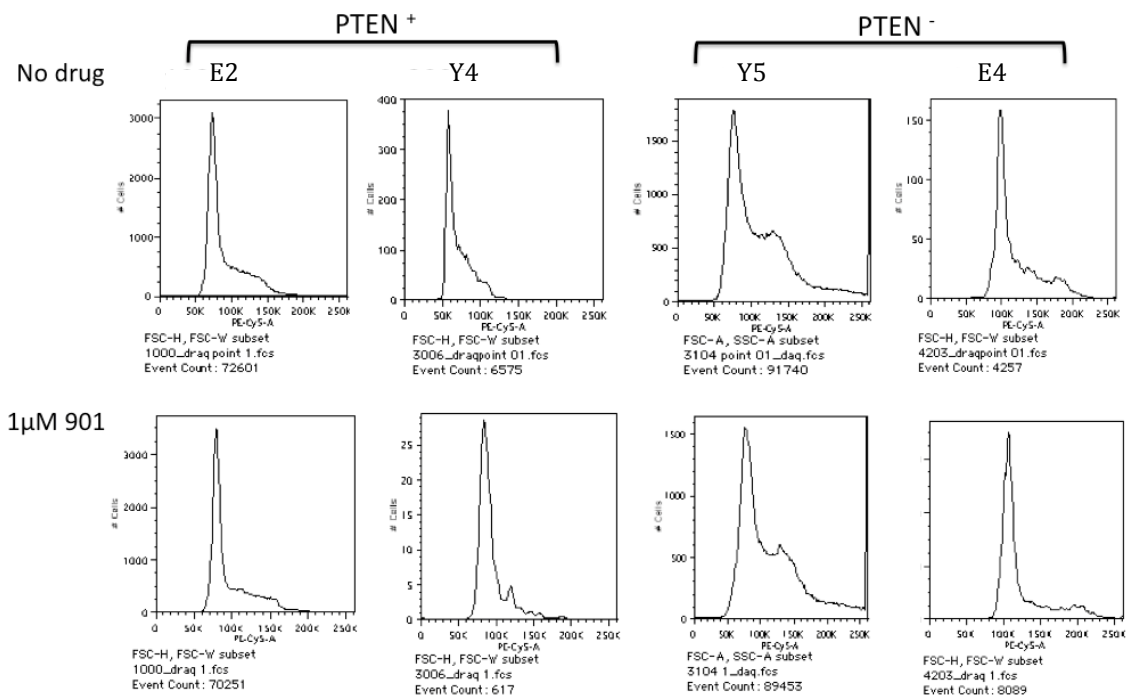


Figure 3 – T-ALL lines show no changes in cell cycle in the presence of PD0325901. T-ALL lines with and without PTEN expression show no gross differences in cell cycle after treatment with 1µM PD0325901. DNA stain Draq 5 was used 48 hours after treatment with PD0325901.

lines express equal or lower levels of the anti-apoptotic proteins MCL-1 and BCL-xl at 0, and that these levels decreased after exposure to PD0325901 (Figure 4). By contrast, cell lines resistant to inhibition of MEK by PD0325901 show equal or higher levels of these proteins in basal conditions and their expression increases or remains the same after drug exposure.

While our studies implicated hyper-activated PI3K signaling in resistance to PI3K-induced apoptosis, these data were correlative in nature. We therefore assessed the response of T-ALL cells to a combination of AKT and MEK inhibitors to test the hypothesis that reducing PI3K signaling in resistant lines would sensitize them to PD0325901. We exposed T-ALL cells to an intermediate concentration of MK2206 (0.1 μ M) that reduced pAKT to levels seen in cell lines with intact PTEN expression (Supplemental Figure 6 in Chapter 2) and a range of MEK doses. Exposing resistant T-ALL cells lacking PTEN expression to MK2206 increased sensitivity to MEK inhibition (Figure 5).

We also collected lysates from cell lines treated with a combination of PD0325901 and MK2206 as well as MK2206 alone, and performed Western blotting. These experiments showed that the expression of pro-apoptotic proteins BCL-xl and MCL-1 remained stable or increased in resistant cells treated with single agents. However, combined MEK and PI3K inhibition decreased the expression of both proteins to levels that were similar to cell lines that are sensitive to MEK inhibition alone (Figure 5).

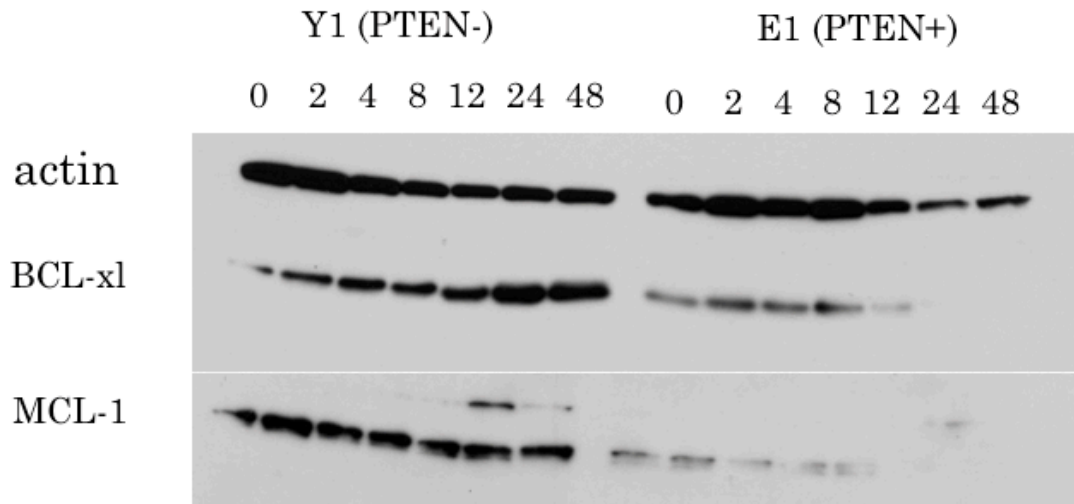


Figure 4 - Varied expression of pro-survival proteins in the presence of PD0325901. *PTEN* null cell lines express equal or higher basal levels of BCL-xl and MCL-1 and levels increase or remain steady after exposure to drug. Cell lines that express *PTEN* express lower levels of these proteins and in the presence of drug the expression decreases further. Time indicated is hours after exposure to drug.

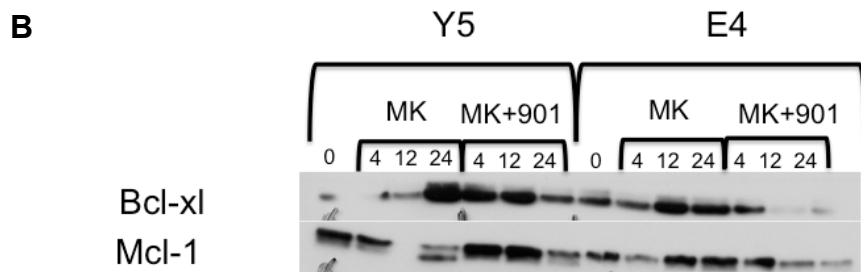
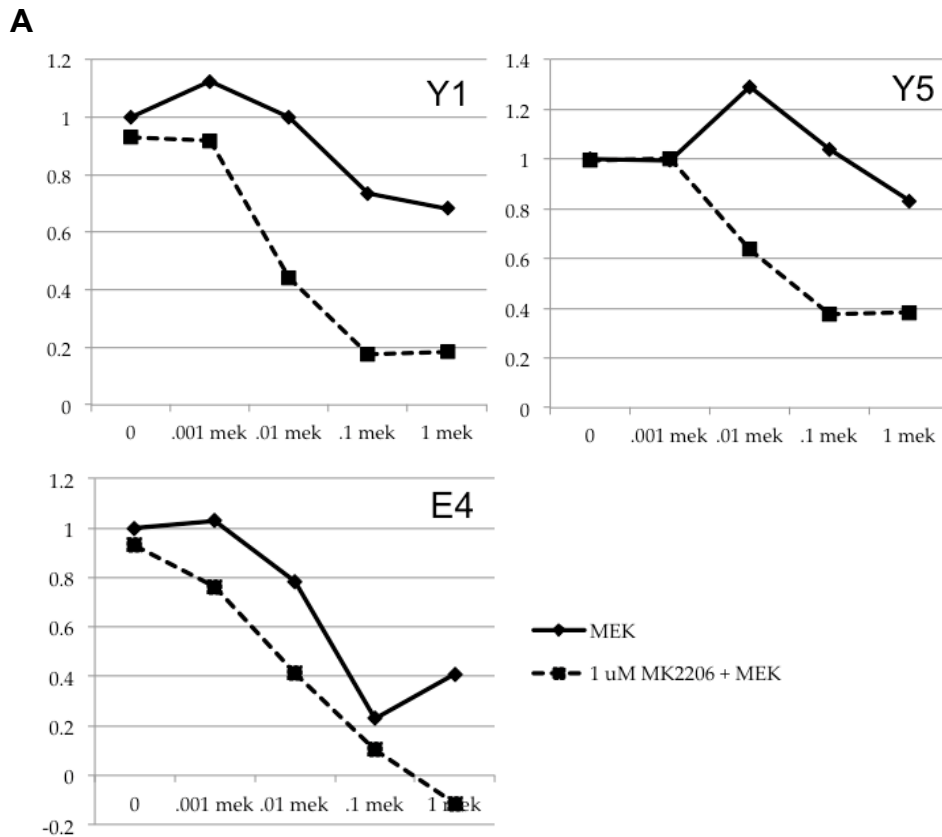


Figure 5 - Inhibition of AKT alters sensitivity to PD0325901 and expression of pro-survival proteins. (A) Increasing doses of MEK inhibitor PD0325901 alone and in combination with 1 μ M MK2206 (B) Western blot analysis of lysates of cells treated with MK2206 alone and with PD0325901 show altered expression of pro-survival proteins BCL-xl and MCL-1 in the combination treated samples. Levels of pro-survival proteins decrease over time after exposure to PD0325901 and MK2206.

Knockdown of PTEN alters sensitivity to PD0325901. Because cell lines with intact PTEN expression are uniquely sensitive to MEK inhibition, we asked if altering PTEN expression would modulate sensitivity.

We designed short-interfering RNA (siRNA) hairpins based on published sequences and annealed them into a lentivirus vector.¹¹⁻¹³ Efficient knockdown of PTEN protein expression was confirmed in NIH 3T3 cells (Figure 6). We transduced T-ALL cell lines with these hairpins, and after 72 hours placed the cells in 0.1 μ M PD0325901. After 72 hours we increased the dose to 1 μ M, waited 72 hours, then performed flow cytometry.

Cell lines with intact PTEN expression that were treated with the hairpin survived in PD00325901 at levels similar to cell lines lacking PTEN that were resistant to PD0325901 (Figure 7). Additionally, cells from lines with PTEN that were alive in the presence of PD0325901 expressed the hairpin at much higher frequency, indicating a growth advantage, whereas cells from lines that express no PTEN expressed the hairpin at low levels.

Western blots from cell lines with PTEN expression that have been exposed to the hairpin showed increases in AKT, BCL-xl, and MCL-1 (Figure 7), similar to what is seen in second site cell lines that have lost PTEN expression.

Together with studies in which we exposed PD0325901-resistant T-ALL cell lines to both MEK and AKT inhibitors, these data implicate loss of PTEN expression as a critical determinant of sensitivity of MEK inhibitions and suggests that activated AKT mediates resistance through BCL-xl and MCL-1 expression.

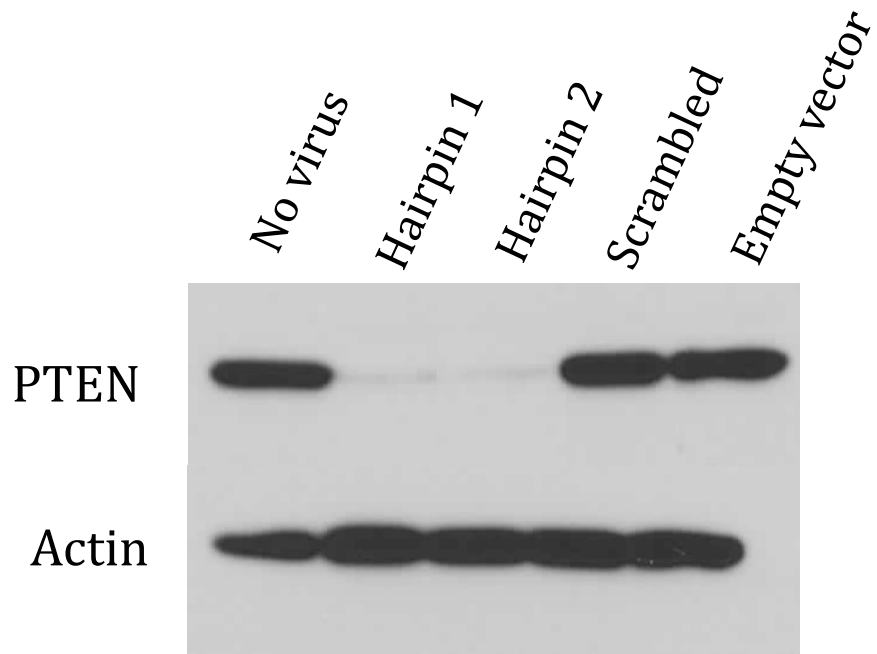


Figure 6 - Knockdown of PTEN using siRNA vectors. Western blot showing efficient knockdown of PTEN in NIH3T3 cells.

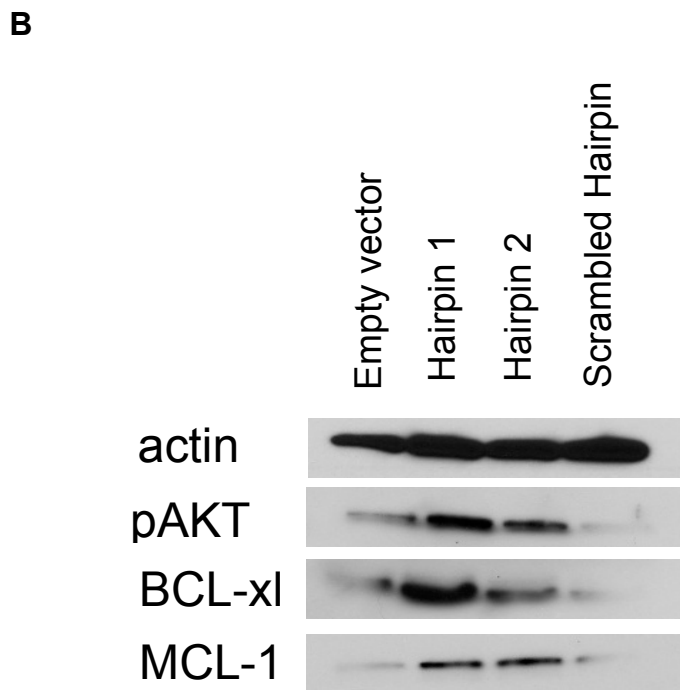
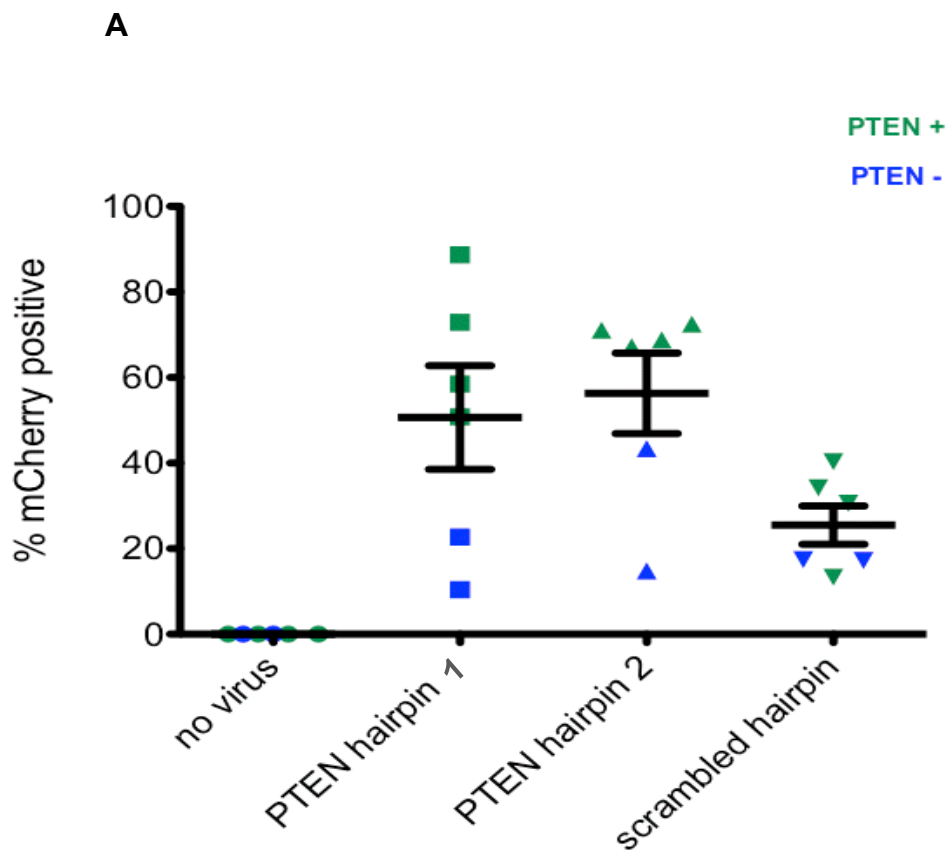


Figure 7 - PTEN knockdown alters sensitivity to PD0325901 and expression of pro-survival proteins. (A) Percentage of live cells expressing hairpins in the presence of PD0325901 indicates a selective advantage for PTEN⁺ cells to express PTEN siRNA hairpins. (B) PTEN knockdown increases expression of pAkt, BCL-xl and Mcl-1.

Discussion

Second-site mutants of Ras are a unique biological system that facilitate studies of distinct downstream Ras effectors. As Ras is yet undruggable, these second-site mutants can shed insight into which downstream pathways are most important for cancer initiation and maintenance. Adding chemical inhibitors to this genetically-defined system provides further information regarding signaling pathways that are required for proliferation and survival.

To determine if pathway activation of second site mutants could influence responses to chemical inhibition, cell lines were treated with a variety of inhibitors (Figure 1). Interestingly, both E37G and Y64G cell lines were sensitive to inhibition of the PI3K pathway irregardless of PTEN status. This was surprising given that in lines without PTEN expression, pAKT levels were significantly higher. It has previously been thought that higher activation of a pathway is correlated to a greater sensitivity to inhibition of the pathway, as cells that have increase flux through a pathway may become dependent on that increased signal. Second-site T-ALL cell lines are sensitive to PI3K pathway inhibition, regardless of basal pathway activation.

To elucidate the effects PD0325901 was having in sensitive T-ALL cells, we assessed cell cycle status and apoptosis in the presence of this drug (Figures 2, 3). Chemically inhibiting the Raf/MEK/ERK pathway can alter proliferation, as demonstrated in thyroid cancer cell lines, or cause cells to undergo apoptosis, as seen in studies on multiple myeloma, non-small cell lung cancer, and ovarian cancer.

¹⁴⁻¹⁷ While we observed no changes in cell cycle status in sensitive T-ALL cells

treated with PD0325901, there was a marked increase in apoptosis, as measured by cleaved Caspase 3. Cell lines that were sensitive to inhibition of pERK by PD0325901 demonstrated lower basal levels of the anti-apoptotic proteins BCL-xl and MCL1, and levels decreased over time after exposure to PD0325901. By contrast, resistant second-site cell lines showed higher basal levels of these proteins that persisted or increased in the presence of PD0325901 (Figure 4).

We investigated if treating our second-site cell lines that were resistant to PD0325901 with an AKT inhibitor would alter their sensitivity to pERK inhibition. MEK inhibition has been seen to synergize with PI3K inhibition in many models including non-small cell lung cancer, rhabdomyosarcoma, *NRAS* driven melanomas, breast cancer, and *KRAS* mutant colorectal cancer.¹⁸⁻²⁰ In hematopoietic cells activated PI3K and MEK pathways converge to regulate the cell cycle.²¹

The influence of PTEN status on sensitivity to MEK inhibitors was characterized with the inhibitor E6201 in melanoma cell lines, where wild-type PTEN correlated with sensitivity to MEK inhibition and resistance correlated with PI3K pathway activation, as we saw in our studies.²² Similarly, in *KRAS* mutant colorectal cell lines, PI3K activation through loss of PTEN led to reduced sensitivity resistance to PD0325901.²³ The resistant phenotype was seen more robustly in cell lines lacking PTEN compared to those with activating *PIK3CA* mutations, which the authors interpreted as indicating that either loss of PTEN activated the pathway more potently, or loss of PTEN had other effects on the cell that allowed them to survive despite MEK inhibition. A combination of a PD0325901 and inactivation of *PIK3CA* resulted in the cells becoming sensitive to PD0325901, similar to we saw in

our experiments. In breast cancer cell lines, PTEN loss was demonstrated to be a negative predictor of MEK sensitivity, and PI3K inhibition synergized with MEK inhibition to decrease cell proliferation.²⁴ In an ovarian cancer mouse model generated by Kras^{G12D} expression and tissue-specific PTEN deletion, tumors were resistant to PI3K inhibition by PF-04691502, but when combined with PD0325901 these tumors regressed.¹⁴

In our studies, when cell lines were treated with PD0325901 and MK2206, lines that were resistant to ERK inhibition became sensitive, indicating that high levels of phosphorylated AKT is not just a bio marker of resistance to PD0325901, but AKT is mediating the resistant phenotype (Figure 7).

Phosphorylated AKT serves a strong pro-survival function in cells. Phosphorylated AKT directly regulates apoptosis by inhibiting the pro-apoptotic protein Bad, causing it to dissociate from pro-survival Bcl-2 family members BCL-2 and BCL-xl, which allows them to localize to the surface of the mitochondria where they block cytochrome c release.^{25,26} Cytochrome c is a heme protein and an intermediate in apoptosis that is released from the mitochondria and signals to the endoplasmic reticulum to release calcium, which triggers more cytochrome c in a positive feedback loop.²⁷ When calcium levels are high enough, cytochrome c is released at such levels that it activates caspase 9, which activates caspases 7 then 3, and the cell undergoes apoptosis.²⁸ AKT also directly blocks apoptosis through phosphorylating Bax, which hinders its ability to localize to the mitochondria and make pores to stimulate cytochrome c release.²⁹ Several forkhead transcription factors are also direct targets for AKT, and when phosphorylated by AKT they are

sequestered in the cytoplasm, unable to localize to the mitochondria and mediate the mitochondrial independent death pathway.³⁰ Indirectly, phosphorylated AKT inhibits GSK3 β , which, when activated, degrades Mcl-1. Mcl-1 works on the surface of the mitochondria to block cytochrome c release and this inhibit apoptosis, so in the presence of AKT, Mcl-1 is able to exert its pro-survival function. Activated AKT can also activate Mdm2, which negatively regulates p53.³¹

Because of the known pro-survival role of AKT and the finding that PD0325901-sensitive T-ALL cells were undergoing apoptosis, we performed Western blotting to determine if pro-survival proteins were being altered in the presence of drug, and if sensitive and resistant cell lines had altered levels of these proteins (Figure 4). Indeed, we found that cell lines that retained PTEN expression and were sensitive to MEK inhibition expressed low basal levels of the pro-survival proteins BCL-xl and MCL-1. Alternatively, cell lines lacking PTEN expression had high AKT levels and also showed higher levels of these proteins in basal conditions, which remained steady or increased in the presence of PD0325901.

The Raf/MEK/ERK pathway also plays a role in apoptosis, though it is thought to be less pivotal than AKT. ERK activates transcription factors that can lead to upregulation of Bcl-2 family members.³² Phosphorylation of BIM by ERK decreases the interaction of BIM and BAX, and decreases BIMs pro-apoptotic function.³³ Mcl-1 is also phosphorylated by ERK, and this phosphorylation slows Mcl-1 protein turnover.³⁴

The discovery that pro-survival proteins differed between sensitive and resistant cell lines leads us to hypothesize that a cells ability to survive in the

presence of PD0325901 is largely dependent on its inability to avoid apoptosis. Cells with high levels of AKT have likewise high levels of pro-survival protein MCL-1, and BCL family members in the cell are blocking cytochrome c release and inhibiting apoptosis. In cell lines with PTEN, phosphorylated AKT is reduced and thus the pro-survival effects are diminished. This makes cells more sensitive to cell death by decreases in phosphorylated ERK, as the cells lose the contribution of the Raf/MEK/ERK pathway to their survival, and as they express PTEN and have low levels of phosphorylated AKT, had lower activity of pro-survival proteins to begin with.

There are no previous reports correlating the expression of pro-survival Bcl-2 family members at baseline in cells with elevated AKT. However, the differences we observed could be due post-translational mechanisms or the involvement of other pathways known to regulate expression of pro-survival proteins such as Ets transcription factors, NF-kappaB signaling, or activated integrins.³⁵⁻³⁷

When our second-site cell lines were treated with a combination of PD0325901 and MK2206, the lines that had been resistant to inhibition became sensitive. Western blots showed that levels of pro-survival proteins BCL-xl and MCL-1 increased or did not change in the presence of MK2206 alone, but in the presence of the combination, these proteins decreased to levels seen in sensitive sell lines (Figure 5).

The failure of MK2206 to reduce expression of pro-survival proteins may be explained by the complex compensatory network of pro-survival proteins in the cell. It may be that in cells with a high basal level of these proteins, shutting down

phosphorylated ERK or AKT alone is not enough to cause the levels of pro-survival proteins to fall and apoptosis to occur, but a combination of a shut down in both the MEK/ERK and PI3K pathways causes the cells to undergo apoptosis.

We sought to determine if PTEN was responsible for the changes in AKT that allowed for resistance to PD0325901, so hairpins were designed to knockdown PTEN. Cells were transduced and treated with PD0325901, and collected for analysis by FACs. We showed that cell lines that retained PTEN expression and were sensitive to PD0325901 were made resistant when they expressed the hairpin (Figure 6). A scrambled hairpin had no effect, and the PTEN siRNA did not affect cell lines lacking PTEN expression.

Experiments in colorectal cancer cell lines mentioned previously showed that PI3K activation due to loss of PTEN enhanced resistance to PD0325901.²³ These authors engineered a *KRAS* mutant cell line to express an shRNA targeted to PTEN. Similar to our findings, they observed that decreasing PTEN levels in cells sensitive to PD0325901 reversed the sensitivity.²³ Likewise in the breast cancer study, RNA-interference knockdown in Kras-driven tumor cells decreased the cells sensitivity to PD0325901. These data support our conclusion that loss of PTEN expression may be responsible for decreased sensitivity to MEK inhibition in Kras driven cancers.²⁴

Our studies show that cell lines with and without PTEN are equally sensitive to inhibition of AKT, that inhibition of AKT and MEK in combination cause cell lines that were resistant to MEK inhibition to become sensitive, and that pro-survival proteins are altered in cell lines that are sensitive to PD0325901. Though further investigations are needed to determine whether MCL-1 and BCL-xl are required for

a resistant phenotype and to prove that PTEN is mediating this response through AKT, our results argue that activated AKT through loss of PTEN plays a role in drug sensitivity through the actions of pro-survival proteins BCL-xl and MCL-1. Activation of AKT through loss of PTEN renders cells resistant to MEK inhibition.

Materials and Methods

Proliferation Assays. T-ALL second site cell lines were plated at a density of 30,000/100 μ L in 96 well plates. Drug was added in varying concentrations in triplicate. After 48 hours, 20 μ L CellTiter 96® AQueous Non-Radioactive Cell Proliferation Assay (Promega, USA) was added and the plates were incubated for 4 hours. Plates were read according to the manufacturer's instructions. Growth curves were established as percentages of maximal growth in DMSO and IC₅₀ values were calculated.

Western Blots. Cells were collected and subsequently lysed in a RIPA buffer, quantitated by Bradford assay, and run on 10% TGX gels (BioRad). Blots were blocked with 5% milk in TBS-T for 20 minutes and in primary antibody overnight. Antibodies used for immunoblotting included BclX (Epitomics) and actin and Mcl1 (Cell Signaling).

Apoptosis and Cell Cycle Assays. T-ALL second site cell lines were plates to a density of 50,000 cells per well in 1 μ M PD0325901. After 48 hours, the cells were collected, fixed with paraformaldehyde, and treated with an antibody against cleaved Caspase-3 (BD) or DNA stain Draq 5 (Invitrogen). FACS data were acquired

with LSRII (BD Biosciences) using FACSDiva software and analyzed with FlowJo (Tree Star).

PTEN Hairpin constructs. Published hairpin sequences to PTEN were modified to 19mers with compatible ends for the pSicoR vector. Oligos ordered from IDT and annealed via PCR, ligated, and checked by miniprep and sequencing (MCLab).

Transfection and Transduction With PTEN Constructs. Pten hairpin lentivirus was made using Fugene reagent (Promega) and 293T cells. After 48 hours, supernatants were collected, filtered, and concentrated by ultracentrifugation (25,000 g for 90 minutes). After resuspension, second site T-ALL cell lines were transduced with virus. 100,000 cells were plated in 2mls of media with virus in a 6-well plate and spun at 2500rpm for 2 hours in the presence of 1x polybrene, then incubated for an additional 2 hours before 6ml of clean media was added.

Sensitivity Assays with PTEN knockdown. 72 hours after transduction cell lines were placed in .01 μ M PD0325901. After 72 more hours, the doses of drug was increased to 1 μ M. 72 hours after the doses increase, cell lines were collected and analyzed by FACS as described above. Cell sorting for Western blot analysis was done on a FACS Aria III.

References

1. Apse B, Blair JA, Gonzalez B, et al. Targeted polypharmacology: discovery of dual inhibitors of tyrosine and phosphoinositide kinases. *Nature Chemical Biology*. 2008-10-12 2008;4(11):691-699.
2. Dumont FJ, Staruch MJ, Koprak SL, et al. Distinct mechanisms of suppression of murine T cell activation by the related macrolides FK-506 and rapamycin. *J Immunol*. 1990-01-01 1990;144(1):251-258.
3. Salvesen GS. Caspases: opening the boxes and interpreting the arrows. *Cell Death and Differentiation*. 2002-01-04 2002;9(1):3-5.
4. Walters J, Pop C, Scott FL, et al. A constitutively active and uninhibitable caspase-3 zymogen efficiently induces apoptosis. *Biochem J*. Dec 15 2009;424(Pt 3):335-345.
5. Smith PJ, Wiltshire M, Davies S, et al. A novel cell permeant and far red-fluorescing DNA probe, DRAQ5, for blood cell discrimination by flow cytometry. *J Immunol Methods*. Oct 29 1999;229(1-2):131-139.
6. Karaman MW, Herrgard S, Treiber DK, et al. A quantitative analysis of kinase inhibitor selectivity. *Nature Biotechnology*. 2008-01-08 2008;26(1):127-132.
7. Kerr JFR, Wyllie AH, Currie AR. Apoptosis: A Basic Biological Phenomenon with Wide-ranging Implications in Tissue Kinetics. *Br J Cancer*. Aug 1972;26(4):239-257.
8. Green DR. *Means to an End; Apoptosis and Other Cell Death Mechanisms*: Cold Spring Harbor Press; 2011.

9. Chao DT, Korsmeyer SJ. BCL-2 FAMILY: Regulators of Cell Death. *Annu Rev Immunol.* 2003-11-28 1998;16:395-419.
10. Zamzami N, Brenner C, Marzo I, et al. Subcellular and submitochondrial mode of action of Bcl-2-like oncoproteins. *Oncogene* 1998-04-27 1998;16(17):2265.
11. Ventura A, Meissner A, Dillon CP, et al. Cre-lox-regulated conditional RNA interference from transgenes. *Proc Natl Acad Sci U S A.* Jul 13 2004;101(28):10380-10385.
12. Reynolds A, Leake D, Boese Q, Scaringe S, Marshall WS, Khvorova A. Rational siRNA design for RNA interference. *Nat Biotechnol.* Mar 2004;22(3):326-330.
13. Luikart BW, Schnell E, Washburn EK, et al. Pten Knockdown in vivo Increases Excitatory Drive onto Dentate Granule Cells. *J Neurosci.* Mar 16 2011;31(11):4345-4354.
14. Kinross KM, Brown DV, Kleinschmidt M, et al. In Vivo Activity of Combined PI3K/mTOR and MEK Inhibition in a KrasG12D;Pten Deletion Mouse Model of Ovarian Cancer. *Molecular Cancer Therapeutics.* 2011-08-01 2011;10(8)1440-9.
15. Kandil E TK, Ma J, Abd Elmageed ZY, et al. Synergistic inhibition of thyroid cancer by suppressing MAPK/PI3K/AKT pathways. Available online 2 April 2013 2013;4804(13):246.
16. Meng J DB, Fang B, Bekele BN, et al. Combination Treatment with MEK and AKT Inhibitors Is More Effective than Each Drug Alone in Human Non-Small Cell Lung Cancer In Vitro and In Vivo. *PLOS ONE.* 2010/11/29 2010;5(11).

17. Kim K KS, Fulciniti M, Li X, et al. Blockade of the MEK/ERK signalling cascade by AS703026, a novel selective MEK1/2 inhibitor, induces pleiotropic anti - myeloma activity in vitro and in vivo. *British Journal of Haematology*. 2010;149(4):537-549.
18. Jokinen E, Laurila N, Koivunen JP. Alternative dosing of dual PI3K and MEK inhibition in cancer therapy. *BMC Cancer*. 2012-12-21 2012;12(1):612.
19. Guenther MK GU, Fulda S. Synthetic lethal interaction between PI3K/Akt/mTOR and Ras/MEK/ERK pathway inhibition in rhabdomyosarcoma. *Cancer Letters*. Available online 16 May 2013 2013;13:379-390.
20. Britten CD. PI3K and MEK inhibitor combinations: examining the evidence in selected tumor types. *Cancer Chemotherapy and Pharmacology*. 2013;71(6):1395-1409.
21. Shelton JG, Blalock WL, White ER, Steelman LS, McCubrey JA. Ability of the Activated PI3K/Akt Oncoproteins to Synergize with MEK1 and Induce Cell Cycle Progression and Abrogate the Cytokine-Dependence of Hematopoietic Cells. *Cell Cycle*. 2004;3(4):501-510.
22. Byron SA, Loch DC, Wellens CL, et al. Sensitivity to the MEK inhibitor E6201 in melanoma cells is associated with mutant BRAF and wildtype PTEN status. *Molecular Cancer*. 2012-10-05 2012;11(1):75.
23. Wee S, Jagani Z, Xiang KX, et al. PI3K Pathway Activation Mediates Resistance to MEK Inhibitors in KRAS Mutant Cancers. *Cancer Research*. 2009-05-15 2009;69(4286).

24. Hoeflich KP, O'Brien C, Boyd Z, et al. In vivo Antitumor Activity of MEK and Phosphatidylinositol 3-Kinase Inhibitors in Basal-Like Breast Cancer Models. *Clinical Cancer Research*. 2009-07-15 2009.
25. Hay N. The Akt-mTOR tango and its relevance to cancer. *Cancer Cell*. Sep 2005;8(3):179-183.
26. Datta SR, Brunet A, Greenberg ME. Cellular survival: a play in three Akts. *Genes and Development*. 1999-11-15 1999.
27. Xuesong Liu CNK, Jie Yang, Ronald Jemmerson and Xiaodong Wang. Induction of Apoptotic Program in Cell-Free Extracts: Requirement for dATP and Cytochrome c. *Cell*. July 12 1996 1996;86(1):147-157.
28. Boehning D, Patterson RL, Sedaghat L, Glebova NO, Kurosaki T, Snyder SH. Cytochrome c binds to inositol (1,4,5) trisphosphate receptors, amplifying calcium-dependent apoptosis. *Nature Cell Biology*. 2003-11-09 2003;5(12):1051-1061.
29. Gardai SJ, Hildeman DA, Frankel SK, et al. Phosphorylation of Bax Ser184 by Akt regulates its activity and apoptosis in neutrophils. *J Biol Chem*. May 14 2004;279(20):21085-21095.
30. Brunet A BA, Zigmund MJ, Lin MZ, Juo P, Hu LS, Anderson MJ, Arden KC, Blenis J, Greenberg ME. Akt Promotes Cell Survival by Phosphorylating and Inhibiting a Forkhead Transcription Factor. *Cell*. 1999;96(6):857-868.
31. Stiles BL. PI-3-K and AKT: Onto the mitochondria. *Advanced Drug Delivery Reviews*. 30 November 2009 2009;61(14):1276-1282.

32. Chang F, Steelman LS, Shelton JG, et al. Regulation of cell cycle progression and apoptosis by the Ras/Raf/MEK/ERK pathway (Review). *Int J Oncol*. Mar 2003;22(3):469-480.
33. McCubrey JA, Steelman LS, Abrams SL, et al. Targeting survival cascades induced by activation of Ras/Raf/MEK/ERK, PI3K/PTEN/Akt/mTOR and Jak/STAT pathways for effective leukemia therapy. *Leukemia*. 2008-03-13 2008;22(4):708-722.
34. Schubert K, Duronio V. Distinct roles for extracellular-signal-regulated protein kinase (ERK) mitogen-activated protein kinases and phosphatidylinositol 3-kinase in the regulation of Mcl-1 synthesis. *Biochem J*. 2001-06-01 2001;356(Pt 2):473-480.
35. Borjes J-C, Willerford DM, Grevin D, et al. Increased T-cell apoptosis and terminal B-cell differentiation induced by inactivation of the Ets-1 proto-oncogene. *Nature*. 1995-10-19 1995;377(6550):635-638.
36. Sheikh MS, Huang Y. Death Receptor Activation Complexes: It Takes Two to Activate TNF Receptor 1. *Cell Cycle*. 2003;2(6):549-551.
37. Stupack DG, Cheresch DA. Get a ligand, get a life: integrins, signaling and cell survival. *Cell Science*. 2002-10-01 2002;115:3729-3738.

Chapter 4: Mechanism of PTEN Silencing in T-ALL Cell Lines

Introduction

Phosphatidylinositol (3,4,5)-triphosphate [PtdIns(3,4,5)P₃] phosphatase and tensin homolog (PTEN) is one of the most commonly mutated tumor suppressors in cancer. ¹ PTEN is the major regulator of cellular levels of PtdIns(3,4,5)P₃, and its major roll in the cell is to catalyze the integral second messenger PtdIns (3,4,5)P₃ to phosphatidylinositol (4,5)- biphosphate [PtdIns(4,5)P₂]. ² High levels of PtdIns(3,4,5)P₃ decreases signaling of downstream receptor tyrosine kinases including the PI3 kinase pathway, and it is through this negative regulation of PI3K/AKT signaling that PTEN is thought to exert its tumor suppressor activity. ³ AKT activation is dependent on PtdIns(3,4,5)P₃, so dephosphorylation of PtdIns(3,4,5)P₃ by PTEN leads to inhibition of AKT. Loss of PTEN expression leads to activated AKT as it is recruited by a build up of PtdIns(3,4,5)P₃ at the plasma membrane, and an increase in flux through the PI3K pathway leading to increases in cell proliferation, metabolic activities, and a decrease in apoptosis. ⁴

PTEN is mutated in many human cancers, including skin, prostate, endometrial carcinoma, and glioblastoma multiforme, and individuals with germline PTEN mutations are predisposed to multiple cancers. ⁵ PTEN plays a role in a variety of essential cellular functions including leukemic stem cell self renewal through mTOR, cell cycle progression and DNA repair through RAD51, proliferation and apoptosis through AKT, and recently, PTEN has been shown to act in a non-PI3K dependent manner to regulate eukaryotic translation initiation factor 2 α kinase 2 (eIF2 α K2), JNK, and SRC. ⁶⁻⁸

PTEN is ubiquitously expressed in human cells, but its expression is carefully controlled.⁹ One such control of PTEN is epigenetic silencing. In several cancer types, the promoter region of PTEN is highly methylated, resulting in the region being less transcriptionally active.¹⁰ Additionally, PTEN transcription can be altered by changes in the chromatin.¹¹ Histone acetylation/deacetylation is controlled by the transcription factor SALL4, which represses PTEN through recruitment of an ATPase and histone deacetylase complex.¹² A lack of methylation in several genes including PTEN correlated with good prognosis in T-ALL patients, and promoter methylation and subsequent silencing of PTEN has been observed in gliomas, glioblastomas, JMML, gastric carcinoma, hepatocellular carcinoma, non-small cell lung carcinoma, melanoma, and breast, prostate, and colorectal cancers.¹³⁻¹⁷

PTEN expression is lost and PI3K signaling is activated in 5 of the 6 second-site T-ALL cell lines that harbor Y64G mutations (Figure 2 in Chapter 2). Quantitative real-time PCR indicated markedly reduced mRNA expression levels of PTEN (Supplemental Figure 2 in Chapter 2). One E37G line, E4/4203, has no PTEN expression but harbors a somatic mutation in PTEN (Supplemental Figure 2 in Chapter 2). The one Y64G cell line that does not lose PTEN expression, Y4/3006, had a 6 nucleotide insertion in the switch II region of Ras, between codons 69 and 70. This in-frame insertion partially activates the PI3K and is seen in patients with lung cancer, colon cancer, and JMML.^{18,19} DNA sequencing of the 5 Y64G T-ALL cell lines without PTEN expression revealed no mutations, so we sought to determine the mechanism of *Pten* silencing in these lines.

Results

Bisulfite sequencing does not alter PTEN DNA Sequence. Because DNA methylation is an important regulator of gene expression and the *Pten* promoter is often methylated in cancer, we performed bisulfite sequencing of second-site T-ALL cell lines.

Genomic DNA from cell lines underwent bisulfite modification, where cells are treated with sodium bisulfite, which converts unmethylated cytosines to thymines but leaves methylated cytosines unchanged.²⁰ Samples are then purified, and sent for DNA sequencing.

DNA sequencing revealed no differences between T-ALL cell lines treated and untreated with bisulfite (Figure 1). In the presence of methylated promoters, we would expect that bisulfite sequencing would result in DNA that would consist of thymines and cytosines, but sequencing confirmed the absence of any cytosines across all the regions studied, showing no evidence of methylation in the promoter region of *Pten*.

5 azacytidine Does Not Alter PTEN Expression. 5-azacytidine inhibits DNA methyltransferases and induces hypomethylation.²¹ We hypothesized that if PTEN is methylated in our second-site cell lines and methylation is leading to the loss of

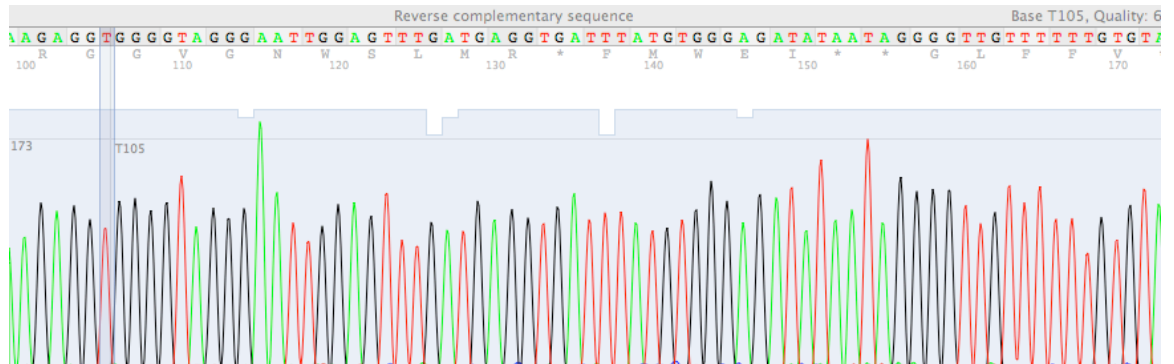


Figure 1 – Bisulfite sequencing of PTEN deficient cells. Genomic DNA from T-ALLs that have lost PTEN expression underwent bisulfite conversion, which revealed no protected cytosines, as evidenced by the loss of cytosines in sequenced samples. Line shown is Y5 but is representative of all Pten- lines and all primer sets tested.

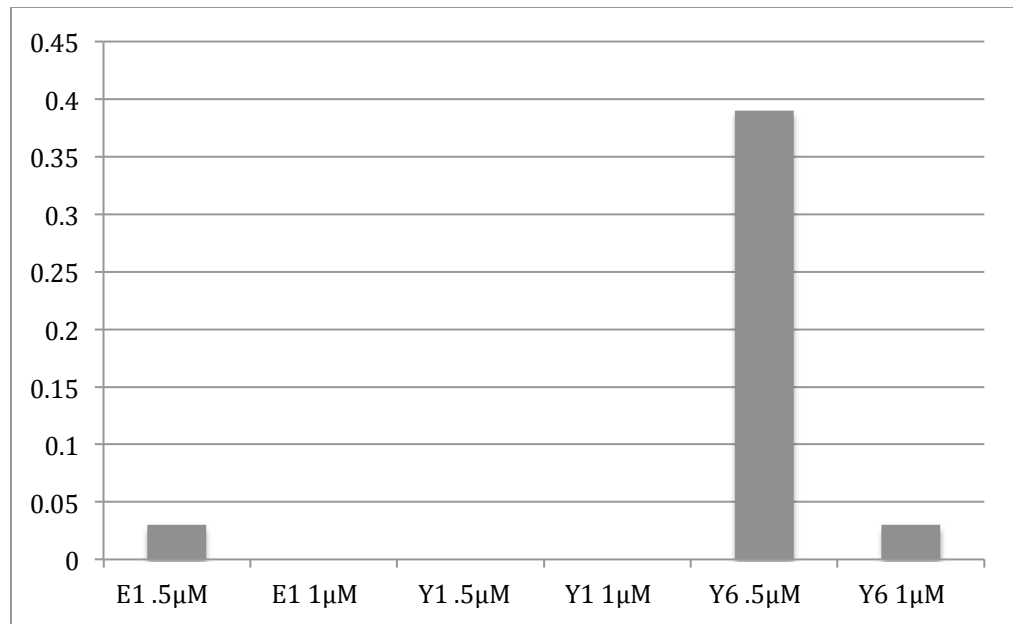
PTEN expression, treating cells with an inhibitor of methylation may reverse this effect. Therefore, we exposed cell lines lacking PTEN expression to 1.0 or 0.5 μ M doses of 5-azacytidine for 3 days. We reasoned that if PTEN was re-expressed as a result of 5-azacytidine treatment that this might result in a decrease in proliferation as the PI3K pathway was inhibited. However, no gross changes in proliferation were seen and cell lines were collected for qRT-PCR to evaluate PTEN levels. Although we were able to detect PTEN in our PTEN⁺ lines, no changes in PTEN mRNA were seen after treatment in 5-azacytidine, further leading us to presume that methylation is not the mechanism by which PTEN expression is lost in our cell lines (Figure 2).

To confirm that the dose of 5-azacytidine we were using was biologically active, a published study was replicated wherein 5-azacytidine was seen to increase expression of ZNF645 in 293T cells (Figure 2).²² The same doses used on our second-site cell lines did indeed induce expression of a known methylated and transcriptionally repressed gene.

Trichostatin A Does Not Re-Activate PTEN. Trichostatin A is a histone deacetylase inhibitor with epigenetic activity.²³ Histone deacetylases remove acetyl groups from amino acids on histone. This removal allows histones to bind DNA more tightly, condensing the DNA and decreasing transcription. HDAC inhibitors increase histone acetylation and decrease the deacetylation, making DNA more accessible on the histone.²⁴ In addition to its action on the chromatin, Trichostatin A has been demonstrated to induce PTEN transcription and is known to promote Egr-1 expression. Egr-1 is the main transcription factor regulating PTEN, and up-

regulation of Egr-1 has been seen to increase PTEN expression.²⁵ Finally, histone acetyltransferase synergistically activates PTEN transcription with Egr-1, which implicates the role of histone acetylation in PTEN regulation.²⁶

A



B

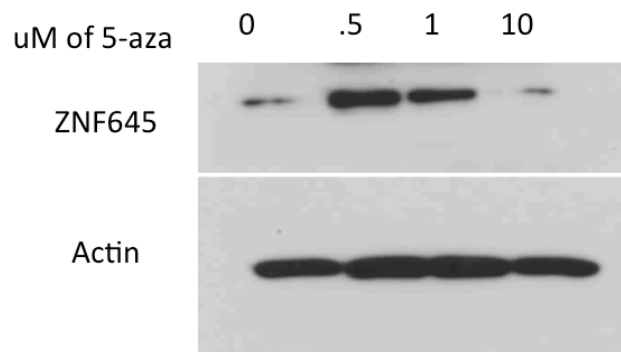


Figure 2 - 5-azacytidine treatment does not alter PTEN expression. (A) qRT-PCR on samples treated with .5 and 1µM 5-azacytidine did not indicate re-expression of PTEN as determined by fold values using delta-delta Ct. (B) Western blots of 293T cells treated with .5 and 1µM 5-azacytidine did reveal re-expression of ZNF645.

We asked if histone deacetylation was responsible for the loss of PTEN expression in our second-site cell lines. We set up proliferation assays of our second-site cell lines in the presence of varying doses of Trichostatin A. When the control well was confluent, wells were counted. We hypothesized that if histone modification was responsible for PTEN loss, treatment of Trichostatin A could reverse this effect and cause re-expression of PTEN in our lines, which might then decrease proliferation through PTEN's effects of the PI3K pathway. Although all of our cell lines were sensitive to doses of Trichostatin A, we observed no measurable differences in the sensitivity of lines with and without PTEN to an HDAC inhibitor (Figure 3).

After 96 hours in Trichostatin A, cell lines were collected for Western blotting to determine if expression of PTEN was altered in the presence of drug. We saw no re-expression of PTEN in lines with PTEN loss after treatment with Trichostatin A. As a control, we looked at levels of H3, a histone protein involved in nucleosome structure.²⁷ H3 is known to be acetylated, so it served as a positive control for our studies and validated the doses of Trichostatin A used in our cell lines were sufficient to cause modulate H3 (Figure 4).

Finally, after cells were treated with Trichostatin A for 96 hours, they were collected and RNA was isolated for Qrt-PCR. We saw no induction of PTEN in lines after treatment of Trichostatin A (Figure 5), leading us to surmise that histone

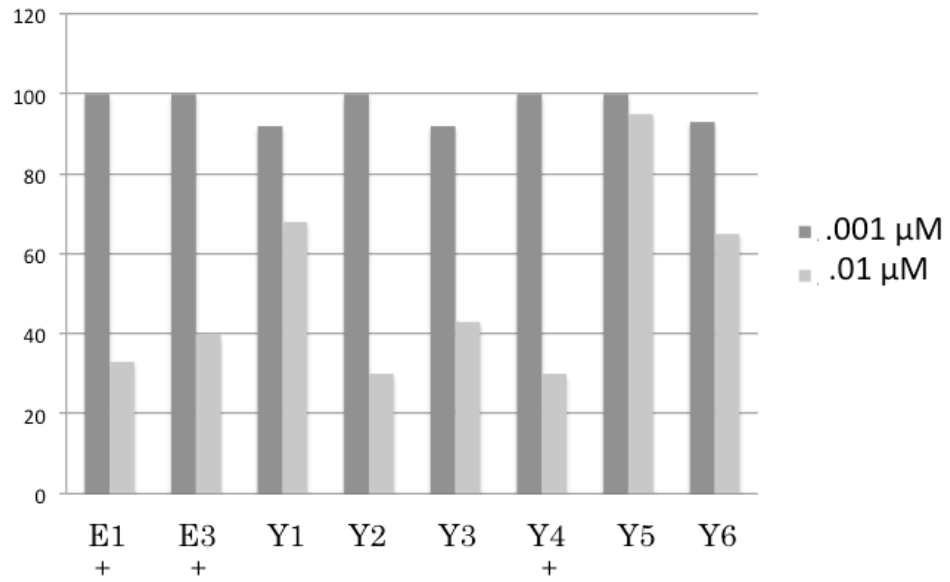


Figure 3 – Cell lines show no changes in proliferation in response to treatment with Trichostatin A. Proliferation assays of T-ALL cells treated with varying doses of Trichostatin A. Values are shown as percent of control (DMSO) well. Plus signs indicate lines that express PTEN.

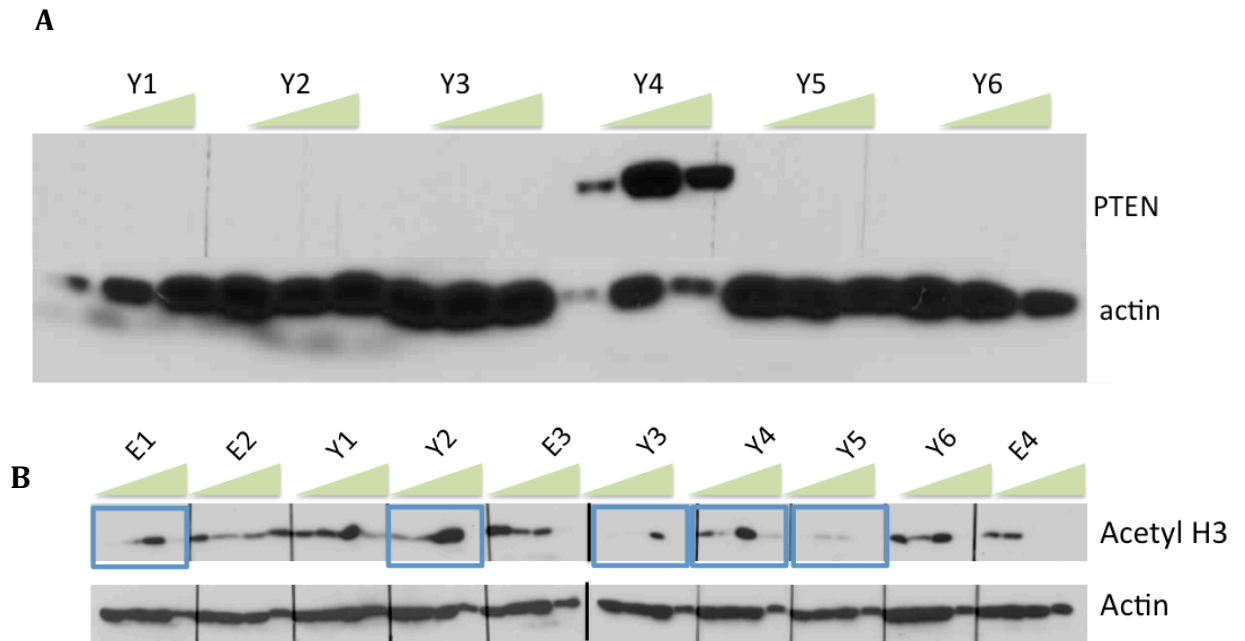


Figure 4 - Trichostatin A does not alter PTEN expression. Western blot analysis of T-ALL cells treated with Trichostatin A indicates that (A) PTEN levels are not altered after 96 hours of Trichostatin A treatment and (B) Trichostatin A at doses used in our experiments was able to increase expression of known acetylated protein H3. Blue boxes indicate lines with little or no H3 expression at basal levels where induction of H3 was observed after Trichostatin A treatment. Green triangles indicate increasing doses of drug from 0-.01 in A and 0-.1 in B.

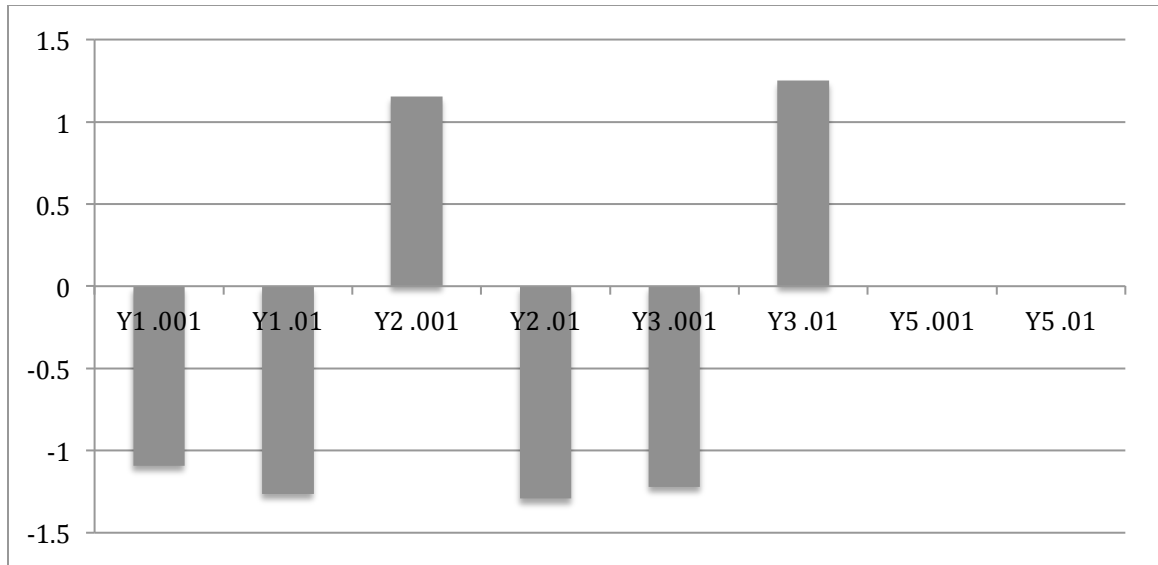


Figure 5 - Fold change of PTEN in T-ALL cell lines exposed to Trichostatin A. qRT-PCR indicated negative or insignificant changes in PTEN mRNA expression when cell lines were exposed to Trichostatin A. Fold values were calculated using delta-delta CT.

modification is unlikely to be the mechanism of PTEN loss in these cells.

EpiQ Analysis Does Not Implicate Chromatin Remodeling. To further investigate the role of chromatin remodeling in the loss of PTEN in our cell lines, EpiQ analysis was performed. EpiQ uses RT-PCR to quantitate the structure of chromatin, which can exist in 2 states within the nucleus. Heterochromatin is inaccessible to nucleases, and is thus transcriptionally silent.²⁸ It is unable to be digested due to its tightly wound nature, and therefore in our experiments is able to be amplified by PCR and will not result in a threshold change when analyzed by RT-PCR.

Euchromatin, on the other hand, is unwound DNA. It is available and easily accessible to nucleases, and is able to be digested. As such, it is unable to be amplified by PCR and will therefore result in a large threshold shift in RT-PCR.

We exposed our second-site T-ALL cell lines to a chromatin buffer either containing a nuclease or nuclease free. Genomic DNA was isolated and chromatin structure was assessed by RT-PCR. Results are normalized to a known epigenetically silenced gene, and are displayed as accessibility percentages, where 95-100% is fully accessible, 65-95 is mostly accessible, 20-65 indicates low accessibility, and 0-20% is highly inaccessible chromatin. The percentages are calculated by comparing the delta Ct of the digested versus undigested samples of each cell line and comparing the values to the known epigenetically silenced reference genes values for the same cell line (Figure 7).

Results using the EpiQ kit were mixed and were never reproducible across

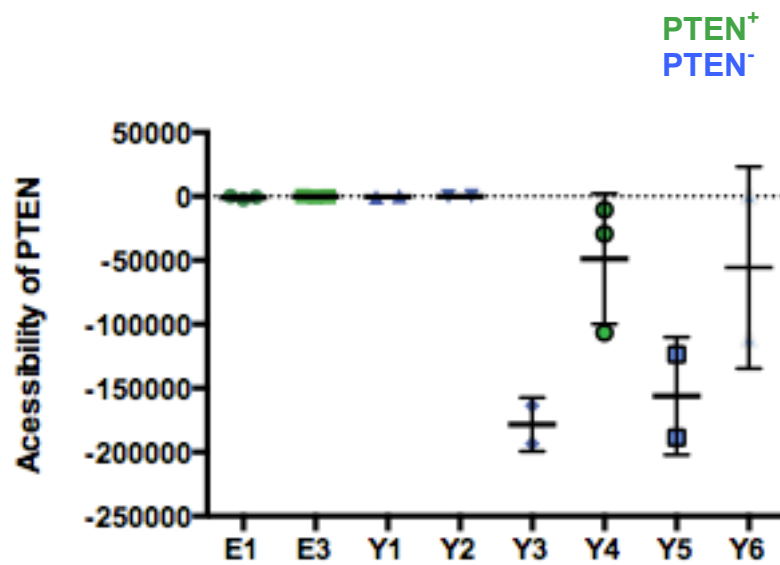


Figure 6 – EpiQ Analysis of PTEN chromatin structure. Percent accessibility of PTEN promoter. Values are determined by calculating comparing the delta Ct of known epigenetically silenced gene and that of PTEN.

RT-PCR runs. While some experiments yielded results seeming to indicate that the chromatin in lines without PTEN expression were in an inaccessible position, subsequent runs did not verify this result, and our data therefore did not support chromatin remodeling as the mechanism underlying PTEN silencing.

Discussion

PTEN is regulated by a variety of processes within the cell. In cancer there is varied evidence that epigenetic regulation of PTEN plays a role in drug response, disease progression, and tumor maintenance.¹⁰ We sought to investigate if PTEN was being epigenetically silenced in our second-site T-ALL cell lines that do not exhibit PTEN expression as a way to re-activate the PI3K pathway.

Bisulfite sequencing did not indicate that the promoter of *Pten* is methylated in our cell lines. Sequencing did not reveal any protected thymine residues (Figure 1). This method relies heavily on the design of primers for areas in the promoter likely to be methylated. Although our primers were designed using a program designed to help determine likely CpG islands and using published sequences used in previous *Pten* methylation studies, it is possible that there is methylation of the *Pten* promoter but that we just never designed the appropriate primers to detect it.

Our experiments with 5-azacytidine did not indicate that PTEN was being negatively regulated by methylation (Figure 2). The doses we used induced the

expression of ZNF645, a gene silenced by methylation (Figure 3), but the experiments never yielded any change in PTEN expression.²²

Likewise, exposing T-ALL cell lines to Trichostatin A did not result in an induction of PTEN expression. We expected that if PTEN expression was being influenced by histone acetylation and chromatin structure, Trichostatin A might reverse the effect. We examined time points commonly used in the literature, but saw no changes by either proliferation assay, Western blot, or RT-PCR (Figures 4,5,6).²⁹

Finally, analysis of chromatin accessibility by nuclease digestion and RT-PCR did not yield a clear positive result. Experimentally the results were inconsistent. This could perhaps be corrected for by optimizing the time of nuclease digestion and the amount of nuclease used. Values for the reference gene, which is essential for calculating accessibility were not ideal, which could be due to it being in a partially accessible configuration in our cell lines. Some cell lines also contain endogenous nuclease activity, so it is possible that this experiment could have been successful with more optimization.

Although we focused our studies on epigenetic silencing, PTEN expression is highly regulated in the cell by various mechanisms, many of which can lead to its decreased expression, any of which may be responsible for the lack of PTEN in our second-site cell lines and all of which could be explored further.

PTEN is regulated by phosphorylation. Its membrane recruitment and lipid

phosphatase activity is dependent on phosphorylation in its C-terminal tail.³⁰ By contrast, PTEN phosphorylation at Thr366 leads to degradation of the protein.^{31,32}

PTEN can be subject to ubiquitylation by E3 ligases. NEDD4, XIAP, and WWP2 have all been shown to ubiquitylate PTEN, though only NEDD4 is well-studied.^{33,34} NEDD4 ubiquitylates PTEN in a context-dependent manner, downregulating PTEN when the PI3K pathway is required for neuronal survival.³⁵ In breast cancer the relationship between NEDD4 and PTEN has been observed to be altered by other proteins. Authors observed that RAK phosphorylation of PTEN stabilizes and prevents PTEN from binding to NEDD4, rescuing PTEN from degradation.³⁶

PTEN is susceptible to degradation due to oxidation.³⁷ Changes in the catalytic activity by oxidation can occur directly by ROS in the active site forming a di-sulfide bond or indirectly, as oxidation of PTEN binding partner PARK7 induces binding to PTEN and the subsequent inhibition of lipid phosphatase activity.³⁸

S-nitrosylation is another mechanism of PTEN regulation. Nitric Oxide induces PTEN S-nitrosylation, inactivating its lipid phosphatase activity via NEDD4 degradation. Pten can also be S-nitrosylated by NO, and the degree of S-nitrosylation of PTEN has been correlated with reduced PTEN levels and increases in AKT activation in early Alzheimer disease.³⁹

In addition to post-translational modifications, PTEN is regulated by many non-coding RNAs. Expression of miRNAs that have been observed to down-regulate

PTEN have been found in patients with metabolic disease, Cowden disease, and leukemia and have been demonstrated to promote tumorigenesis or advance disease.⁴⁰⁻⁴⁴ In addition to miRNAs themselves, regulators of miRNA that modulate PTEN have also been discovered and found to be altered in disease states, as miR-19, a miRNA known to decrease PTEN expression is upregulated by MYC.⁴⁵ Interestingly, the PTEN pseudogene *PTENP1* has been shown to act as a sort of miRNA decoy, playing a role in the regulation of PTEN by sequestering miRNA targeting PTEN and thus preserving PTEN expression.^{46,47}

Although we were unable to determine the mechanism by which PTEN is silenced in our second-site T-ALL cell lines, it is a scientifically important question that can and should be answered by further studies.

Materials and Methods

Bisulfite Sequencing. Bisulfite conversion was performed using the EZ DNA Methylation-Direct Kit (Zymo Research). Briefly, second-site T-ALL cell lines were collected and digested with Proteinase K. Bisulfite conversion was performed using the C-T Conversion Reagent, heated to 98 degrees and the lowered to 64 degrees for 3.5 hours. The resulting product was bound to a spin column, washed, eluted, and sent for immediate sequencing.

5 Azacitidine Studies. Second-site T-ALL cell lines were plated to a density of 2 million per 3 milliliters of media in 12-well plates. 5-azacytidine (Sigma) was added to a final concentration of .5 and 1 μ M. New drug was added every 24 hours, and cell lines were collected at 96 hours. RNA was isolated using the RNeasy Mini Kit (Qiagen) and cDNA made with SuperscriptIII (Invitrogen). Taqman PTEN primers (Invitrogen) were used in a gene expression Qrt-PCR assay (ABI Invitrogen) run on an AB 7900 using Taqman Gene Expression Master Mix (Invitrogen).

Trichostatin A Experiments. Trichostatin A (Sigma) was added to second-site T-ALL cell lines plated to a density of 2 million per 3 milliliters of media in a 12-well plate. Drug was added at concentrations of .001, .01, and .1 μ M. Trichostatin A was added fresh daily and cell lined were counted on a hemocytometer when the DMSO well was confluent (96 hours). Lysates were collected for Western blot and run on a 10% gel as described previously. Antibodies used were from Cell Signaling. Qrt-PCR was performed as described above.

EpiQ Analysis. EpiQ (BioRad) experiments were performed as described in the manufacturers instructions. In summary, a chromatin buffer is added to cells and incubated in a tissue culture incubator for one hour. Ethanol is added and genomic DNA is isolated. qPCR was performed using EpiQ Chromatin SYBR Supermix (BioRad) on an AB 7900. Data were analyzed using the EpiQ chromatin kit data analysis tool.

References

1. Waite KA EC. Protean PTEN: Form and Function. *Am J Hum Genet.* 2002;70(4):829-844.
2. Maehama T, Dixon JE. The Tumor Suppressor, PTEN/MMAC1, Dephosphorylates the Lipid Second Messenger, Phosphatidylinositol 3,4,5-Trisphosphate. *Journal of Biological Chemistry.* 1998-05-29 1998;273(22):13375-13378.
3. Chu EC TA. PTEN regulatory functions in tumor suppression and cell biology. *Med Sci Monit.* 2004;10(10):235-241.
4. Yamada KM, Araki M. Tumor suppressor PTEN: modulator of cell signaling, growth, migration and apoptosis. *J Cell Sci.* 2001-07-01 2001;114(13):2375-2382.
5. Li J, Yen C, Liaw D, et al. PTEN, a Putative Protein Tyrosine Phosphatase Gene Mutated in Human Brain, Breast, and Prostate Cancer. *Science.* 1997-03-28 1997;275(5308):1943-1947.
6. Tamguney T, Stokoe D. New insights into PTEN. *J Cell Sci.* 2007-12-01 2007;120(23):4071-4079.
7. Manning BD CL. AKT/PKB Signaling: Navigating Downstream. *Cell.* 2007;129(7):1261-1274.
8. Song MS, Salmena L, Pandolfi PP. The functions and regulation of the PTEN tumour suppressor. *Nat Rev Mol Cell Biol.* May 2012;13(5):283-296.

9. Zhang P CJ, Guo XL. New insights into PTEN regulation mechanisms and its potential function in targeted therapies. *Biomed Pharmacother*. October 2012 2012;66(7):485–490.
10. Hollander MC, Blumenthal GM, Dennis PA. PTEN loss in the continuum of common cancers, rare syndromes and mouse models. *Nature Reviews Cancer*. 2011-03-24 2011;11(4):289-301.
11. Ikenoue T, Inoki K, Zhao B, Guan K-L. PTEN Acetylation Modulates Its Interaction with PDZ Domain. *Cancer Research*. 2008-09-01 2008;68(17):6908-6912.
12. Lu J JH, Kong N, Yang Y, Carroll J, Luo HR, Silberstein LE, Yupoma, Chai L. Stem Cell Factor SALL4 Represses the Transcriptions of PTEN and SALL1 through an Epigenetic Repressor Complex. *PLOS ONE*. 2009/5/18 2009;4(5).
13. Roman-Gomez J, Jimenez-Velasco A, Agirre X, Prosper F, Heiniger A, Torres A. Lack of CpG Island Methylator Phenotype Defines a Clinical Subtype of T-Cell Acute Lymphoblastic Leukemia Associated With Good Prognosis. *J Clin Oncol*. 2005-10-01 2005;23(28):7043-7049.
14. Whang YE, Wu X, Suzuki H, et al. Inactivation of the tumor suppressor PTEN/MMAC1 in advanced human prostate cancer through loss of expression. *Proc Natl Acad Sci U S A*. 1998 April 28 1998;95(9):5246-5250.
15. Goel A, Arnold CN, Niedzwiecki D, et al. Frequent Inactivation of PTEN by Promoter Hypermethylation in Microsatellite Instability-High Sporadic Colorectal Cancers. *Cancer Research*. 2004-05-01 2004;64(9):3014-3021.

16. Khan S, Vora J. PTEN promoter is methylated in a proportion of invasive breast cancers. *International Journal of Cancer*. 2004;112(3):407-410.
17. Wang L WW, Zhang Y, Guo SP, Zhang J, Li QL. Epigenetic and genetic alterations of PTEN in hepatocellular carcinoma. *Hepatology Research*. 2007;37(5):389-396.
18. Schmid K, Oehl N, Wrba F, Pirker R, Pirker C, Filipits M. EGFR/KRAS/BRAF Mutations in Primary Lung Adenocarcinomas and Corresponding Locoregional Lymph Node Metastases. *Clin Cancer Res*. 2009-07-15 2009;15(14):4554-4560.
19. Wójcik P KJ, Okoń K, Zazula M, Moździoch I, Niepsuj A, Stachura J. KRAS mutation profile in colorectal carcinoma aand novel mutation—internal tandem duplication in KRAS. *Pol J Pathol*. 2008;59(2):93-96.
20. Frommer M, McDonald LE, Millar DS, et al. A genomic sequencing protocol that yields a positive display of 5-methylcytosine residues in individual DNA strands. *Proc Natl Acad Sci U S A*. Mar 1 1992;89(5):1827-1831.
21. Chiak A. Biological Effects of 5-Azacytidine in Eukaryotes. *Oncology*. 1974;30(5):405-422.
22. Bai G, Liu Y, Zhang H, et al. Promoter demethylation mediates the expression of ZNF645, a novel cancer/testis gene. *BMB Rep*. Jun 2010;43(6):400-406.
23. Vanhaecke T, Papeleu P, Elaut G, Rogiers V. Trichostatin A-like hydroxamate histone deacetylase inhibitors as therapeutic agents: toxicological point of view. *Curr Med Chem*. Jun 2004;11(12):1629-1643.

24. Shankar S, Srivastava RK. Histone Deacetylase Inhibitors: Mechanisms and Clinical Significance in Cancer: HDAC Inhibitor-Induced Apoptosis. *Advances in Experimental Medicine and Biology*. 2007;615:261-298.
25. Su L, Cheng H, Sampaio AV, Nielsen TO, Underhill TM. EGR1 reactivation by histone deacetylase inhibitors promotes synovial sarcoma cell death through the PTEN tumor suppressor. *Oncogene*. 2010-05-31 2010;29(30):4352-4361.
26. Pan L LJ, Wang X, Han L, Zhang Y, Han S, Huang B. Histone deacetylase inhibitor trichostatin a potentiates doxorubicin - induced apoptosis by up - regulating PTEN expression. *Cancer*. 2007;109(8):1676-1688.
27. Lachner M, O'Carroll D, Rea S, Mechtler K, Jenuwein T. Methylation of histone H3 lysine 9 creates a binding site for HP1 proteins. *Nature*. 2001-03-01 2001;410(6824):116-120.
28. Rando OJ, Chang HY. Genome-wide views of chromatin structure. *Annu Rev Biochem*. 2009;78:245-271.
29. Cai Y, Cui W, Chen W, et al. The effects of a histone deacetylase inhibitor on biological behavior of diffuse large B-cell lymphoma cell lines and insights into the underlying mechanisms. *Cancer Cell Int*. 2013;13:57.
30. Vazquez F, Matsuoka S, Sellers WR, Yanagida T, Ueda M, Devreotes PN. Tumor suppressor PTEN acts through dynamic interaction with the plasma membrane. *Proc Natl Acad Sci U S A*. 2006 March 7 2006;103(10):3633-3638.
31. Odriozola L, Singh G, Hoang T, Chan AM. Regulation of PTEN Activity by Its Carboxyl-terminal Autoinhibitory Domain. *Journal of Biological Chemistry*. 2007-08-10 2007;282(32):23306-23315.

32. Rahdar M, Inoue T, Meyer T, Zhang J, Vazquez F, Devreotes PN. A phosphorylation-dependent intramolecular interaction regulates the membrane association and activity of the tumor suppressor PTEN. *Proc Natl Acad Sci U S A*. 2008-12-29 2008;106(2):480-485.
33. Maddika S, Kavela S, Rani N, et al. WWP2 is an E3 ubiquitin ligase for PTEN. *Nature Cell Biology*. 2011-05-01 2011;13:728-733.
34. Themsche CV, Leblanc V, Parent S, Asselin E. X-linked Inhibitor of Apoptosis Protein (XIAP) Regulates PTEN Ubiquitination, Content, and Compartmentalization. *Journal of Biological Chemistry*. 2009-07-31 2009;284(31):20462-20466.
35. Drinjakovic J JH, Campbell DS, Strohlic L, Dwivedy A, Holt CE. E3 ligase Nedd4 promotes axon branching by downregulating PTEN. *Neuron*. 2010;65(3):341-357.
36. Yim EK PG, Dai H, Hu R, Li K, Lu Y, Mills GB, Meric-Bernstam F, Hennessy BT, Craven RJ, Lin SY. Rak Functions as a Tumor Suppressor by Regulating PTEN Protein Stability and Function. *Cancer Cell*. 2009;15(4):301-314.
37. Lee SR YK, Kwon J, Lee C, Jeong W, Rhee SG. Reversible inactivation of the tumor suppressor PTEN by H₂O₂. *Journal of Biological Chemistry*. 2002;277(23):20336-20342.
38. Kim YC, Kitaura, H., Taira, T., Iguchi-Ariga, S. M. and Ariga, H. Oxidation of DJ-1-dependent cell transformation through direct binding of DJ-1 to PTEN. *Int J Oncol*. 2009;35:1331-1341.

39. Numajiri N, Takasawa K, Nishiya T, et al. On-off system for PI3-kinase-Akt signaling through S-nitrosylation of phosphatase with sequence homology to tensin (PTEN). *Proc Natl Acad Sci U S A*. 2011 June 21 2011;108(25):10349-10354.
40. Xiao C, Srinivasan L, Calado DP, et al. Lymphoproliferative disease and autoimmunity in mice with elevated miR-17-92 expression in lymphocytes. *Nat Immunol*. 2008 April 2008;9(4):405-414.
41. Olive V, Bennett MJ, Walker JC, et al. miR-19 is a key oncogenic component of mir-17-92. *Genes and Development*. 2009-12-15 2009;23(24):2839-2849.
42. Mavrakis KJ, Wolfe AL, Oricchio E, et al. Genome-wide RNAi screen identifies miR-19 targets in Notch-induced acute T-cell leukaemia (T-ALL). *Nat Cell Biol*. 2010 April 2010;12(4):372-379.
43. Meng F HR, Wehbe-Janek H, Ghoshal K, Jacob ST, Patel T. Source. MicroRNA-21 Regulates Expression of the PTEN Tumor Suppressor Gene in Human Hepatocellular Cancer. August 2007 2007;133(2):647-658.
44. Ma X KM, Choudhury SN, Becker Buscaglia LE, Barker JR, Kanakamedala K, Liu MF, Li Y. Loss of the miR-21 allele elevates the expression of its target genes and reduces tumorigenesis. *Proc Natl Acad Sci U S A*. 2011;108(25):10144-10149.
45. Mu P, Han Y-C, Betel D, et al. Genetic dissection of the miR-17~92 cluster of microRNAs in Myc-induced B-cell lymphomas. *Genes and Development*. 2009-12-15 2009;23(24):2806-2811.

46. Poliseno L, Salmena L, Zhang J, Carver B, Haveman WJ, Pandolfi PP. A coding-independent function of gene and pseudogene mRNAs regulates tumour biology. *Nature*. 2010 June 24 2010;465(7301):1033-1038.
47. Salmena L PL, Tay Y, Kats L, Pandolfi PP. A ceRNA Hypothesis: The Rosetta Stone of a Hidden RNA Language? *Cell*. 2011;146(3):353-358.

Chapter 5: Conclusions and Future Directions

Concluding Remarks

Our studies of T-ALL cell lines generated from leukemias that were initiated by expressing “second site” *KRAS* mutations in mouse bone marrow unexpectedly showed that PTEN expression strongly modulated sensitivity to MEK inhibition. Further analysis indicates that this sensitivity is due to a decrease in pro-survival proteins, as susceptible cells succumb to apoptosis. Additionally, we have shown that AKT phosphorylation is required for the pro-survival proteins BCL-xl and MCL-1 to be expressed and lines to remain resistant to MEK inhibition. These data indicate that it is not only increased pathway activation that drives whether a given drug will be effective, but a complex interplay of feedback and signaling must be considered.

Future Directions

In our work we have described the response of various second-site T-ALL cell lines to MEK inhibition by PD0325901. These studies have informed us of the role of PTEN as a marker of drug sensitivity. We showed through a knockdown experiment that decreasing PTEN expression in our second site cell lines that are sensitive to MEK inhibition altered the sensitivity and caused cells to become more resistant to PD0325901. These data reinforce the idea that PTEN is responsible for the sensitive phenotype. However, to fully elucidate the role of PTEN as the gatekeeper of sensitivity, further study is required.

First, to more fully prove that PTEN is the driver of MEK sensitivity in our system it would be important to re-introduce PTEN into the lines that are deficient

for it, to determine if PTEN expression can reverse resistance to PD0325901. E37G and Y64G mutants are different genetically and biochemically, so it is important to firmly establish that though varied, expression of just the PTEN protein can alter the resistant phenotype we observed.

Through our experiments we showed that even partial inhibition of AKT caused cell lines that had lost expression of PTEN become sensitive to MEK inhibition by PD0325901. Our data indicates that PTEN, acting through its lipid phosphatase activity to regulate AKT levels, is altering sensitivity to MEK inhibition.

The drug we used in our combination study, MK2206, is a specific AKT inhibitor.¹ It would be interesting to note if other PI3K inhibitors would likewise cause sensitivity to PD0325901 in cell lines without PTEN expression. Although BCL-xl and MCL-1 are both regulated by AKT and their levels correlate with resistance, perhaps other pro-survival proteins could likewise alter the resistant phenotype. Apoptosis is tightly controlled in the cell, with much redundancy.² Using inhibitors targeting different nodes of the PI3K pathway could elucidate other mechanisms by which cell lines may become resistant to MEK inhibition.

As an alternative to utilizing chemical inhibitors, RNA knockdown studies could also help to elucidate the specific role of AKT for drug resistance. Decreasing AKT in the cell in this manner and performing proliferation assays would allow us to determine if PTEN is exerting its effect strictly through its regulation of AKT. Although the main lipid phosphatase activity of PTEN is through regulation of PtdIns(3,4,5)P₃ and thus AKT levels in the cell, PTEN exhibits non-canonical, non-PI3K related activity as well. PTEN loss has been shown to activate the JNK pathway

independent of AKT activation, and based on *in vitro* studies PTEN is able to dephosphorylate Ser, Tyr, and Thr residues and focal adhesion kinase (FAK) and cAMP responsive-element-binding protein (CREB).³⁻⁵ Loss of PTEN can also lead to activation of non-receptor tyrosine kinase SRC and conferred resistance to HER2 breast cancer cell lines.⁶ It is possible that although AKT is clearly involved in the resistant phenotype, PTEN may be altering sensitivity to MEK inhibition in a non-canonical manner.

We found that the levels of pro-survival proteins BCL-xl and MCL-1 were increased in cell lines that are resistant to MEK inhibition. To determine if these proteins are responsible for the resistant phenotype, it would be necessary to alter their expression and assess responses to PD0325901. ABT-737 is an inhibitor of Bcl2 proteins and is active against BCL-xl but not MCL-1.⁷ Preliminary studies in our laboratory have showed no effect on sensitivity to PD0325901 when this drug is used on PTEN deficient second-site T-ALL cell lines. However, studies in a mouse lymphoma model have shown that inhibition of MCL-1 is required for ABT-737 to effectively induce apoptosis in cell lines with MCL-1 expression.⁸ This data indicate that MCL-1 inactivation is capable of sensitizing resistant cells and that these 2 pro-survival proteins work together in the evasion of apoptosis. Designing a hairpin to MCL-1 and using it alone and in combination with ABT-737 would elucidate the role of these 2 specific pro-survival proteins in the response to MEK inhibition. Alternatively, hairpins to NOXA, which negatively regulates MCL-1 and targets it for degradation could be designed and used in combination with ABT-737.⁹ Alternatively, the inhibitor TW-37 could be used. This drug has been demonstrated

to target MCL-1 and BCL-xl in B-cell lymphomas.¹⁰ As an alternative to inhibitor studies, the role of MCL-1 and BCL-xl in sensitivity to PD0325901 could be assessed through the generation of constructs to over-express MCL-1 and BCL-xl proteins in lines which express PTEN and show sensitivity to MEK inhibition. It would be interesting to note if both of these proteins are required for resistance to develop.

Our studies of the regulation of PTEN did not elucidate the mechanism by which PTEN expression is lost in our second-site cell lines. We sought to determine if PTEN was silenced through epigenetic mechanisms through bisulfite sequencing, 5-azacytidine and Trichostatin A treatment, and epiQ analysis. That all our results were negative indicates that PTEN is being regulated by another mechanism than methylation or chromatin remodeling.

PTEN can be down regulated by phosphorylation events, oxidation, ubiquitylation, and S-nitrosylation.¹¹ Additionally, PTEN interacts with and the lipid phosphatase activity is increased by interaction with p85.¹² Interactions with shank-interacting protein-like 1 (SIPL1) or PtdIns(3,4,5)P₃- RAC-exchanger 2 (PREX2) can decrease PTENs lipid phosphatase activity.^{13,14} Since PTEN is not mutated in our T-ALL cells, any of these mechanisms for down regulating PTEN may be acting in our lines.

Our experiments indicate the role of anti-apoptotic proteins in resistance to MEK inhibition and the role of PTEN in mediating this response. That so many of our cell lines have lost PTEN expression suggests its importance as a mechanism by which cells will re-wire and re-activate lost pathways. The mechanism by which PTEN loss occurs is important for our understanding of potential effects of Ras

effector pathway inhibition.

References

1. Hirai H, Sootome H, Nakatsuru Y, et al. MK-2206, an Allosteric Akt Inhibitor, Enhances Antitumor Efficacy by Standard Chemotherapeutic Agents or Molecular Targeted Drugs In vitro and In vivo. *Molecular Cancer Therapeutics*. 2010-07-01 2010;9(1956).
2. Degterev A, Yuan J. Expansion and evolution of cell death programmes. *Nat Rev Mol Cell Biol*. May 2008;9(5):378-390.
3. Vivanco I, Palaskas N, Tran C, et al. Identification of the JNK signaling pathway as a functional target of the tumor suppressor PTEN. *Cancer Cell*. Jun 2007;11(6):555-569.
4. Gu T, Zhang Z, Wang J, Guo J, Shen WH, Yin Y. CREB is a novel nuclear target of PTEN phosphatase. *Cancer Res*. Apr 15 2011;71(8):2821-2825.
5. Tamura M, Gu J, Matsumoto K, Aota S, Parsons R, Yamada KM. Inhibition of cell migration, spreading, and focal adhesions by tumor suppressor PTEN. *Science*. Jun 5 1998;280(5369):1614-1617.
6. Zhang S, Huang WC, Li P, et al. Combating trastuzumab resistance by targeting SRC, a common node downstream of multiple resistance pathways. *Nat Med*. Apr 2011;17(4):461-469.

7. Oltersdorf T, Elmore SW, Shoemaker AR, et al. An inhibitor of Bcl-2 family proteins induces regression of solid tumours. *Nature*. 2005-05-15 2005;435(7042):677-681.
8. van Delft MF WA, Mason KD, Vandenberg CJ, Chen L, Czabotar PE, Willis SN, Scott CL, Day CL, Cory S, Adams JM, Roberts AW, Huang DC. The BH3 mimetic ABT-737 targets selective Bcl-2 proteins and efficiently induces apoptosis via Bak/Bax if Mcl-1 is neutralized. *Cancer Cell*. 2006;10(5):389-399.
9. Rooswinkel RW, Kooij Bvd, Verheij M, Borst J. Bcl-2 is a better ABT-737 target than Bcl-xL or Bcl-w and only Noxa overcomes resistance mediated by Mcl-1, Bfl-1, or Bcl-B. *Cell Death & Disease*. 2012-08-01 2012;3(8).
10. Mohammad RM, Goustin AS, Aboukameel A, et al. Preclinical Studies of TW-37, a New Nonpeptidic Small-Molecule Inhibitor of Bcl-2, in Diffuse Large Cell Lymphoma Xenograft Model Reveal Drug Action on Both Bcl-2 and Mcl-1. *Clinical Cancer Research*. 2007-04-01 2007;13(7):2226-2235.
11. Shi Y, Paluch BE, Wang X, Jiang X. PTEN at a glance. *Journal of Cell Science*. 2012-10-15 2012;125(20):4687-4692.
12. Chagpar RB, Links PH, Pastor MC, et al. Direct positive regulation of PTEN by the p85 subunit of phosphatidylinositol 3-kinase. *Proc Natl Acad Sci U S A*. 2010-03-23 2010;107(12):5471-5476.
13. Fine B, Hodakoski C, Koujak S, et al. Activation of the PI3K Pathway in Cancer Through Inhibition of PTEN by Exchange Factor P-REX2a. *Science*. 2009-09-04 2009;325(5945):1261-1265.

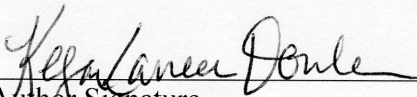
14. He L, Ingram A, Rybak AP, Tang D. Shank-interacting protein-like 1 promotes tumorigenesis via PTEN inhibition in human tumor cells. *J Clin Invest*. 2010-06-01 2010;120(6):2094-2108.

Publishing Agreement

It is the policy of the University to encourage the distribution of all theses, dissertations, and manuscripts. Copies of all UCSF theses, dissertations, and manuscripts will be routed to the library via the Graduate Division. The library will make all theses, dissertations, and manuscripts accessible to the public and will preserve these to the best of their abilities, in perpetuity.

Please sign the following statement:

I hereby grant permission to the Graduate Division of the University of California, San Francisco to release copies of my thesis, dissertation, or manuscript to the Campus Library to provide access and preservation, in whole or in part, in perpetuity.



Author Signature

7-10-13

Date